

Aus der Medizinischen Universitätsklinik und Poliklinik Tübingen
Abteilung Innere Medizin II
(Schwerpunkt: Hämatologie, Onkologie, Klinische Immunologie,
Rheumatologie)

**Evaluation of myelo-monocytic differentiation of
congenital neutropenia patient derived induced
pluripotent stem cells**

**Inaugural-Dissertation
zur Erlangung des Doktorgrades
der Medizin**

**der Medizinischen Fakultät
der Eberhard Karls Universität
zu Tübingen**

**vorgelegt von
Stalman, Dorothea Juliane Luise**

2022

Dekan: Professor Dr. B. Pichler

1. Berichterstatter: Professor Dr. J. Skokowa, Ph.D

2. Berichterstatter: Professor Dr. P.J. Lang

Tag der Disputation: 27.04.2022

Meiner Familie

Table of content

Table of content	IV
List of figures	VIII
List of tables	IX
List of abbreviations	X
1 Introduction	1
1.1 Hematopoiesis	1
1.1.1 Transcriptional regulation in hematopoiesis and myeloid decision making.....	3
1.1.2 Steady state and emergency granulopoiesis	5
1.2 Severe congenital neutropenia (CN)	6
1.2.1 History	7
1.2.2 Genetic background and pathogenesis.....	8
1.2.3 Prognosis and treatment.....	9
1.2.4 Leukemic progression in CN	11
1.3 <i>FLT3</i>	12
1.4 <i>FLT1</i>	13
1.5 Induced pluripotent stem cells (iPSCs).....	14
1.6 Aim.....	16
2 Material and Methods	17
2.1 Material	17
2.1.1 Cell culture standard medium and buffer	17
2.1.2 Cell lines	18
2.1.3 Antibodies	19

2.1.4	Cytokines and organic compounds	20
2.1.5	Cell culture chemicals	20
2.1.6	Cell culture equipment	21
2.1.7	Molecular biology standard medium and buffer	22
2.1.8	Primers.....	23
2.1.9	Competent cells	25
2.1.10	Vector and virus.....	25
2.1.11	Antibodies western blot	26
2.1.12	Molecular biology chemicals.....	27
2.1.13	Molecular biology equipment.....	29
2.1.14	Software	30
2.2	Methods	31
2.2.1	Polymerase chain reaction (PCR)	31
2.2.2	Electrophoresis and gel extraction	32
2.2.3	Cloning.....	32
2.2.3.1	Digestion.....	33
2.2.3.2	Dephosphorylation	34
2.2.3.3	Gel electrophoresis and gel extraction.....	34
2.2.3.4	Insert purification.....	34
2.2.3.5	Ligation	34
2.2.3.6	Transformation.....	35
2.2.3.7	Mini-preparation	36
2.2.3.8	Maxi-preparation	36
2.2.4	Sequencing	36
2.2.5	Primer design.....	36
2.2.6	Transfection	37
2.2.7	RNA Isolation and cDNA Synthesis	37
2.2.8	Real-time PCR.....	38
2.2.9	Western blot.....	38
2.2.10	Virus production and -titration.....	40
2.2.11	Bortezomib treatment	40
2.2.12	Generation of induced pluripotent stem cells (iPSC)	41

2.2.13	iPSC maintenance.....	42
2.2.14	Embryoid bodies (EB) formation and hematopoietic differentiation	42
2.2.15	Flow cytometry (FACS)	43
2.2.15.1	Single staining FACS	43
2.2.15.2	Multicolor FACS	44
2.2.16	DNA isolation, -gene amplification and mutational analysis	45
2.2.17	Alkaline Phosphatase staining.....	46
2.2.18	Cytospin slides preparation	46
2.2.19	Immunocytochemistry.....	46
3	Results	47
3.1	Patient case	47
3.2	Analysis of V194M- <i>FLT3</i> mutation using an overexpression system	50
3.2.1	Production of a wildtype <i>FLT3</i> vector	50
3.2.2	Production of V-194M- <i>FLT3</i> vector using site directed mutagenesis .	51
3.2.3	Comparison of the expression levels of WT- and mutant <i>FLT3</i> in transfected 293FT cells.....	52
3.2.4	Production of the <i>FLT3</i> mutant- and <i>FLT3</i> WT – lentiviral particles ...	54
3.3	Evaluation of the effect of Bortezomib on the expression level of V194M <i>FLT3</i>	55
3.3.1	<i>FLT3</i> receptor surface expression in <i>FLT3</i> vector transfected and Bortezomib treated 293FT cells (flow cytometry).....	56
3.3.2	<i>FLT3</i> protein expression in <i>FLT3</i> vector transfected and Bortezomib treated 293FT cells (Western blot).....	57
3.4	Production and characterization of CN patient iPS cells	58
3.4.1	Alkaline Phosphatase staining of undifferentiated iPSC colonies	58
3.4.2	Flow cytometry of undifferentiated patient iPS cells for pluripotency markers.....	59
3.4.3	Real-time PCR for the pluripotency- and 3-germ layer markers.....	61

3.4.4 Immunocytochemistry of spontaneously differentiated CN patient iPS cells	63
3.5 Comparison of CN patient vs. healthy donor iPS cell hematopoietic and myeloid differentiation	64
3.5.1 Early differentiation: <i>FLT3</i> and <i>FLT1</i> expression analysis	64
3.5.2 Intermediate and late differentiation: comparison of CN patient vs. healthy donor iPS cells	66
3.5.2.1 Multicolor FACs analysis of suspension cells	66
3.5.2.1.1 Myeloid differentiation of iPSCs	67
3.5.2.1.2 Myeloid differentiation using various culture conditions	69
3.5.2.2 Morphology analysis of iPSC suspension cells	71
4 Discussion	76
4.1 V194M- <i>FLT3</i> mutation and its implication on mRNA, protein and receptor expression levels	79
4.2 Evaluation of the impact of Bortezomib on the expression level of V194M <i>FLT3</i>	80
4.3 Production and characterization of patient derived iPSC	81
4.4 Comparison of the hematopoietic differentiation of the index CN patient vs. healthy donor iPSC	83
4.4.1 Early differentiation into mesodermal lineage: <i>FLT3</i> and <i>FLT1</i> expression analysis	83
4.4.2 Analysis of the late hematopoietic differentiation of iPSCs	84
4.5 Conclusion	88
5 Abstract/Zusammenfassung	89
5.1 Abstract	89
5.2 Zusammenfassung	90

6	References.....	91
7	Declaration of authorship.....	104
8	Acknowledgement	105

List of figures

Figure 1. Hematopoiesis: from stem cell to peripheral blood cell	2
Figure 2. Steady state and emergency granulopoiesis.....	6
Figure 3. From somatic cell to induced pluripotent stem cells and beyond: iPSC development, technics and opportunities	15
Figure 4. Lentiviral vector used for the cloning of <i>FLT3</i>	33
Figure 5. Histological comparison of bone marrow samples from healthy individuals, a typical CN patient and the index patient	48
Figure 6. Electrophoresis of lentiviral vector backbone and <i>FLT3</i> insert, Sanger Sequencing of <i>FLT3</i> -WT vector and sequencing primer coverage of the <i>FLT3</i> gene	51
Figure 7. Sanger Sequencing of V194M- <i>FLT3</i> mutated vector	52
Figure 8. Results of the <i>FLT3</i> mRNA/protein expression analysis in transfected 293FT cells.....	54
Figure 9. Virus titration of <i>FLT3</i> control/empty virus, WT- <i>FLT3</i> virus and mutant V194M- <i>FLT3</i> virus.....	55
Figure 10. Mean fluorescence intensity (MFI) of <i>FLT3</i> in <i>FLT3</i> -vector transfected and Bortezomib (BZ)/DMSO treated HEK293FT cells	57
Figure 11. Western blot of <i>FLT3</i> protein in <i>FLT3</i> vector (control, WT and mutant) transfected and treated 293FT cells.....	58
Figure 12. AP staining of patient derived IPS colonies.....	59
Figure 13. Flow cytometry evaluation of SSEA4 and Tra1-60 expression in undifferentiated iPSC cells of CN patient (OKPBL2 and OKPBL6) and healthy donor (CD34IPSC16)	60

Figure 14. Real-time PCR analysis of pluripotency markers in undifferentiated CN patient (OKPBL2 and OKPBL6) and healthy donor (CD34IPS) iPS cells compared to mature CD34 ⁺ cells.....	62
Figure 15. mRNA expression levels of markers of ectodermal and endodermal differentiation in spontaneously differentiated CN patient and healthy donor iPS cell- vs. undifferentiated iPS cells.....	63
Figure 16. Immunocytochemistry of spontaneously differentiated patient iPS cells	63
Figure 17. Mean fluorescent intensity (MFI) (Mean sample-mean isotype) of <i>FLT3</i> expression at early stages of hematopoietic differentiation of CN patient vs. healthy donor EBs	65
Figure 18. MFI of <i>FLT1</i> expression at early stages of hematopoietic differentiation of CN patient vs. healthy donor EBs.	66
Figure 19. Analysis of myeloid differentiation of healthy donor and patient derived iPS- Suspension cells day 12-26	68
Figure 20. Assessment of myeloid differentiation of healthy donor and patient derived iPSCs stimulated with different cytokine mixes (IL3, IL3-GCSF, IL3-GCSF- <i>FLT3L</i>).....	70
Figure 21. Morphology analysis of CN patient vs. healthy donor floating cell development in different treatment groups	73
Figure 22. Morphology analysis of monocyte development of CN patient vs. healthy donor iPSC suspension cells development in different treatment groups (IL3, IL3-GCSF, IL3-GCSF- <i>FLT3L</i>)	75

List of tables

Table 1. PCR reaction mix	31
Table 2. Digestion reaction mix, modified from New England Biolabs AgeI-HF and AfeI-restriction enzyme protocol	33
Table 3. Ligation mix, modified from New England Biolabs Quick Ligation kit protocol	35
Table 4. Real-time PCR cycling protocol.....	38

Table 5. Polyacrylamide gel	39
Table 6. Multicolor FACS antibody panel for late myeloid differentiation.....	44
Table 7. FLT3 amplification mix.....	45
Table 8. Patient bone marrow and differential blood count prior to rhG-CSF and rhGM-CSF treatment.....	47

List of abbreviations

AFP	Alpha-Fetoprotein
AP	Alkaline phosphatase
APC	Allophycocyanin fluorescence
APEL	Albumin Polyvinylalcohol Essential Lipids
BCIP	5-Bromo-4-Chloro-3-indolyl phosphate
bFGF	Basic fibroblast growth factor
BFP	Blue fluorescence protein
BMP-4	Bone morphogenetic protein-4
BSA	Bovine serum albumin
CaCl ₂	Calcium chloride
CD	Cluster of differentiation
cDNA	Complementary DNA
c-kit	CD117/SCF receptor
cm	centimeter
Ctrl	control
CY7	Cyanine-7
DAPI	4',6-diamidino-2-phenylindole
ddH ₂ O	Double-distilled water
D-MEM	Dulbecco's Modified Eagle Medium
DMSO	Dimethyl sulfoxide
DNA	deoxyribonucleic acid
DNMT	DNA methyltransferase
dNTP	Deoxyribose nucleoside triphosphates
EB	Embryoid bodies

EDTA	Ethylenediaminetetraacetic acid
FACS	Fluorescence activated cell sorting
FCS	Fetal calf serum
FITC	Fluorescein isothiocyanate
<i>FLT1</i>	Vascular Endothelial Growth Factor Receptor 1/ Fms Related Tyrosine Kinase 1
<i>FLT3</i>	CD135/ Fms Related Tyrosine Kinase 3
<i>FLT3L</i>	<i>FLT3</i> ligand
FMO	Fluorescence minus one
Gag-pol	Viral packaging gene
G-CSF	Granulocyte-colony stimulating factor
h	hour
HCl	Hydrochloric acid
HEPES	hydroxyethyl piperazineethanesulfonic acid
hVEGFR1	Human vascular endothelial growth factor receptor 1/ <i>FLT1</i>
IgG1	Immunoglobulin G1
IL	Interleukin
iPSCs	Induced pluripotent stem cells
kB	kilo base
kDa	kilo dalton
LB	Lysogeny broth
M	Molarity (mol/L)
MFI	mean fluorescence intensity
MgCl	Magnesium chloride
min	minutes
ml	milliliter
MMC-SNL	Mitomycin treated SNL cells
MOI	Multiplicity of infection

mRNA	Messenger ribonucleic acid
NaCl	Sodium chloride
Nanog	Transcriptional factor for the maintenance of pluripotency in embryonic stem cells
NBT	Nitro blue tetrazolium
Nr.	number
NTM	Buffer containing Tris, NaCl and MgCl (2.1.1.1.6)
OSKM	Plasmid containing OCT3/4, SOX2, KLF4 and c-MYC
PAX6	Paired box protein 6
PBMNC	Peripheral blood mononuclear cells
PBS	Phosphate buffered saline
PCR	Polymerase chain reaction
PE	Phycoerythrin
PFA	Paraformaldehyde
PI	Propidium iodide
Rcf	Relative centrifugal force
RNA	Ribonucleic acid
Rpm	Revolutions per minute
RSV	Long terminal repeat (LTR) viral promoter
RT	Reverse transcriptase
RT-PCR	Real-time polymerase chain reaction
RUNX1	Runt-related transcription factor 1/ acute myeloid leukemia 1 protein
s	second
SCF	c-kit ligand
SCN	Severe congenital neutropenia
SOX 2	Sex determining region Y-box 2
SOX 17	Sex determining region Y-box 17
SSEA-4	stage-specific embryonic antigen-4

TBE	Tris-Borate-EDTA Buffer
TBST	Buffer made from Tris base, NaCl and Tween20
TEMED	Tetramethylethylenediamin
TFM	Transfer medium for virus production (2.1.1.1.5)
TPO	Thrombopoietin
Tra1-60	Podocalyxin, Pluripotency marker in stem cell characterization
Tra1-85	CD147/Oka blood group antigen
Tris	Tris(hydroxymethyl)aminomethane
TUBB3	β -Tubulin III
UV	ultraviolet
V	Voltage
V194M	<i>FLT3</i> mutation Valin to Methionine at the amino acid position 194
VEGF	Vascular endothelial growth factor
VSV-G	Viral envelope gene
WT	Wildtype
$\Delta\Delta CT$	Relative fold gene expression
μg	Microgram
μl	Microliter
μM	Micromolar
7AAD	7-Aminoactinomycin D
$^{\circ}\text{C}$	Degree Celsius

1 Introduction

1.1 Hematopoiesis

Hematopoiesis is the process of proliferation and differentiation from multipotent hematopoietic stem cells (HSC) to mature peripheral blood cells. It is a complex system that gives rise to all cellular components of the blood and is regulated by several transcription factors, colony stimulating factors and their receptors.

Hematopoietic stem cells derive from the lateral plate mesoderm (Hoang, Lambert and Martin, 2016). During embryonal development, the site of hematopoiesis shifts from the initial yolk sac to the aorto-gonad mesonephros (AGM) region, followed by the placenta, fetal liver, thymus and finally the bone marrow (Müller *et al.*, 1994; Gekas *et al.*, 2005; Orkin and Zon, 2008). While the early hematopoiesis (“primitive” hematopoiesis) is focused on generation of erythrocytes, macrophages and megakaryocytes, the system matures along with the embryo to a “definitive” adult hematopoiesis featuring all hematopoietic progenitors and mature cells (Orkin and Zon, 2008).

Multicolor fluorescence activated cell sorting (FACS) has enabled us to distinguish progenitor cells according to their surface markers. Remarkable progress has been made in understanding phenotype and the relationships of progenitor cells to one another. Nevertheless, the exact map of differentiation remains a subject of discussion (Weissman, Anderson and Gage, 2002; Adolfsson *et al.*, 2005; Forsberg *et al.*, 2006; Drissen *et al.*, 2016).

All blood cells are descending from long-term HSC (LT-HSC), which are characterized by the ability for unlimited self-renewal and multipotency (Spangrude, Heimfeld and Weissman, 1988; Uchida and Weissman, 1992; Morrison and Weissman, 1994). While the skill for self-renewal is lost in the following hierarchy levels, short-term HSC (ST-HSC) and multipotent progenitors (MPP) preserve their multipotency (Weissman, Anderson and Gage, 2002; Rosenbauer and Tenen, 2007).

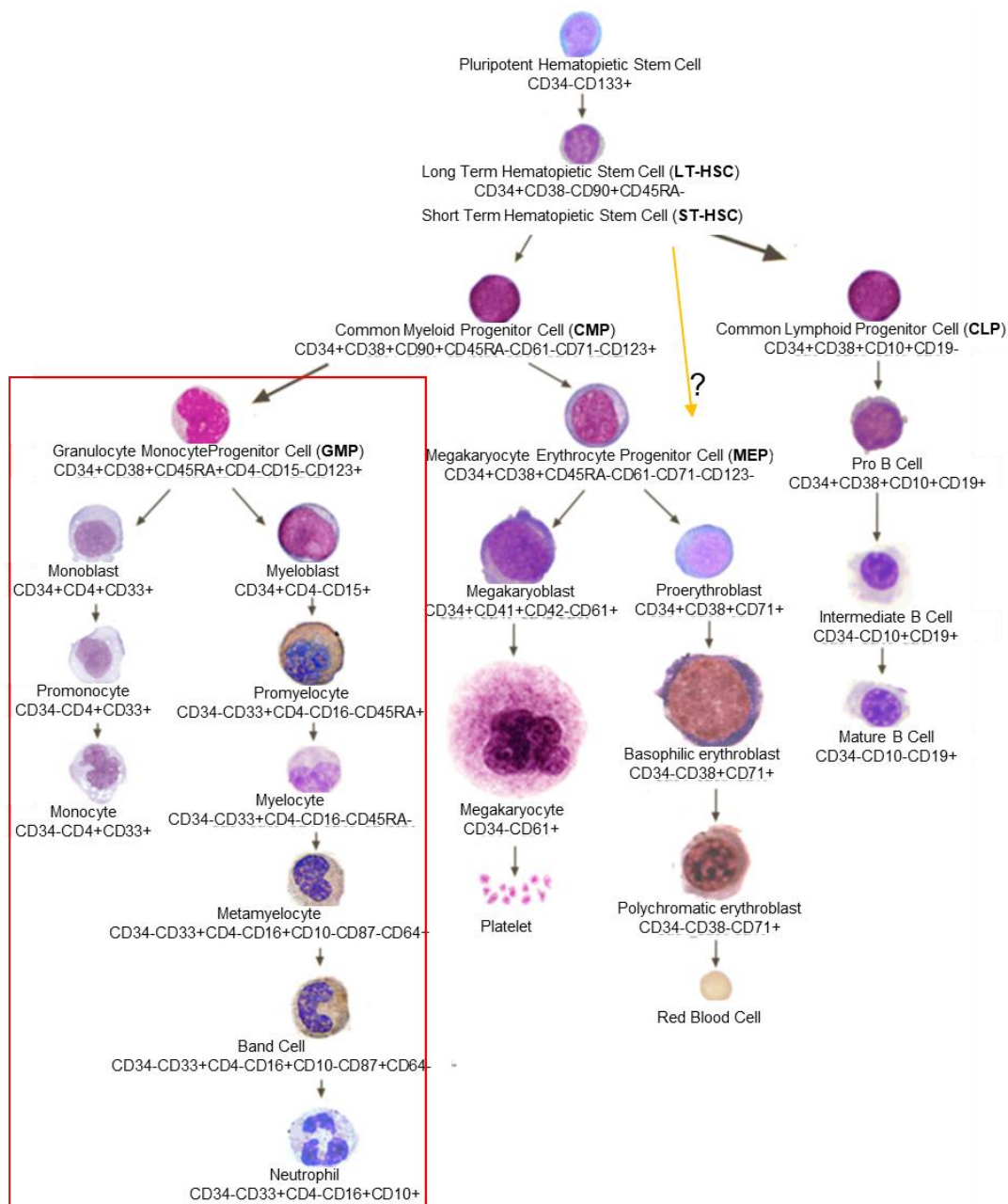


Figure 1. Hematopoiesis: from stem cell to peripheral blood cell

Hematopoietic differentiation from pluripotent hematopoietic cells to mature peripheral blood cells. Schematic phenotype and common surface antigen expression. MEP development from ST-HSC is matter of discussion, as indicated by yellow arrow (modified from Attar, 2014).

With the appearance of common lymphoid progenitors (CLP) and common myeloid progenitors (CMP), different branches of hematopoiesis arise. Progeny of the CLP are the B- and T-lymphocytes, as well as the natural killer (NK) cells. The common myeloid progenitors (CMP), on the other hand, give rise to the granulocyte/monocyte progenitors (GMP) and megakaryocyte/erythroid

progenitors (MEP). It is still in discussion whether the megakaryocyte/erythroid progenitors (MEP) derive exclusively from the CMP (Weissman, Anderson and Gage, 2002) or from an earlier division of the ST-HSC as well (Adolfsson *et al.*, 2005).

The GMP splits subsequently in the monocytic and granulocytic branches. The granulocytic branch comprises of the myeloblast, promyelocyte, myelocyte, metamyelocyte, band cell, and mature polymorphonuclear neutrophils (Attar, 2014).

1.1.1 Transcriptional regulation in hematopoiesis and myeloid decision making

Transcription factors are DNA-binding proteins that regulate gene activity. They are essential for cell fate determination of hematopoietic progenitors and influence hematopoiesis additionally through up- or downregulation of specific colony stimulating factors as the macrophage-colony stimulating factor (M-CSF), the granulocyte-colony stimulating factor (G-CSF) and the granulocyte/macrophage-colony stimulating factor (GM-CSF) (Smith *et al.*, 1996; Zhang *et al.*, 1997; Barreda, Hanington and Belosevic, 2004).

The transcription factors SCL and RUNX1 are essential for priming mesodermal stem cells to fulfil a hematopoietic destiny (Rosenbauer and Tenen, 2007; Hoang, Lambert and Martin, 2016). Both SCL^{-/-} and RUNX1^{-/-} mice have proven to be non-viable and show no hematopoietic development (Shivdasani, Mayer and Orkin, 1995; Okuda *et al.*, 1996). In adult hematopoiesis, both transcription factors are not important for maintenance of HSC, but influence the differentiation (Rosenbauer and Tenen, 2007). RUNX1 deficiency inhibits lymphoid differentiation and megakaryocytic development (Ichikawa *et al.*, 2004) while SCL blocks megakaryocytic and erythrocytic maturation (Mikkola *et al.*, 2003).

PU.1 is expressed to various degrees at different stages of hematopoiesis, being highly expressed in HSC, CMP, CLP, GMP, granulocytes, monocytes and modestly in B-cells while being suppressed during erythrocytic and T-cell development (Back *et al.*, 2005; Nutt *et al.*, 2005). PU.1 deletion in adult

hematopoiesis impairs the development from MPPs to CLP and CMP; though stimulating a disruptive granulopoiesis with accumulation of promyelocytes and myelocytes in bone marrow and spleen of PU.1^{-/-} mice (Dakic *et al.*, 2005). Moreover, sensitivity for M-CSF, GM-CSF and IL-6 was found to be reduced in this model (Dakic *et al.*, 2005). It has been suggested that the level of PU.1 expression guides differentiation either towards macrophages (high expression) or B-lymphocytes (low expression) (DeKoter and Singh, 2000). Furthermore, CMPs with high PU.1 expression seem to be primed for granulocytic/monocytic development while those eluding PU.1 develop towards erythrocytes (Back *et al.*, 2005; Nutt *et al.*, 2005). One can conclude that PU.1 is important for the MPP to CMP/CLP development and steers differentiation towards monocyte granulocyte development.

Another group of important transcription factors activating myelopoiesis are CCAAT/enhancer-binding proteins (C/EBP α , C/EBP β , C/EBP ϵ).

C/EBP α is a transcription factor that is associated with HSCs and myeloid lineage differentiation, being highly expressed in granulocytes and to a lower degree in monocytes (Radomska *et al.*, 1998; Akashi *et al.*, 2000). Similar to the importance of PU.1 for the CMP production, C/EBP α is necessary for the differentiation of CMPs towards GMPs (Zhang *et al.*, 2004).

It is well established that the C/EBP α to PU.1 ratio governs the progenitor cell fate in monocyte or neutrophil direction (Reddy *et al.*, 2002; Dahl *et al.*, 2003). PU.1 upregulation is a signal for monocytic differentiation while C/EBP α guides CMPs towards neutrophil development (Dahl *et al.*, 2003; Ross *et al.*, 2004; Laslo *et al.*, 2006).

Moreover, the granulocyte colony stimulating factor receptor (G-CSFR) was shown to be absent in C/EBP α -deficient mice and they subsequently did not develop mature neutrophils and eosinophils (Zhang *et al.*, 1997).

In recent years, our group has found **LEF-1** transcription factor to play an essential role in the activation of C/EBP α (Skokowa *et al.*, 2006). Additionally, LEF-1 has been shown to interact with and inhibit PU.1 (Rosenbauer *et al.*, 2006). LEF-1 has since been identified to be ubiquitinated and downregulated due to hyperactivity of STAT5 (activated signal transducer and activator of

transcription 5), a process that could be reversed *in vitro* by the proteasome inhibitor Bortezomib (Dong *et al.*, 1998; Gupta *et al.*, 2014).

IRF8 is another transcription factor influencing the cell fate of the bipotential GMP. IRF8 deficiency has shown to shift differentiation towards granulopoiesis, while reintroduction of the gene improved monocytic differentiation in a mouse based model (Scheller *et al.*, 1999; Tamura *et al.*, 2000). IRF8 effects on monocytic/granulocytic differentiation were recently reproduced using induced pluripotent stem cell (iPSC) technology (Sontag *et al.*, 2017).

1.1.2 Steady state and emergency granulopoiesis

Having a short half-life (hours to days), neutrophils need constant replacement in steady state conditions (Tak *et al.*, 2013). That being said, approximately $0.5-1 \times 10^{11}$ granulocytes are produced every day in adults (Dancey *et al.*, 1976). For local infections, this continuously generated neutrophil pool can be utilized and has an adequate strength in fighting the infection (Manz and Boettcher, 2014). As soon as foreign pathogens are perceived, granulocytes are being recruited and by matter of chemotaxis led to the infected tissue (Borregaard, 2010). There, neutrophils start eliminating foreign pathogens via phagocytosis, bactericidal granule proteins and neutrophil extracellular traps (NETs) (Kolaczkowska and Kubes, 2013). Apoptotic neutrophils themselves are being phagocytosed by macrophages, which in turn reduce neutrophil production via downregulation of the IL23-IL17A-G-CSF axis (Schwarzenberger *et al.*, 2000; Borregaard, 2010).

Steady state granulopoiesis is dependent on the granulocyte colony stimulating factor (G-CSF)- and its C/EBP α - downstream signaling pathway (Manz and Boettcher, 2014). G-CSF not only supports neutrophil production, it has been found to regulate neutrophil release from bone marrow (Semerad *et al.*, 2002). C/EBP α on the other hand primes neutrophil differentiation (1.1.1) and acts additionally as the responsible transcription factor for the CSF3R transcription leading to G-CSFR expression (Manz and Boettcher, 2014).

The number of neutrophils can increase dramatically during “emergency” situations, such as severe bacterial infections or blood loss. Neutrophil

generation rises, cellular turnover accelerates and high numbers of mature and immature neutrophils are released into the peripheral blood (left shift) (Manz and Boettcher, 2014). In contrast to steady state granulopoiesis, “emergency” granulopoiesis is reliant on C/EBP β activation (Hirai *et al.*, 2006). Upon G-CSF stimulation nicotinamide phosphoribosyltransferase (NAMPT) is upregulated, leading through a series of enzymatic reactions to an increase in nicotinamide adenine dinucleotide (NAD⁺) levels and sirtuin 1 (SIRT1) activation (Skokowa *et al.*, 2009). Ultimately, C/EBP α and C/EBP β are upregulated and G-CSF synthesis as well as G-CSFR expression are elevated, closing the autoregulatory feedback loop (Skokowa and Welte, 2009).

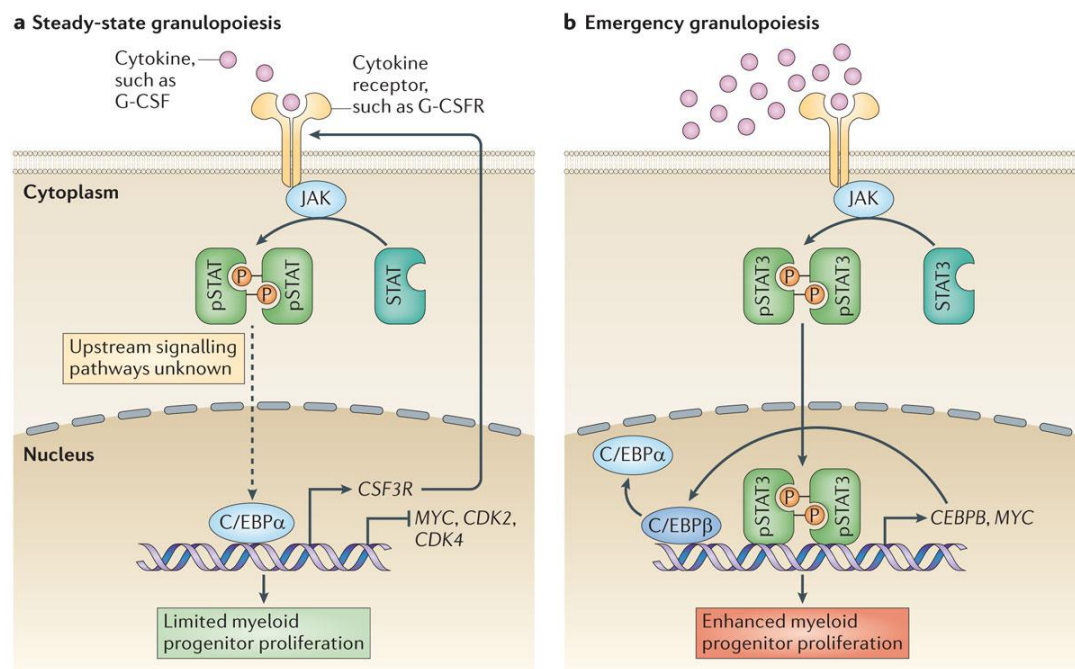


Figure 2. Steady state and emergency granulopoiesis

Regulation of steady state and emergency granulopoiesis. CSF3R (G-CSF receptor) expression is regulated in steady state by the transcription factor C/EBP α in response to upstream signals (STAT, JAK, cytokine-receptor interaction). The emergency granulopoiesis in contrast is dependent on C/EBP β (Manz and Boettcher, 2014).

1.2 Severe congenital neutropenia (CN)

Severe congenital neutropenia (CN) is a heterogenous group of disorders of the myeloid differentiation, defined by a maturation arrest at the promyelocyte/myelocyte stage and an absolute neutrophil count (ANC) of <

$0,5 \times 10^9/L$. Due to the lack of functional mature neutrophils, patients are susceptible for severe bacterial infections starting in their neonatal period. Frequent are e.g. infections of the skin, oral cavity, ears, and respiratory tract (Spoor, Farajifard and Rezaei, 2019). The differential blood count is characterized by severe neutropenia ($< 0,5 \times 10^9 /L$) and an association to monocytosis, eosinophilia and hyper-gammaglobulinaemia (Donadieu *et al.*, 2017). The diagnosis, however, is often delayed as a full differential blood count as well as multiple ANCs over the course of several weeks to verify the persistency of the neutropenia, is seldomly performed early on (Skokowa *et al.*, 2018). Furthermore, with a prevalence of 10:1.000.000 inhabitants, CN is considered an orphan disease (Donadieu *et al.*, 2013).

Neutropenia in neonates may have a variety of explanations: from simple viral infections (e.g.), iatrogenesis, allo- and autoimmune origin, bone marrow deficiency (Fanconi anemia, GATA2 deficiency), multiple syndromes (e.g. Shwachmann-Diamond syndrome, WHIM syndrome, Glycogen storage disease Ib, Barth syndrome), to isolated neutropenia (severe congenital neutropenia, cyclic neutropenia) (Spoor, Farajifard and Rezaei, 2019).

To observe patient care and register disease outcome, neutropenia patients are registered in the severe chronic neutropenia international registry (SCNIR) that was established in 1994 (Dale *et al.*, 2003).

1.2.1 History

Historically, this phenotype was introduced by Dr. Kostmann in 1956, as he was studying hematopoietic defects in a consanguineous family in the remote area of Norrbotten, Sweden (Kostmann, 1956). Dr. Kostmann observed that newborn patients were struggling with frequent bacterial infections of skin, gingiva, ear, lung and urinary tract due to persistent granulocytopenia or agranulocytosis. Despite antibiotic therapy, all patients passed away during the first months of their life as a result of e.g. septicemia, peritonitis or severe enteritis (Kostmann, 1975). Due to the pattern observable in the initial family, he suspected an autosomal recessive inheritance (Kostmann, 1956). Furthermore, he speculated

that the defect in the granulocytic maturation was based in a deficiency of a serum factor (Kostmann, 1975).

1.2.2 Genetic background and pathogenesis

Nowadays, we know that the Kostmann syndrome is only one subtype of congenital neutropenia (CN) and that, depending on the subtype, there are autosomal recessive and dominant, as well as X-linked and mitochondrial patterns of inheritance at work (Skokowa *et al.*, 2018). CN, while still not completely understood in its pathogenesis, can be caused by numerous mutations in different genes. Up to date, there are more than 30 genes that are known to be responsible for CN, many of which leading to neutropenia in combination with pancreatic insufficiency, bone marrow insufficiency or metabolic diseases (Skokowa, Zeidler and Welte, 2018; Spoor, Farajifard and Rezaei, 2019). However, with ongoing research, we can expect the number of involved CN-causing genes to continue to grow. For some genes, numerous mutation sites have been discovered (Xia and Link, 2008). Moreover, some patients with mutations in more than one CN specific gene have been reported (Germeshausen *et al.*, 2010), while in other patients no known CN-specific gene mutations were detected.

The autosomal recessive CN, specifically the Kostmann syndrome, is most commonly caused by **HAX1** mutations (Klein *et al.*, 2007). *HAX1* encodes for the HCLS1-associated protein X-1 (*HAX-1*) which in turn binds to the HCLS1 protein (hematopoietic lineage cell-specific protein) (Suzuki *et al.*, 1997; Klein *et al.*, 2007). The latter is an important player in the G-CSF receptor signaling cascade (Skokowa *et al.*, 2012). Homozygous *HAX1* mutations occur most often in consanguineous pedigrees like the original family Dr. Kostmann described in 1956 in northern Sweden or in remote areas of Anatolia (Klein *et al.*, 2007). Other genes responsible for autosomal recessive CN, include e.g. *G6PC3*, *GFI1* and *STK4* (Horwitz *et al.*, 2013).

The majority of CN cases belong to the autosomal dominant subtype of inheritance and are associated with mutations in the **ELANE** gene (formerly known as ELA2) (Dale *et al.*, 2000). Interestingly, mutations in *ELANE* can lead to two different phenotypes: the typical congenital neutropenia with a permanent ANC < 0,5x10⁹/L and cyclic neutropenia (CyN). The latter is a milder version of neutropenia with a 21-day-periodic oscillation of the ANC (Horwitz *et al.*, 2007). The pathomechanism of this genotype-phenotype correlation is yet to be entirely understood.

ELANE encodes for the neutrophil elastase (NE). In CN patients, accumulation of a misfolded NE, stress of the endoplasmic reticulum (ER) and stimulation of the unfolded protein response (UPR) are central aspects of the pathomechanism (Köllner *et al.*, 2006; Xia and Link, 2008).

Interestingly, LEF-1 and C/EBP α downregulation in granulocytic progenitor cells was found as a characteristic of severe congenital neutropenia (HAX-1 and *ELANE* mutated forms), but not in cyclic or idiopathic neutropenia (Skokowa *et al.*, 2006). Furthermore, PU.1 expression in bone marrow cells of CN patients was found to be slightly upregulated in CN patients myeloid progenitors compared to healthy donor cells (Skokowa *et al.*, 2006).

1.2.3 Prognosis and treatment

Congenital neutropenia was for the longest time a devastating diagnosis for child and family. Up to the 1980's, even with full antibiotic treatment, mortality exceeded 80% (Kostmann, 1956; Gilman, Jackson and Guild, 1970). About half of the patients died during their first year of life, and in the following years up to the age of 4, mortality was estimated to be about 6-7% per year (Alter BP, 2003).

The introduction of G-CSF in 1985 (Welte *et al.*, 1985) can be considered a milestone in CN therapy. Just 4 years later, the first successful treatment of 5 congenital neutropenia patients with the new agent was published, showing an increase of the ANC from below 100 to 1300-9500 cells/ μ l and maturation of myeloid cells in bone marrow samples (Bonilla *et al.*, 1989). Even more

importantly, chronic infections improved and the number of infections and the necessity for intravenous antibiotics decreased with these patients (Bonilla *et al.*, 1989; Dale *et al.*, 1993).

Life expectancy under daily subcutaneous G-CSF injections improved dramatically. After 10 years of observation of 374 G-CSF treated CN patients, the cumulative incidence of death due to sepsis was calculated to have decreased to 8% (Rosenberg *et al.*, 2006).

Side effects of the granulocyte colony stimulating factor, as noticed in the phase III trial, included splenomegaly, bone pains, headaches and rashes (Dale *et al.*, 1993). Over time, an increase in malignant progression, acute myeloid leukemia (AML) and myelodysplastic syndrome (MDS) had to be added to the list. This will be discussed further in section 1.2.4.

Though a sufficient level of neutrophils can be reached by this treatment, patients continue to suffer from infections and periodontal disease. A deficiency of neutrophil's antibacterial peptide LL-37 as well as reduced chemotaxis might be an explanation (Elsner *et al.*, 1992; Pütsep *et al.*, 2002; Karlsson *et al.*, 2007).

Unfortunately, about 10% of CN patients are considered unresponsive to normal dosages of G-CSF ($>50\mu\text{g}/\text{kg}/\text{d}$ and an ANC $< 0.5 \times 10^9/\text{L}$) (Bonilla *et al.*, 1994; Skokowa *et al.*, 2018).

The only definitive cure for this bone marrow failure syndrome is allogeneic Hematopoietic Stem Cell Transplantation (HSCT). Due to the obvious life threatening risks, HSCT is restricted to patients who failed other therapeutic options (G-CSF non responder or poor infection control) or clonal transformation indicates a shift to malignancy (Fioredda *et al.*, 2015). In one of the largest multicenter retrospective studies, 136 SCN-post-HSCT patients from Europe and middle east were analyzed between 1990 and 2012, showing the best outcome for patients below the age of 10 and with an HLA-matched related or unrelated donor (Fioredda *et al.*, 2015). A three year overall survival rate of 82%, transplant related mortality of 17% as well as risks for graft failure and graft-versus-host reaction in 1/5 of patients emphasize the severity of the procedure (Fioredda *et al.*, 2015).

To reduce risks of malignant transformation and finding new acceptable therapeutic alternatives and combinational therapies, research is ongoing. A promising approach for *ELANE*-mutated show recent studies that are investigating the possibility of treatment with NE-Inhibitors. So far, *in vitro* studies have found that treatment of CN hematopoietic and myeloid progenitors with NE inhibitors resulted in the C/EBP α upregulation, UPR stress relief and BCL2 downregulation, all of which are essential aspects in the NE controlled maturation pathway (Nayak *et al.*, 2015). Furthermore, some NE-Inhibitors have shown promising effects on cell survival and myeloid differentiation of CN patients cells *in vitro* (Makaryan *et al.*, 2017).

1.2.4 Leukemic progression in CN

Severe congenital neutropenia is known to be a preleukemic syndrome. Since the late 1960's, there have been sporadic reports of leukemia in congenital neutropenia patients (Miller, 1969; Gilman, Jackson and Guild, 1970). Interest spread, when 1995, after the first few years of G-CSF treatment along with a rise in survival, the incidence of acute myeloid leukemia (AML) and myelodysplastic syndrome (MDS) increased (Dong *et al.*, 1995; Imashuku *et al.*, 1995; Kalra *et al.*, 1995; Weinblatt *et al.*, 1995). In 2010, a prospective study following the progress of 374 CN patients concluded that after 15 years of G-CSF treatment the cumulative incidence for AML/MDS was 22%, while the cumulative incidence for lethal sepsis in 10 years decreased to 10% (Rosenberg *et al.*, 2010). Patients who showed a poor response to G-CSF treatment, requiring more than 8 μ g/kg/d, were identified as having a poor prognosis with high numbers of AML/MDS progression (40%) or death due to sepsis (14%) after 10 years of treatment (Rosenberg *et al.*, 2006).

The reason for the leukemogenic transformation was found in the acquisition of additional somatic mutations. Today we know that most common for CN-AML/MDS patients are mutations of the G-CSF receptor (CSF3R) (88%), RUNX1 (76%) or chromosomal abnormalities as monosomy 7 or trisomy 21 (Skokowa *et al.*, 2014). RUNX1 mutations, while characteristic for CN-AML/MDS, are rare (2,9%) in cases of de-novo AML/MDS (Skokowa *et al.*,

2014). Interestingly, truncating mutations of the G-CSF receptor can appear years before the progress to overt leukemia and even disappear under detection limit spontaneously in some patients (Bernard *et al.*, 1998). The mechanism of leukemic transformation is subject of ongoing investigations. Common hypothesis is that G-CSF stimulates *CSF3R* mutated hematopoietic stem cell (HSC) clones, leading to an increase in proliferation and clonal advantage, while additional mutations such as *RUNX1* may lead to overt leukemia (Skokowa *et al.*, 2014).

1.3 *FLT3*

FMS-like tyrosine kinase 3 (*FLT3*) gene is located on chromosome 13q12 and encodes a receptor tyrosine kinase (RTK) which holds important functions in hematopoiesis (Rosnet *et al.*, 1993; Stirewalt and Radich, 2003). The membrane-bound receptor contains five immunoglobulin-like extracellular domains, a transmembrane domain, a juxtamembrane domain and two linked intracellular tyrosine kinase domains (Stirewalt and Radich, 2003). As such, it resembles other class III receptor tyrosine kinases like the macrophage colony-stimulating factor (M-CSF) receptor (FMS) and SCF receptor KIT (steel factor receptor) in structure, exon/intron organization and even sequence (Agnès *et al.*, 1994). Like M-CSFR and SCF receptor, *FLT3* is vastly involved in hematopoietic differentiation. *FLT3*, also known as *FLK-2*, has been identified as a marker for the loss of self-renewal in HSC, being expressed in ST-HSC and increasingly so in MPPs (Adolfsson *et al.*, 2001; Christensen and Weissman, 2002). *In vitro* studies have found that *FLT3* ligand (*FLT3L*) stimulates cell growth of uncommitted CD34⁺ progenitors and development of early B-cell progenitors (Ray *et al.*, 1996; Rusten *et al.*, 1996). This effect is inducible by combination with other growth factors for example interleukine-3 (IL-3), G-CSF, M-CSF, GM-CSF, erythropoietin (EPO), and SCF (Gabbianelli *et al.*, 1995; Rusten *et al.*, 1996). Interestingly, isolated *FLT3L* stimulation triggers predominantly monocytic differentiation (Gabbianelli *et al.*, 1995). However, studies with *FLT3* knockout mice showed little changes in adult hematopoiesis (Mackarehtschian *et al.*, 1995).

FLT3 mutations have been identified in about 1/3 of patients with acute myeloid leukemia (AML) (Kayser *et al.*, 2009; Papaemmanuil *et al.*, 2016). Most frequent are internal tandem duplications (ITD) (approx. 30% of AML patients) in the juxtamembrane domain and missense mutation of the intracellular tyrosine kinase domains (TKD) (up to 13% of patients in certain AML-subgroups) (Bacher *et al.*, 2008; Papaemmanuil *et al.*, 2016). Both types of mutations effect intracellular domains of the receptor and allow ligand independent activation, STAT-5 and MAP-Kinase pathway stimulation leading to unrestricted cell proliferation (Hayakawa *et al.*, 2000; Kiyoi *et al.*, 2002; Spiekermann *et al.*, 2002). Investigations on *FLT3*-tyrosine kinase inhibitors as targeted therapeutic drug in AML are ongoing (Patnaik, 2018).

Contrary to *FLT3*-ITD/TKD mutations, *FLT3*-V194M (rs146030737) is a mutation which is relatively unknown. It is located in exon 5 which translates to the extracellular part of the receptor. This missense mutation has been identified as possibly damaging by PolyPhen-2 (<http://genetics.bwh.harvard.edu/pph2/>) (Adzhubei *et al.*, 2010). However, using SIFT and PMUT web tools, Fröhling *et al.* have predicted no pathological consequence for this mutation (Fröhling *et al.*, 2007). Nevertheless, in 2017 it was found that this particular mutation can be associated with a monocytic phenotype (Mousas *et al.*, 2017).

1.4 *FLT1*

The vascular endothelial growth factor receptor 1 (*VEGFR1/FLT1*) is a receptor tyrosine kinase with seven extracellular immunoglobulin like domains. It exists in a membrane bound as well as in a shortened, soluble form (Shibuya, 2001). *FLT1* is known to modulate embryonic angiogenesis and endothelial cell migration (Ji *et al.*, 2018). *FLT1* mRNA is upregulated in activated monocytes and the binding of VEGF to *FLT1* promotes monocyte migration (Shibuya, 2001). Furthermore, *FLT1* expression was found to be stimulated by Wnt ligand in retinal myeloid cells, leading ultimately to a suppression of angiogenesis (Stefater *et al.*, 2011).

The heterozygote missense mutation *FLT1* - P1201L (rs140861115) has been named by PolyPhen-2 (<http://genetics.bwh.harvard.edu/pph2/>) (Adzhubei *et al.*, 2010) as possibly damaging.

1.5 Induced pluripotent stem cells (iPSCs)

In 2006, the world was first introduced to induced pluripotent stem cells (iPSC) (Takahashi and Yamanaka, 2006). Dr. Takahashi and Dr. Yamanaka had found a way to reprogram somatic cells by transiently reintroducing four transcription factors (Oct4 + Sox2 + Klf4 + c-Myc = OSKM) that were known to be essential for embryonic stem cell maintenance (Avilion *et al.*, 2003; Cartwright, 2005; Li *et al.*, 2005).

As a result, they discovered that the new cells had the ability to differentiate into all three germ layers and were suitable for long-term cell culture (Takahashi and Yamanaka, 2006). As such, iPSCs resemble embryonic stem cells (ES), though eluding the ethical dilemma of destroying human embryonic blastocysts (Diecke *et al.*, 2014).

Different cell reprogramming techniques have been established since: genome integrative systems (Retroviral and Lentiviral) and non-integrative systems (episomal vectors, Sendai RNA-viral, Protein- and mRNA-systems) (Yamanaka, 2012; Diecke *et al.*, 2014).

OSKM-transcription factors have been studied for their importance in the reprogramming process. C-Myc was found to facilitate the step of attaching OSK to the enhancer regions of reprogramming genes (Soufi, Donahue and Zaret, 2012). OCT4, SOX2, and KLF4 are part of a balanced system, each participant leading in a different direction (mesodermal, ectodermal and epidermal), thus concluding in a compromising pluripotency (Shu *et al.*, 2013; Kim *et al.*, 2015). Other combinations of transcription factors, e.g. GATA6+GMNN, have been successfully used for reprogramming as well (Shu *et al.*, 2013).

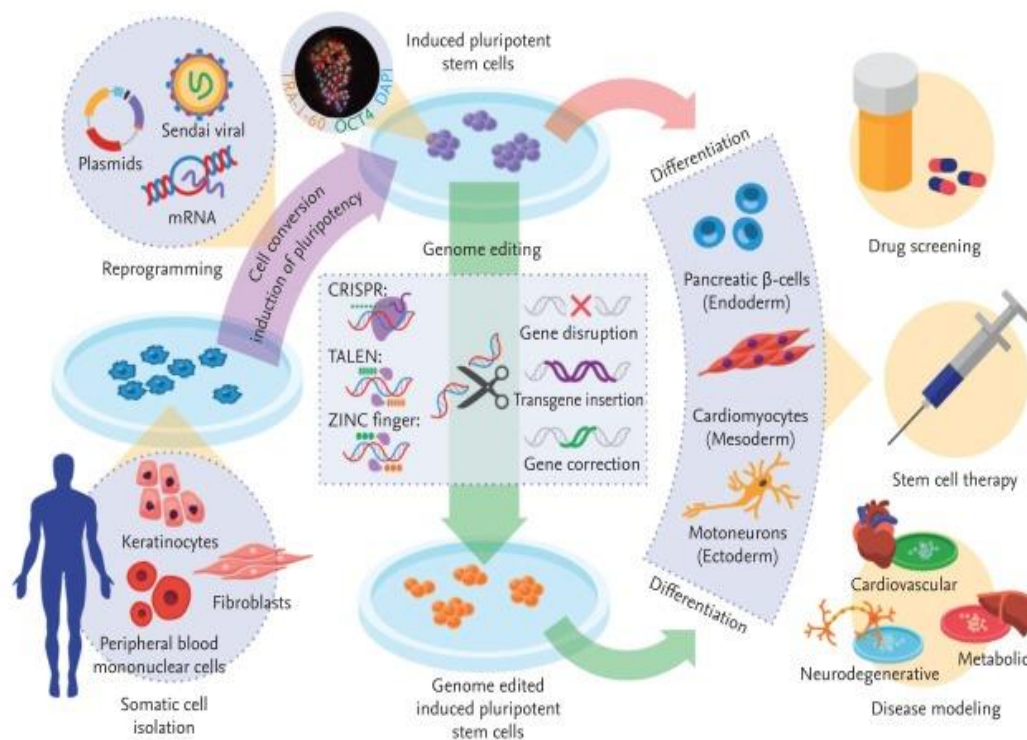


Figure 3. From somatic cell to induced pluripotent stem cells and beyond: iPSC development, technics and opportunities

Starting in the lower left corner of the image, somatic cells are isolated, reprogrammed using different techniques and can either be gene edited by CRISPR-Cas9 or directly differentiated into all three germ layers. Among the potential usages are disease modeling (+/- CRISPR-Cas9 corrected iPSC lines), research for drug effects and stem cells for further therapeutic use (Diecke *et al.*, 2014).

iPSCs differentiation starts with the formation of embryoid bodies (EB), which are spherical structures of iPSC that start to organize themselves and differentiate to cells of the three germ layers, mimicking early embryonic development (Brickman and Serup, 2017). The density of the cell aggregates and stimulation with certain cytokines guides differentiation towards an endodermal, mesodermal or ectodermal cell fate (Rothová *et al.*, 2016; Brickman and Serup, 2017).

Especially in studying hematopoietic diseases and impaired differentiation, iPSCs have proven to be of great value. In recent studies it was shown that bone marrow myeloid progenitors/precursors and their iPSC developed

equivalents have analogous levels of expression for genes concerning the innate immune system and granulocytic functions (Nayak *et al.*, 2015).

Moreover, Nayak *et al.* have shown that iPSCs of *ELANE*-mutated SCN patients accurately mirror the maturation arrest at the promyelocytic/myelocytic (CD45+CD34-CD33+CD11b-CD15+/low) stage as well as the characteristic neutropenia (Nayak *et al.*, 2015).

Promising results have been accomplished using gene correction of iPSCs featuring a *HAX1* or dystrophin gene mutation with CRISPR-Cas9 (Li *et al.*, 2016; Pittermann *et al.*, 2017).

1.6 Aim

Aim of this study is to understand the role of V194M-*FLT3* mutation in myelomonocyte differentiation. For this, a new iPS cell line from a CN patient with this specific mutation and an unusually strong shift from neutrophil development towards monocytosis will be developed.

By comparing patient vs. healthy donor iPSC development and early hematopoietic differentiation, we are hoping to gain new insights in myeloid differentiation and specifically lineage determination of granulocyte-macrophage progenitors.

Early embryoid body formation and *FLT1/FLT3* expression throughout the first days of differentiation will be analyzed.

Moreover, we aim to establish an *FLT3*-wild type and *FLT3*-V194M-mutated expression vector to evaluate the role of this particular mutation on mRNA, protein expression levels as well as on hematopoietic differentiation. The potential effect of Bortezomib on the expression level of mutated *FLT3* will be investigated.

2 Material and Methods

2.1 Material

2.1.1 Cell culture standard medium and buffer

iPSCs-Medium	<u>volume</u>	<u>company</u>
Dulbecco's Modified Eagle Medium Nutrient Mixture F-12 HAM (D-MEM F12)	384 ml	Sigma-Aldrich (St. Louis, USA)
KSR (Knockout Serum Replacement)	100ml	Thermo Fisher scientific (Waltham, USA)
L-Glutamin (200mM)	5ml	Biochrom (Berlin, Germany)
2-Mercapto Ethanol (50mM)	1ml	Thermo Fisher scientific (Waltham, USA)
Penicillin/Streptomycin (1000U/ml)	5ml	Biochrom (Berlin, Germany)
NEAA (Non-Essential Amino Acid 100x)	5ml	Thermo Fisher scientific (Waltham, USA)

SNL-Medium= DMEM Full	<u>volume</u>	<u>company</u>
Dulbecco's Modified Eagle Medium (DMEM)	500ml	Thermo Fisher scientific (Waltham, USA)
FCS-inactivated	50ml	Sigma-Aldrich (St. Louis, USA)
Penicillin/Streptomycin (1000U/ml)	5ml	Biochrom (Berlin, Germany)

Expansion-Medium	<u>concentration</u>	<u>company</u>
Stemline II Hematopoietic Stem Cell Expansion Medium		Sigma-Aldrich (St. Louis, USA)
FCS- inactivated	10%	Sigma-Aldrich (St. Louis, USA)
Penicillin/Streptomycin (10.000U/ml / 10.000µg/ml)	1%	Biochrom (Berlin, Germany)
L-Glutamine (200mM)	1%	Biochrom (Berlin, Germany)
Recombinant human IL-3	20ng/ml	R&D Systems (Minneapolis, USA)
Recombinant human IL-6	20ng/ml	R&D Systems (Minneapolis, USA)
Recombinant human TPO	20ng/ml	R&D Systems (Minneapolis, USA)
Recombinant Human SCF/C-Kit Ligand	50ng/ml	R&D Systems (Minneapolis, USA)

Recombinant human <i>FLT3L</i>	50ng/ml	R&D Systems (Minneapolis, USA)
-----------------------------------	---------	--------------------------------

FACS Buffer – 3% PBS/BSA	<u>volume/mass</u>	<u>company</u>
PBS	500ml	Lonza (Basel, Switzerland)
Bovine Serum Albumin (BSA)	15mg	Sigma-Aldrich (St. Louis, USA)

Transfer Medium (TFM)	<u>volume</u>	<u>company</u>
Dulbecco's Modified Eagle Medium (DMEM)	500ml	Thermo Fisher scientific (Waltham, USA)
FCS-inactivated	50ml	Sigma-Aldrich (St. Louis, USA)
Penicillin/Streptomycin (1000U/ml)	5ml	Biochrom (Berlin, Germany)
HEPES Buffer Solution 1M	1ml	Thermo Fisher scientific (Waltham, USA)

NTM-Buffer	<u>concentration</u>	<u>company</u>
ddH2O		
Tris	0,1M	Carl Roth (Karlsruhe, Germany)
NaCl	0,1M	Carl Roth (Karlsruhe, Germany)
MgCl	0,05M	Promega (Madison, USA)

Laemmli-Buffer 3x	<u>volume</u>	<u>company</u>
0.5M Tris-HCl	2.5ml	Carl Roth (Karlsruhe, Germany)
Glycerol	2ml	
10% SDS	4ml	Carl Roth (Karlsruhe, Germany)
0,1% Bromophenol Blue	0.5ml	
ddH2O	1ml	

2.1.2 Cell lines

	<u>provided by</u>
Mitomycin treated (MMC)-SNL-Feeder cells	Culture collections - Public Health England (Salisbury, UK)
CD34IPSC16 (healthy donor)	(Lachmann <i>et al.</i> , 2014)
HD34E1	Azadeh Zahabi (Skokowa Lab, Tübingen)
OKPBL2 /6	Houra Loghmani and Dorothea Stalman (Skokowa Lab, Tübingen)

Human embryonal kidney (HEK)293FT- cells	Skokowa Lab, Tübingen
--	-----------------------

2.1.3 Antibodies

Antibody	Cat.Nr. / Lot Nr. (company)
FITC Mouse Anti-Human CD16	555406/ 74339 - BD Biosciences (Franklin Lakes, USA)
PE Mouse Anti-Human CD15	555402/5098658 - BD Biosciences (Franklin Lakes, USA)
7AAD (51-68981E)	559925/4177939 - BD Biosciences (Franklin Lakes, USA)
PE/Cy7 Anti-Human CD11b	301322/B193552 - BioLegend (San Diego, USA)
APC Anti-Human CD135	313308/B192464 - BioLegend (San Diego, USA)
APC-H7 Mouse Anti-Human CD14	560180/5167936 - BD Biosciences (Franklin Lakes, USA)
Brilliant Violet 510 Anti-Human CD45	304036/ B204188 - BioLegend (San Diego, USA)
Anti-hVEGFR1/ <i>FLT1</i> phycoerythrin conjugated Mouse IgG1	FAB321P/LFR1212121 - R&D Systems (Minneapolis, USA)
PE-conjugated Mouse IgG1 Isotype control	556029/0000064454 - BD Biosciences (Franklin Lakes, USA)
APC Mouse IgG1k Isotype control	555751/ 3312634 - BD Biosciences (Franklin Lakes, USA)
Anti-human Tra-1-60 PE	12-8863-80/E02186-1633 – eBioscience (San Diego, USA)
Anti-hTra-1-85 Fluorescein conjugated mouse IgG1	FAB31695F/LUX0411081 - R&D Systems (Minneapolis, USA)
Anti-h/mSSEA-4 Phycoerythrin conjugated mouse IgG3	FAB1435P/LNK1110091 - R&D Systems (Minneapolis, USA)
IgG Isotype control Phycoerythrin conjugated mouse IgG3	IC007P/AAIY0209011 - R&D Systems (Minneapolis, USA)
Mouse IgG1 Isotype control Fluorescein conjugated	IC002F/LGY0812101 - R&D Systems (Minneapolis, USA)
Anti-hSOX17-hSOX17 affinity purified Goat IgG	AF1924/ KGA0815042 - R&D Systems (Minneapolis, USA)
Monoclonal Anti- β -Tubulin III antibody (mouse)	T8660/103M4830 - Sigma-Aldrich (St. Louis, USA)
Anti-goat IgG (FITC conjugated)	F7367/113M4807V - Sigma-Aldrich (St. Louis, USA)
Goat anti-mouse (FITC conjugated)	AP308F/2430517 - Merck Millipore (Burlington, USA)

2.1.4 Cytokines and organic compounds

	<u>company</u>
Recombinant human IL-3	R&D Systems (Minneapolis, USA)
Recombinant human IL-6	R&D Systems (Minneapolis, USA)
Recombinant human TPO	R&D Systems (Minneapolis, USA)
Recombinant human SCF/C-Kit Ligand	R&D Systems (Minneapolis, USA)
Recombinant human <i>FLT3L</i>	R&D Systems (Minneapolis, USA)
Recombinant human FGF basic	Peptrotech (Rocky Hill, USA)
Recombinant human BMP-4	R&D Systems (Minneapolis, USA)
Recombinant human VEGF 165	R&D Systems (Minneapolis, USA)
Recombinant human G-CSF	Stemcell technologies (Vancouver, Canada)
L-Ascorbic Acid	Sigma-Aldrich (St. Louis, USA)
Valproic Acid Sodium salt	Sigma-Aldrich (St. Louis, USA)

2.1.5 Cell culture chemicals

Dulbecco's Modified Eagle Medium Nutrient Mixture F-12 HAM (D-MEM F12)	Sigma-Aldrich (St. Louis, USA)
Chloroquin 25mM	Sigma-Aldrich (St. Louis, USA)
Poly-L-Lysin 0,01% Solution	Sigma-Aldrich (St. Louis, USA)
2xHBS (HEPES buffered saline)	Sigma-Aldrich (St. Louis, USA)
Propidiumiodid (PI)	Thermo Fisher scientific (Waltham, USA)
DAPI (1mg/ml)	Thermo Fisher scientific (Waltham, USA)
Lenti-x-concentrator	Clontech-Takara Bio (Mountain View, USA)
Gelatin (sterile)	Sigma-Aldrich (St. Louis, USA)
Rock Inhibitor	Wako Pure Chemicals Industries (Osaka, Japan)
Accutase	Thermo Fisher scientific (Waltham, USA)
STEMdiff APEL Medium	Stemcell technologies (Vancouver, Canada)
Corning Matrigel Growth Factor Reduced (GFR) Basement Membrane Matrix	Corning (Corning, USA)
Paraformaldehyde (PFA)	Sigma-Aldrich (St. Louis, USA)
Sucrose	Serva (Heidelberg, Germany)
RPMI Medium 1640(1x) + GlutaMAX-I	Thermo Fisher scientific (Waltham, USA)
Polybrene 10mg/ml	Merck Millipore (Burlington, USA)
BCIP (5-Bromo-4-chloro-3-indolyl	Sigma-Aldrich (St. Louis, USA)

phosphate p-toluidine salt)	
NBT (Nitro Blue Tetrazolium Tablets)	Sigma-Aldrich (St. Louis, USA)
Lipofectamine 2000 (1mg/ml)	Thermo Fisher scientific (Waltham, USA)
Retronectin	Clontech-Takara Bio (Mountain View, USA)
Bovine serum Albumin (BSA)	Sigma-Aldrich (St. Louis, USA)
Trypan blue stain (0,4%)	Thermo Fisher scientific (Waltham, USA)
Trypsin-EDTA 0,05%	Thermo Fisher scientific (Waltham, USA)
Bortezomib	Sigma-Aldrich (St. Louis, USA)
CaCl ₂ Dihydrate (2,5M)	Sigma-Aldrich (St. Louis, USA)
Wright-Giemsa stain set	Sigma-Aldrich (St. Louis, USA)
HBSS (Hank's balanced salt solution)	Thermo Fisher scientific (Waltham, USA)
HEPES Buffer Solution 1M	Thermo Fisher scientific (Waltham, USA)
Stemline II hematopoietic stem cell expansion medium	Sigma-Aldrich (St. Louis, USA)
PBS	Lonza (Basel, Switzerland)
Anti-mouse IgK negative control compensation Particles Set	BD Biosciences (Franklin Lakes, USA)
Triton X-100	Sigma-Aldrich (St. Louis, USA)

2.1.6 Cell culture equipment

	<u>company</u>
Cell culture petri dish, Nunclon Deltasurface, 3,5cm	Thermo Fisher scientific (Waltham, USA)
Tissue culture dish, 6cm	Corning (Corning, USA)
Sterile Nunclon Delta Surface 6-well plate	Thermo Fisher scientific (Waltham, USA)
Falcon 12 Well Clear Flat Bottom TC-Treated Multiwell Cell Culture Plate	Corning (Corning, USA)
Multi-well 24 Well companion plate	Thermo Fisher scientific (Waltham, USA)
TC-Plate 96 well Suspens. K	Sarstedt (Nümbrecht, Germany)
TC Flask T75	Sarstedt (Nümbrecht, Germany)
Centrifuge 5810R	Eppendorf (Hamburg, Germany)
Centrifuge Heraeus Megafuge 1.0R	Thermo Fisher scientific (Waltham, USA)
Cytospin4 cytocentrifuge <ul style="list-style-type: none"> • Cytoclip • Cytofunnel • Shandon white filter cards 	Thermo Fisher scientific (Waltham, USA)

Menzel-glasses, ground edges, frosted end	Thermo Fisher scientific (Waltham, USA)
BBD 6220 CO2 Incubator	Thermo Fisher scientific (Waltham, USA)
HEMA-TEK slide stainer	Ames Miles Laboratories (Elkhart, USA)
Electric Pipetting aid - Pipetus	Hirschmann Laborgeräte GmbH (Eberstadt, Germany)
Serological pipette <ul style="list-style-type: none"> • 5ml • 10ml • 25ml 	Sarstedt (Nümbrecht, Germany)
Olympus CKX41 Microscope	Olympus Life Science (Tokyo, Japan)
Wilovert S Microscope	Helmut Hund GmbH (Wetzlar, Germany)
Counting chamber-M-NZ-Disposable Hemocytometer chips Neubauer Improved	NanoEnTek (Seoul, Korea)
HERA Safe HS12 Hood	Heraeus Instruments (Hanau, Germany)
FACs Tubes -Falcon 5ml polystyrene round –bottom tube with cell-strainer	Corning (Corning, USA)
Cell scrapper	Sarstedt (Nümbrecht, Germany)
FACS Canto II Cytometer	BD Biosciences (Franklin Lakes, USA)

2.1.7 Molecular biology standard medium and buffer

Wet transfer buffer (1x)	
Tris base (25mM)	3.03 g
Glycine (192mM)	14.41 g
Methanol	200 ml
ddH2O	Up to 1000 ml

Running buffer	
Tris (0.25M)	60.6 g
Glycerine	288.4 g
SDS (Natriumdodecylsulfat) 1%	20 g

ddH2O	Up to 2000 ml
-------	---------------

TBST buffer	
Tris base (25mM)	2.423 g
NaCl	8.006 g
Tween 20	1 ml
ddH2O	Up to 1000 ml

2.1.8 Primers

	sequence	Tm in °C
OK- <i>FLT3</i> -Mutation site		
<i>FLT3_V194M_F</i>	5'-TAC ATA CAG CTT GAT GTC AAC TAC-3'	56,55
<i>FLT3_V194M_R</i>	5'-CTG GTC TGC ATA TCT GAG AGC G- 3'	60,61
q- <i>FLT3</i> -for	5'-AAA TGG AAA ACC AGG ACG CC-3'	59,03
q- <i>FLT3</i> -rev	5'-TGG CAC AGC ACC TTA TGT CC-3'	60,32
<i>FLT3</i> -Sequencing primer		
Age1-KZ <i>FLT3</i> -for	5'-GCT TTT AAC CGG TGA GGC CAT GCC GGC GTT G-3'	74,63
Afe1- <i>FLT3</i> -rev	5'-GTC CAC GAG CGC TCT ACG AAT CTT CGA CCT-3'	70,76
<i>FLT3</i> str.t.ch.R478	5'-CCA GCT TGG GTT TCT GTC AT-3'	58,08
<i>FLT3</i> end.ch.F262 5	5'-CCC GTC TGC CTG TAA AAT GGA-3'	60,34
<i>FLT3</i> midCHECK.F	5'-CCC CTT CCC TTT CAT CCA AG-3'	57,85
<i>FLT3</i> midCHECK.	5'-TCT CTG TCC AAG TCC TGT GA-3'	57,62

R		
<i>FLT3</i> checkclon-F	5'-AGC ATC CCA GTC AAT CAG C-3'	57,51
<i>FLT3</i> checkclone-R	5'-CGG TCA CCT GTA CCA TCT GT-3'	59,10
Primer for Site directed Mutagenesis		
g22a_	5'-CAA AGC ACC CAT TCC ATG ATC GGC TCT GGA ACG-3'	71,96
	5'-CGT TCC AGA GCC GAT CAT GGA ATG GGT GCT TTG-3'	71,96
IPS- Characterization Primer		
PAX6-for	5'ACCCATTATCCAGATGTGTTTGCCCG AG-3'	66,86
PAX6-rev	5'ATGGTGAAGCTGGGCATAGGCGGCA G-3'	70,92
FOXA2-for	5'TGGGAGCGGTGAAGATGGAAGGGCA C-3'	70,37
FOXA2-rev	5'TCATGCCAGCGCCCACGTACGACGAC -3'	72,60
AFP-for	5'GAATGCTGCAAACCTGACCACGCTGGA AC-3'	68,75
AFP-rev	5'TGGCATTCAAGAGGGTTTTTCAGTCTG GA-3'	66,26
TUBB3-for	5' TAGACCCCAGCGGCAACTAT-3'	60,69
TUBB3-rev	5'- GTTCCAGGTTCCAAGTCCACC-3'	60,82
MYH6-for	5'-GCCCTTTGACATTGCACTG-3'	60,11
MYH6-rev	5'- GGTTTCAGCAATGACCTTGCC-3'	60,34
T-Brachyury-for	5'- CTGGGTACTCCCAATGGGG-3'	59,08
T-Brachyury-rev	5'- GGT TGG AGA ATT GTT CCG ATG A-	58,66

	3'	
DZ DNMT3B for	5'-ATA AGT CGA AGG TGC GTC GT-3'	59,48
DZ DNMT3B rev	5'-GGC AAC ATC TGA AGC CAT TT-3'	56,96
PRE-forward	5'- GAG TTG TGG CCC GTT GT -3'	62,68
PRE-reverse	5'-TGA CAG GTG GCA ATG CC-3'	63,33
hSox2 F	5'-TTC ACA TGT CCC AGC ACT ACC AGA-3'	63,62
hSox2 R	5'-TCA CAT GTG TGA GAG GGG CAG TGT GC-3'	68,80
LS-Nanog-	5'- RVG AAC ACA GTT CTG GTC TTC TG-3'	
LS-Nanog-	5'-WTC ACA CGG AGA CTG TCT CTC-3'	
cDNA synthesis	company (Cat. No.)	
Oligo (dt)18 primer	Thermo fisher scientific (SO131)	
Random hexamer primer	Thermo fisher scientific (SO142)	

2.1.9 Competent cells

	provided by
Stellar Competent cells	Clontech-Takara Bio (Mountain View, USA)
x-Gold	QuikChange II Site-directed Mutagenesis kit- Agilent Technologies (Santa Clara, USA)

2.1.10 Vector and virus

	description	provided by
Nr. 644	hRUNX1Kontrolle(Age/Afecut religated)pRRlppTcBx3SFhuman	Provided by Prof. Dr. med Axel Schambach

	Runx1.i2EBFP	(MH), Dirk Hoffmann
Nr. 717	<i>FLT3</i> wt in pRRL.PPT.CBX3SF h <i>FLT3</i> .i2.EBFP.puro.pre	Dr. Houra Loghmani + Dorothea Stalman (AG Skokowa, Tübingen)
Nr. 736	<i>FLT3</i> P12Amut in pRRL.PPT.CBX3SF h <i>FLT3</i> .i2.EBFP.puro.pre	Dr. Houra Loghmani + Tessa Skroblyn (AG Skokowa, Tübingen)
Nr. 636	Gag-pol for Lentivirus production	Addgene (Cambridge, USA)
Nr. 497	RSV for Lentivirus Production	Addgene (Cambridge, USA)
Nr. 582	VSV-G for Lentivirus Production	Addgene (Cambridge, USA)
<i>FLT3</i> -WT basis	pDONR223- <i>FLT3</i> Plasmid	Addgene (Cambridge, USA)
OSKM- Virus (second generation)	<ul style="list-style-type: none"> • OSKM plasmid • psPAX2 packaging vector (Addgene) • pMD2.G packaging vector (Addgene) 	Benjamin Dannenmann (AG Skokowa, Tübingen)

2.1.11 Antibodies western blot

	Cat.Nr. (company)
<i>FLT3</i> (8F2) Rabbit mAb	3462S - Cell signaling (Danvers, USA)
b-actin Rabbit mAb	4970S - Cell signaling (Danvers, USA)
Goat anti-rabbit IgG-HRP	F0515 (2004) Santa Cruz (Dallas, USA)

2.1.12 Molecular biology chemicals

5x Phusion HF Buffer	Thermo Fisher scientific (Waltham, USA)
PCR Nucleotide Mix - dNTP (10mM)	Roche Diagnostics (Rotkreuz, Switzerland)
DMSO (100%)	Thermo Fisher scientific (Waltham, USA)
MgCl ₂ (25mM)	Promega (Madison, USA)
Go Taq Hot start Polymerase (5u / μ L)	Promega (Madison, USA)
10x TBE buffer	Lonza (Basel, Switzerland)
Gel red	Biotium (Fremont, Canada)
DNA gel loading dye (6x)	New England Biolabs (Ipswich, USA)
Gel extraction kit 250	Qiagen (Venlo, Netherlands)
Qubit dsDNA HS Assay kit	Thermo Fisher scientific (Waltham, USA)
Quickload 1kb DNA ladder	New England Biolabs (Ipswich, USA)
AgeI-HF- Restriction enzyme	New England Biolabs (Ipswich, USA)
AfeI-Restriction enzyme	New England Biolabs (Ipswich, USA)
10x NEB Buffer = Cut smart Buffer	New England Biolabs (Ipswich, USA)
Calf intestinal alkaline Phosphatase 1u/ μ l (CIAP)	Thermo Fisher scientific (Waltham, USA)
PCR Purification kit	Qiagen (Venlo, Netherlands)
Quick Ligation kit	New England Biolabs (Ipswich, USA)
LB-Medium	Carl Roth (Karlsruhe, Germany)
Agar-Agar, Kobe I	Carl Roth (Karlsruhe, Germany)
Ampicillin (100mg/ml)	Carl Roth (Karlsruhe, Germany)
Nucleospin Plasmid easy pure kit	Macherey-Nagel
Nucleobond Xtra maxi Kit	Macherey-Nagel
Buffer RLT Lysis Buffer 45ml	Qiagen (Venlo, Netherlands)
Rneasy mini kit	Qiagen (Venlo, Netherlands)
Omniscript RT Kit (50)	Qiagen (Venlo, Netherlands)

<ul style="list-style-type: none"> • 10x RT Buffer • Omniscript reverse Transcriptase 	
LightCycler 480 SYBR Green I Master	Roche Diagnostics (Rotkreuz, Switzerland)
Rotiphorese gel 30	Carl Roth (Karlsruhe, Germany)
SDS (Natriumdodecylsulfat) 1%	Carl Roth (Karlsruhe, Germany)
Ammonium Persulfate (AP) 20%	Serva (Heidelberg, Germany)
Temed	Carl Roth (Karlsruhe, Germany)
Tris (0.25M)	Carl Roth (Karlsruhe, Germany)
Glycerin, Rotipuran	Carl Roth (Karlsruhe, Germany)
Methanol	Carl Roth (Karlsruhe, Germany)
Reversible protein staining kit	Thermo fisher scientific (Waltham, USA)
Sodium chloride	Carl Roth (Karlsruhe, Germany)
Tween 20	PanReac AppliChem (Darmstadt, Germany)
Page Ruler prestained Protein ladder	Thermo fisher scientific (Waltham, USA)
Powdered milk	Carl Roth (Karlsruhe, Germany)
Pierce ECL WB Substrate	Thermo fisher scientific (Waltham, USA)
Amersham Protran Premium 0,2µm Nitrocellulose membrane	GE Healthcare life science (Chicago, USA)
Amersham Hyperfilm	GE Healthcare life science (Chicago, USA)
QIAamp DNA mini kit	Qiagen (Venlo, Netherlands)
5x Green GoTaq Flexi Buffer	Promega (Madison, USA)
SeaKem LE Agarose 500g	Lonza (Basel, Switzerland)

2.1.13 Molecular biology equipment

DNA LoBind Tube 1,5ml	Eppendorf (Hamburg, Germany)
Mastercycler nexus GX2	Eppendorf (Hamburg, Germany)
Wide Mini-Sub Cell GT Cell <ul style="list-style-type: none"> • Mini gel caster • Sub-Cell GT UV-Transparent Wide Mini-Gel Tray • 20-well comb • 15-well comb 	Bio-Rad Laboratories (Hercules, USA)
Precision Balance max. 500g	Kern (Balingen, Germany)
PCR Tubes 0,2ml - Multiply μ Strip Pro mix.colour	Sarstedt (Nümbrecht, Germany)
Gel iX20 Imager	Intas (Göttingen, Germany)
Feather sterile disposable scalpel	Sigma-Aldrich (St. Louis, USA)
Qubit 2.0 Fluorometer	Thermo Fisher scientific (Waltham, USA)
Thermomixer compact	Eppendorf (Hamburg, Germany)
Centrifuge 5418	Eppendorf (Hamburg, Germany)
Water bath Haake W13	Gemini B.V (Apeldoorn – Netherland)
New Brunswick scientific Innova 44 Incubator shaker series	Eppendorf (Hamburg, Germany)
Fuego basic Bunsen burner	Carl Roth (Karlsruhe, Germany)
Bacterial cell spreader sterile	Carl Roth (Karlsruhe, Germany)
Bacteria tubes – 14ml PP Tube sterile	Greiner bio-one (Kremsmünster, Austria)
Petri dish	Sarstedt (Nümbrecht, Germany)
Nanodrop spectrophotometer	Thermo Fisher scientific (Waltham, USA)
UVC/T-AR, DNA/RNA UV-cleaner box	BioSan (Riga, Latvia)
96-well Light cycler plate	Sarstedt (Nümbrecht, Germany)

Adhesive q-PCR seal	Sarstedt (Nümbrecht, Germany)
Light cycler 480	Roche Diagnostics (Rotkreuz, Switzerland)
Mini-PROTEAN Tetra Vertical Electrophoresis chamber	Bio-Rad Laboratories (Hercules, USA)
Mini-PROTEAN Tetra Cell Casting Module <ul style="list-style-type: none"> • Gel casting module • Casting stands • Casting frames • Combs • Short and spacer plates • Sample loading guide 	Bio-Rad Laboratories (Hercules, USA)
Mini trans-blot module <ul style="list-style-type: none"> • Gel holder cassettes • Foam pads • Electrode assembly • Cooling unit 	Bio-Rad Laboratories (Hercules, USA)
PowerPac HC power supply	Bio-Rad Laboratories (Hercules, USA)
AGFA CP1000 developing machine	Diagnostic imaging systems (Rapid city, USA)

2.1.14 Software

Windows 10 <ul style="list-style-type: none"> • Excel • Words • PowerPoint 	<ul style="list-style-type: none"> • Data analysis and graphic representation • MD-Thesis • Presentations
FlowJo V10 Software	FACS data analysis
Primer-blast www.ncbi.nlm.nih.gov/tools/primer-	Primer design

<i>blast/</i> (Ye <i>et al.</i> , 2012)	
Primer3input: http://primer3.ut.ee/ (Untergasser <i>et al.</i> , 2012)	Primer design
Chromas Pro 1.76 Software	Sanger sequencing result analysis
Light Cycler 480 software	Real-time PCR data analysis
DIVA FACS Software	Compensation of multicolor FACs
Axiovision 4.8 software	Immunocytochemistry

2.2 Methods

2.2.1 Polymerase chain reaction (PCR)

Aim of the polymerase chain reaction (PCR) was to extract and replicate the full-length functional wildtype *FLT3* gene. PDONR223-*FLT3* plasmid (Addgene) was used as a DNA template. The Age1-KZ*FLT3*-for- and Afe1-*FLT3*-rev-primers (2.1.8) were used which included a start/stop codon, a Kozak region to improve the translational yield and the two restriction sites AgeI and AfeI. The reaction mix was combined as follows:

Table 1. PCR reaction mix

H ₂ O	13,8µl
5x Phusion HF Buffer	4µl
dNTP (10mM)	0,4µl
Primer mix AgeI/AfeI (10pmol/µl)	0,25µl
pDONOR223- <i>FLT3</i> Plasmid (1µg/µl)	0,25µl
DMSO (100%)	0,6µl
MgCl ₂ (25mM)	0,5µl
Go Taq Hot start Polymerase (5u/µl)	0,2µl

An initial temperature of 98°C for 30 seconds, 32 cycles of denaturation for 10 seconds at 98°C, annealing and elongation for 30 seconds at 72°C were

chosen. A final elongation at 72°C for 10 minutes and a reaction stop at 4°C followed.

2.2.2 Electrophoresis and gel extraction

For size dependent separation of the PCR-mix, an electrophoresis on 0,8% agarose gel, made with 1x TBE buffer and gel-red in a 1:10.000 dilution, was used. 6x loading dye and a 1kb DNA ladder was chosen. Electrophoresis was performed for 40 min at 150V.

The result was evaluated under UV light (Gel iX20 imager, Intas) and the *FLT3* band at 3,5kb was cut from the gel manually. To extract the DNA, the Gel Extraction kit (250) (QIAGEN) was used according to the provided protocol.

The DNA concentration was measured with the Qubit 2.0 dsDNA HS Assay, following standard protocol.

2.2.3 Cloning

The aim of the cloning process was to produce a wild type *FLT3*-vector. The vector of choice was "RUNX1wt in pRRL.PPT.CBX3SFhRUNX1.i2.EBFP.puro.pre" and „RUNX1K43Qmut in pRRLppTcBx35FhRunx.I2. EBFP.puro.pre“. Both vectors have the same lentiviral backbone which includes an ampicillin resistance and a blue fluorescent protein (BFP) sequence. Additionally, the vector includes a CBX3 promoter region, which allows viral integration in iPSC genome without epigenetic vector silencing (Hoffmann *et al.*, 2017). The RUNX1 cDNA that was originally a part of the vector, was removed by the *AgeI* and *AfeI* restriction enzymes and was replaced by the *FLT3* full cDNA sequence amplicon.

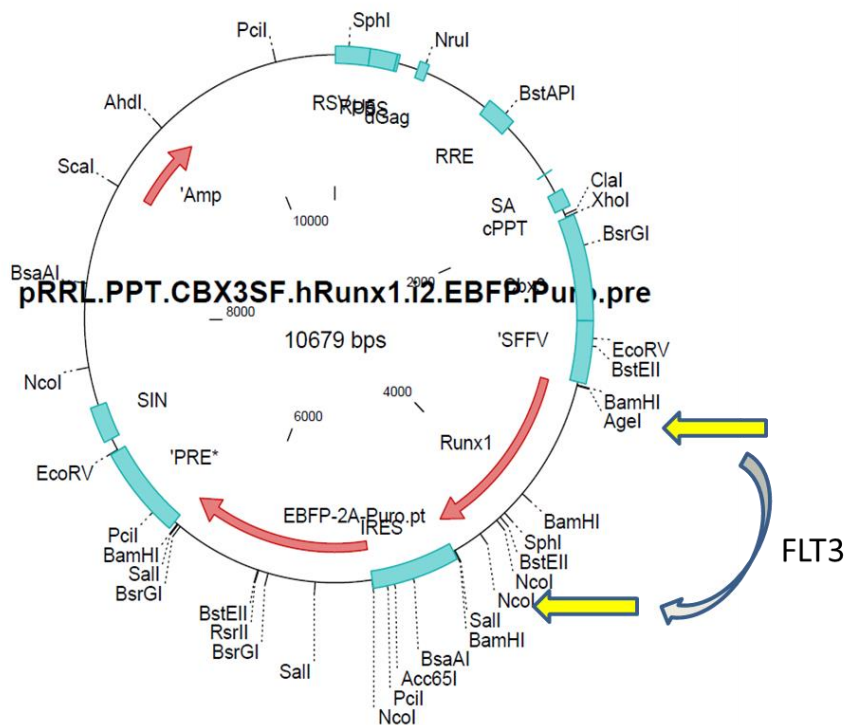


Figure 4. Lentiviral vector used for the cloning of *FLT3*

Lentiviral vector with ampicillin resistance, blue fluorescence protein sequence, CBX3 promoter and *Agel*/*Afel* restriction sites adjacent to the *Runx1* cDNA sequence (Modified after: Prof. A. Schambach, Medizinische Hochschule Hannover, Germany).

2.2.3.1 Digestion

The aim was to extract the *RUNX1* cDNA and insert the *FLT3* wildtype cDNA amplicon (NM_004119). The digestion protocol of the *Agel*-HF- and *Afel*-restriction enzymes (New England Biolabs) was varied to digest the *FLT3* amplicon as well as the vectors of choice.

Table 2. Digestion reaction mix, modified from New England Biolabs *Agel*-HF and *Afel*-restriction enzyme protocol

	Standard Protocol	Vector (1µg/µl) Doubled protocol	<i>FLT3</i> template (34ng/µl)
DNA	1µg	2µg = 2µl	1µg = 34µl
<i>Agel</i> -restriction enzyme	10 units	4µl, 8µl, 8µl	2µl
<i>Afel</i>	10 units	2µl, 4µl, 2µl	1µl

10x NEB Buffer = Cut smart Buffer	5µl	10µl	5µl
H2O	Rest volume for 50µl	82µl, 76µl, 78µl	8µl
Incubation temperature	37°C	37°C	37°C
Incubation time	1h	2h, overnight, 1h	2h

2.2.3.2 Dephosphorylation

To avoid plasmid recirculation, the 5'-end of the vector DNA was dephosphorylated using Calf Intestinal Alkaline Phosphatase (CIAP) (Fermentas). 20 units of CIAP were incubated with the reaction mix for 2h at 37°C.

2.2.3.3 Gel electrophoresis and gel extraction

The vector template was separated by electrophoresis according to the protocol described in 2.2.2.

The 9,5kb band, correlating with the size of the vector backbone, was cut out and the DNA was extracted from the gel, as described in said protocol (Gel Extraction kit (250) by QIAGEN).

2.2.3.4 Insert purification

To isolate the *FLT3* insert from restriction enzymes and DNA fragments of the different size, the restriction enzymes were heat inactivated at 65 °C for 20 min. Afterwards, the PCR product was purified according to the kit instructions (Qiagen).

2.2.3.5 Ligation

A modified version of the New England Biolabs Quick Ligation kit protocol was used. Two different ratios of vector to insert were used: 30ng of vector with a 3-fold and 5-fold molar excess of the insert (calculated with the NEB calculator).

Additionally, three different control groups were prepared for troubleshooting purposes:

- Control 1: uncut vector + no ligase
- Control 2: cut vector + ligase
- Control 3: water + ligase

The vector, the insert and the uncut vector were incubated for 5min at 62°C.

The reaction mix was pipetted as follows:

Table 3. Ligation mix, modified from New England Biolabs Quick Ligation kit protocol

40µl reaction	1:3	1:5	Control 1 Uncut vector	Control 2 Cut vector	Control 3
2x Quick Ligase buffer	20µl	20µl	20µl	20µl	20µl
Enzyme (Ligase)	2µl	2µl	//////////	2µl	2µl
vector	30ng =18µl	30ng=18µl	30ng=0,03µl	30ng=18µl	//////////
Insert	29ng=1,5µl	48ng=2,5µl	//////////	//////////	//////////
Water	0,5µl	//////////	19,7µl	2µl	20µl

After a quick spin down using a centrifuge, the reaction mix was incubated for 5min at 24°C.

2.2.3.6 Transformation

For the transformation, a competent strain of E. coli bacteria (Stellar, Clontech) was used. The modified transformation protocol from New England Biolabs was used.

4µl (approx. 10ng) of the ligation mixture and 100µl of competent cells were gently mixed and incubated for 30min on ice. They were abruptly heated in a 42°C water bath for exactly 30s. The mixture was then added to 950µl of room temperature LB-Medium and kept for 60min at 37°C in an incubator shaker at

250rpm. The bacteria were evenly distributed on Agar plates in three different concentrations (200µl, 400µl, 100µl). The plates were kept drying for a few minutes before being placed upside down in an incubator (37°C) overnight. Single colonies were picked and suspended in 2ml of LB-Medium + ampicillin (1:1000). These tubes were incubated overnight at 37°C and 250rpm shaking.

2.2.3.7 Mini-preparation

For the mini-preparation, the Nucleospin Plasmid easy pure kit (Macherey-Nagel) was used and the corresponding protocol was followed (Pc and Bac, 2011).

The success of the cloning process was evaluated by enzymatic digestion (2.2.3.1), electrophoresis (2.2.2) and Sanger sequencing.

2.2.3.8 Maxi-preparation

Two clones were selected for maxi-preparation. 300ml of LB-Medium, ampicillin (1:1000) and 400µl of minipreparation bacteria was combined and incubated overnight at 37°C and 180rpm.

The Nucleobond Xtra Maxi Kit (MACHEREY-NAGEL, 2020) was used, according to the manufactures protocol.

2.2.4 Sequencing

The absence of unwanted mutations in the *FLT3* cDNA sequence of the cloned wild type *FLT3* vector was confirmed by Sanger sequencing (performed by GATC Biotech). The sequence was analyzed with the ChromasPro 1.76 Software. To examine the whole cloned *FLT3* cDNA Sequence, additional primers (2.1.8) were designed.

2.2.5 Primer design

The primer design was performed using the following websites:

- PubMed: <http://www.ncbi.nlm.nih.gov/pubmed>
- Primer-blast: <https://www.ncbi.nlm.nih.gov/tools/primer-blast/> (Ye *et al.*,

2012)

- Primer3input: <http://primer3.ut.ee/> (Untergasser *et al.*, 2012)

Primers were synthesized by Eurofins Genomics GmbH (Ebersberg, Germany).

2.2.6 Transfection

A 6-well plate was coated with 10% Poly-L-Lysin to improve the attachment of the cells. For this, plates were incubated with Poly-L-Lysin at 37°C for 30-120 min and washed twice with PBS.

$2,5 \times 10^5$ HEK293FT-cells per well were seeded in SNL Medium (2.1.1).

As soon as a confluency of approximately 70% was reached, the medium was changed to pure DMEM to deprive the cells of the FCS. A lipofectamine mix was prepared containing lipofectamine 2000 and pure DMEM in a ratio of 3:197. The mix was incubated at room temperature for 5 min. Plasmid mixes were prepared containing 1µg Plasmid/200µl DMEM. The lipofectamine mix and the plasmid mixes were combined in equal parts and incubated for 20 minutes at room temperature. 400µl of the plasmid/lipofectamine mix per well was added to the cells and cells were incubated for 6-8h at 37°C before the medium was changed to SNL-Medium.

2.2.7 RNA Isolation and cDNA Synthesis

Between 5×10^5 and 5×10^6 cells were collected, washed and resuspended in 350µl the RLT-Buffer. RNA was extracted using the "RNeasy Mini Kit" (Qiagen), according to the manufactures protocol.

The RNA concentration was measured with the nanodrop spectrophotometer (Thermo Fisher scientific) and 500ng of RNA was used for cDNA synthesis.

500ng of RNA was incubated with 2µl of Oligo dT 18 primer (10µM) and the same amount of Random Hexamer Primer (10µM). ddH₂O was added to the reaction mix up to a volume of 31µl. An incubation at 70°C for 5 min and at 4°C for 1 min followed. Per sample, 4µl of 10xRT buffer, 4µl of dNTPs and 1µl of RT enzyme were added. The synthesis proceeded with incubation periods of 2min at room temperature, 60min at 42°C, 10min at 72°C and a cool down to 4°C.

The cDNA was kept at -20°C until further use.

2.2.8 Real-time PCR

In each well of a 96-well plate, 5µl of SYBR Green, 0,8µl of a primer mix for forward and reverse strand (10pmol/µl) and 4,2µl of a 1:20 diluted cDNA sample were combined. The preparation was done at 4°C and the plate was centrifuged for 1 min at 1300 rcf.

The PCR reaction was performed with the Light cycler 480 (Roche life science)

The protocol for the PCR was as follows:

Table 4. Real-time PCR cycling protocol

	time	temperature
Pre-incubation	5min	95°C
Amplification (45 cycles)	10s	95°C
	10s	60°C
	10s	72°C
Melting curve	5s	95°C
	1min	65°C
		97°C
Cooling	30s	40°C

The results were analyzed with the Light Cycler 480 software and Excel.

2.2.9 Western blot

10⁵ cells were fixed in 20µl of laemmli 3x Buffer (2.1.1). The samples were denatured for 7 min at 95°C and then centrifuged for 1 min at 20238 rcf.

Polyacrylamide gels were prepared according to conditions described in **Table 5. Polyacrylamide gel** Table 5, dividing the gel into a lower separation and an upper stacking segments.

10µl of the sample (lysate of approximately 5x10⁴ cells) was loaded per well and the electrophoresis chamber was filled with running buffer (2.1.7). Starting at 80V for approx. 40 min, the voltage of the electrophoresis was later increased to 150V for the remaining running time.

Table 5. Polyacrylamide gel

	Separation gel (2 gels)	Stacking gel (2 gels)
ddH ₂ O	4.3ml	3ml
Tris Base	3ml (1.5M-pH 8.8)	1.5ml (0.5M – pH 6.8)
Acrylamide 30%	3.2ml	1ml
SDS 1%	1.5ml	0.5ml
AP 20%	24µl	12µl
Temed	24µl	12µl

Following the electrophoresis, the proteins were transferred onto a nitrocellulose membrane (0.2µm) (GE Healthcare life science) by blotting for 1h at 4°C and 0.3A submerged in the wet transfer buffer described in 2.1.7.

To confirm equally loading of the proteins, a reversible protein staining kit (Thermofisher scientific) was used to stain the proteins and after evaluation of the protein distribution throughout the samples, protein staining was erased again.

The membrane was washed in TBST Buffer and blocked in 5% milk in TBST for 1h. Lastly, the membrane was treated with the primary antibodies (*FLT3* and β-actin) in a 1:1000 dilution in 5% milk at 4°C overnight.

The next day, the membrane was washed and incubated in the secondary antibody in a dilution of 1:2000 in 5% milk for 2h at room temperature.

After an additional washing step with TBST, the membrane was incubated with the detection reagents (Pierce ECL WB Substrate) for 1 min and images were developed with the AGFA CP1000 developing machine on Amersham Hyperfilms.

2.2.10 Virus production and -titration

For the Wild-type *FLT3*-Vector (#717), the mutant *FLT3*-Vector (#736) and, as a negative control, the empty-vector (#644), containing only the vector backbone, virus particles were produced.

For the virus production, different retroviral packaging vectors were used as follows: 12 µg of gag-pol (#636), 5 µg of RSV (#497), 2 µg VSV-G (#582) as well as 50 µl of 2,5 M CaCl₂, 10 µg of the target vector and 50 µl of H₂O.

This mixture was released into 500 µl of 2xHBS under constant bubble production with a Pasteur pipette. After continued bubbling for another 15-20s and a gentle shake, the mixture was incubated for 20 min at room temperature. HEK293FT cells were exposed to a mixture of TFM medium and 25µM chloroquine in equal parts. The vector mixes were added drop by drop to the HEK293FT-cells and incubated for 12-14h at 37°C.

The medium was changed to pure TFM-Medium and after 24h and 48h the medium with the newly produced virus particles was collected for virus concentration.

The virus concentration was performed according to the provided protocol of Lenti-x concentrator (Clontech).

For titration of the virus, a 24 well plate with HEK293FT cells at 70% confluency was prepared. The medium was changed to 1ml of SNL-Medium + 4 µg/ml polybrene. A serial dilution was prepared, starting with a virus dilution of 1:100. Each following well, the virus concentration was diluted further 1:10. For the mutated-*FLT3*-virus, the dilution row was started at a dilution of 1:20.

The plate was incubated for 72h at 37°C. The cells were collected for FACS analysis to examine the number of live (PI negative) and transduced (BFP positive) cells, therefore characterizing the potency of the virus.

2.2.11 Bortezomib treatment

HEK293FT cells were transfected according to the protocol previously described (2.2.6). 24h after transfection, the cells were treated with different concentrations of Bortezomib (1µM, 10µM, 100µM) as well as three groups of corresponding concentrations of DMSO as vehicle control (1:10.000; 1:1000;

1:100). After 24h, the cells were collected, counted and lysed in Laemmli-Buffer 3x for protein analysis by WB (2.1.1) or FACS (2.2.15.1).

2.2.12 Generation of induced pluripotent stem cells (iPSC)

For the generation of patient-iPS cells, patient peripheral blood mononuclear cells (PBMNC) were expanded for one week in expansion medium (2.1.1). After 6 days, 3 wells of a 24-well plate were coated with retronectin and incubated overnight in a wet chamber at 37°C. Retronectin was removed and the wells were washed for 30 min with PBS/BSA 2% and for 20 min with HBSS/HEPES 2,5%. $1,5 \times 10^5$ PBMNCs per well were seeded and subsequently each well was assigned a different multiplicity of Infection (MOI) (0.5, 1, 2) of the OSKM virus. According to the desired MOI, the titer of the OSKM virus and the number of cells, the required amount of virus was calculated, mixed with 50µl of Stemline Medium and added to the wells.

$$\frac{MOI \times number\ of\ cells\ to\ treat}{Titre} = volume\ of\ virus$$

The plate was centrifuged for 99min at 2000 rcf and 16°C.

The expanded patient cells were collected, washed once with PBS, counted, and centrifuged. After the centrifugation, the supernatant was removed and $1,5 \times 10^5$ cells in 1ml of expansion medium were added to each well. 20min centrifugation at 300g and 16°C followed. The cells were incubated in a wet 37°C chamber for 5 days. On day 6, the cells were collected and pooled together. Afterwards they were resuspended in a mixture of 1,5 ml of new expansion medium and 1,5ml of hIPS maintenance medium (2.1.1) supplemented with bFGF (30ng/ml), L-ascorbic acid (50ng/ml), and valproic acid (332,4 ng/ml). The cells were seeded on an MMC-SNL-cell coated 6cm-dish. On day 9 and day 12, 1,5ml of hIPS maintenance medium with bFGF (30ng/ml) was added. On day 14 and then on every following second day, the medium was changed completely to hIPS medium. On day 30, single colonies were selected and each of these clones was passaged on the MMC-SNL-cell

coated 3,5cm-dish. The following treatment was conducted according to the iPSC-maintenance-protocol (2.2.13).

2.2.13 iPSC maintenance

The iPSC-colonies were cultured in 6cm-dishes on MMC-SNL feeder cells. The 6cm-dishes were coated for 15min with 0,1% sterile gelatin. The surplus of gelatin was aspirated and $3,75 \times 10^5$ feeder cells were plated per 3ml of SNL-medium for one dish. The dishes were incubated overnight at 37°C. After 11 days, the iPSC cell plates were passaged by gently detaching, aspirating and disintegrating the iPSC colonies into smaller fragments. After aspirating the SNL-Medium of the new feeder plate, the iPSC colony fragments were reseeded in 3ml of new iPSC-medium with bFGF (30ng/ml). This medium was changed daily starting the second day after first passage.

2.2.14 Embryoid bodies (EB) formation and hematopoietic differentiation

iPSCs were cultured for 10-15 days in iPSC-Medium supplemented with 30ng/ml of bFGF. Rock Inhibitor in a dilution of 1:1000 was added to the plate and incubated for at least 2 hours. The cell culture medium was aspirated and the cells were incubated for up to 5 min with prewarmed accutase at 37°C. The detaching feeder cells were aspirated and the enzymatic reaction of the accutase was stopped with the FCS containing SNL-Medium. The detaching iPSC-colonies were collected and the cells were counted. The cells were diluted in APEL Medium supplemented with Rock Inhibitor (1:1000) and bFGF (20ng/ml) in a concentration of 20.000 cells per 100µl medium. 100µl of cell suspension was added per well of a 96-well TC plate (Sarstedt). The plate was centrifuged at 1500 rcf for 5 min. at 5°C. The cells built a nice spherical structure at the bottom of the well. The plate was incubated at 37°C overnight. On the second day, 100µl of APEL supplemented with bFGF (40ng/ml) and BMP4 (40ng/ml) was added per well. On the third day, a 6-well plate was coated with matrigel (303µg/ml) in D-MEM F12 and incubated at 37°C overnight. On the fourth day, the embryoid bodies (EBs) were carefully picked

up with a pipette and 10 EBs were added to 1,5 ml of APEL supplemented with VEGF (40µg/ml), SCF (50µg/ml) and IL3 (50µg/ml). Of the previously coated 6-well matrigel plate, the matrigel was aspirated and the surface was washed once with PBS. Afterwards, 10 EBs per well in 1,5 ml medium were plated. On day 8, 1,5 ml of new medium was added containing different cytokines and forming various groups:

- "IL3" = IL3 (100µg/ml)
- "IL3-GCSF" = IL3 (100µg/ml) + G-CSF (100µg/ml)
- "IL3-GCSF-*FLT3L*" = IL3 (100µg/ml) + G-CSF (100µg/ml) + *FLT3L* (100µg/ml)

Starting from day 12, once a week, floating cells were collected and 1,5 ml of the old medium in combination with 1,5ml of new medium with the same cytokines was added to the embryoid body plate again.

2.2.15 Flow cytometry (FACS)

Flow cytometry analysis of cell surface markers was performed on HEK293FT-transfected cells, iPSCs, Embryoid body cells and EB- derived floating cells (suspension cells). Two methods of FACS analysis can be distinguished: single staining FACS evaluates the expression of one specific cell surface marker. Far more challenging is multicolor FACS where multiple surface markers are analyzed at the same time, thus allowing complex information on receptor expression and identification of specific cell populations.

2.2.15.1 Single staining FACS

Attached cells were collected by treating the plate with accutase or trypsin for 5 min at 37°C and stopping the enzymatic reacting with an FCS containing medium. Through vigorous pipetting, single cells suspension was produced, cells were washed and counted.

A minimum number of 10^4 cells were diluted in 50µl of PBS/BSA 3% and pipetted into the FACs tubes. For each cell line, following samples were prepared:

- 1 tube of unstained cells

- 1 tube of isotype control
- 1 tube with the target antibody (sample)
Antibody concentration (μl of antibody/50 μl cell suspension):
 - embryoid body cells (hIPS derived): *FLT3*- 2 μl , *FLT1*-3 μl
 - HEK293FT transfected cells: *FLT3*-0,5 μl

While the antibody and the isotype control were added, as well as during the following incubation time of 20 min, the samples were kept on ice and in the dark. Afterwards, the cells were washed with 1ml of PBS/3% BSA and centrifuged for 5min at 1300rpm and 4°C. The supernatant was discarded and the cells, except for the unstained group, were diluted in cell staining buffer:

- iPS cells: 300 μl of PBS/3% BSA + DAPI (1:1000)
- Transfected 293FT cells: 300 μl of PBS/3% BSA+ PI (1:5000)

The cells were processed on the FACS Canto II Cytometer and the results were analyzed using the FlowJo Software.

2.2.15.2 Multicolor FACS

The primary steps of cell collection, washing and counting were the same as described in 2.2.15.1. 7 FMOs (fluorescence minus one) + 1 sample with all the antibodies (all in) + 1 unstained tube + compensation controls were prepared. The cells were diluted in 50 μl of PBS/3% BSA and added to the FACS tubes. An antibody master mix was prepared as described in table 6.

Table 6. Multicolor FACS antibody panel for late myeloid differentiation

Antibody master mix	Volume
CD45 BV510 / Amcyan	5 μl / 1 μl
CD15 PE	5 μl
CD16 FITC	5 μl
CD11b PE-Cy7	5 μl
CD14 APC-H7	5 μl
CD135 APC	5 μl
7AAD PerCP-Cy5.5	2 μl
PBS	Up to 50 μl

50µl of the antibody master mix was added to each tube and tubes were incubated at 4°C in the dark. For each fluorescent dye, a compensation control was prepared: 1 drop of anti-mouse positive compensation beads + 1 drop of negative compensation beads + an antibody in the same amount as given to the sample. The compensation controls were incubated for 20 min at 4°C in the dark. The compensation controls and cells were washed and diluted in 300µl of PBS/3% BSA. The compensation controls and cells were measured on the FACS Canto II Cytometer, compensated with the DIVA FACS Software and the results were analyzed with the FlowJo V10 Software.

2.2.16 DNA isolation, -gene amplification and mutational analysis

For further investigations, iPS cells were collected and lysed according to the instructions of the “protocol for cultured cells” of the QIAamp DNA mini kit (QIAGEN). The extracted DNA was measured using Qubit 2.0 dsDNA HS Assay (2.2.2). The *FLT3* template was further amplified by PCR reaction to allow a sufficient amount of cDNA for the following Sanger sequencing:

Table 7. FLT3 amplification mix

Green fluorescence buffer	4µl
dNTP (10mM)	0,5µl
Primer mix Agel/Afel (10pmol/µl)	4µl
DNA template	50ng
MgCl ₂ (25mM)	1µl
Go Taq Hot start Polymerase (5u/µl)	0,2µl
H ₂ O	Up to 21µl

The samples were run for 2min at 96°C, followed by 35 circles of 30s of 95°C, 30s of 58°C and 45s of 72°C. Afterwards, the samples were incubated for 2min at 72°C and cooled down to 8°C. The DNA was separated by electrophoresis, followed by an extraction of the 3.5 kb *FLT3* cDNA band according to protocol 2.2.2 and Sanger sequencing was performed as described in 2.2.4.

2.2.17 Alkaline Phosphatase staining

The medium was removed from the iPSC plate. The plate was washed once with PBS. The cells were fixed with 4% PFA-Sucrose and incubated for 2 min at room temperature. The plate was washed again with PBS. Staining dye was added and incubated for 20 min at room temperature in the dark:

- 10ml NTM Buffer (0,1M Tris pH 9,5 + 0,1M NaCl + 0,05M MgCl)
- 333µl NBT
- 35µl BCIP

After washing with PBS, the cells were stored at 4° in PBS.

2.2.18 Cytospin slides preparation

Per cytopsin slide, 10^4 cells were collected, washed and diluted in 150µl PBS. The cells were fixed on the Menzel glass slide by centrifugation at 400rpm on the cytopsin centrifuge. The slides were dried for 1min before they were stained with Wright-Giemsa stain in the HEMA-TEK slide stainer.

2.2.19 Immunocytochemistry

For the characterization of iPS cells, spontaneously differentiated iPSC were stained for SOX17- (endoderm) and TUBB3-(ectoderm) positivity.

iPS cells were collected and washed. Per well of a 96 well TC plate (Sarstedt), 20.000 cells were seeded in iPS maintenance medium. The plate was centrifuged at 1500 rcf, 5 min at 5°C. The cells were incubated at 37°C for 4 days with daily medium exchange. After that, the cells were plated on a matrigel coated 12-well plate. The cells were left for spontaneous differentiation for 26 days with medium changes about every 3 days. After the appearance of certain signs of differentiation (e.g. colony disintegration), immunocytochemistry was performed. The cells were washed with 0.1% PBS/Tween and fixated for 10min with 4% ice-cold PFA. After additional washing, the cells were permeabilized with 0.2% Triton for 10 min. Blocking was performed at room temperature for 1h in 0,1% PBS/Tween+ 1mg/ml BSA. The primary antibodies were diluted as

suggested by the company (SOX17 – 10µg/ml) (anti-b-Tubulin III – 1:400) in this blocking buffer and incubated overnight at 4°C.

The next day, the cells were washed twice for 10min. with 0,1% PBS/Tween and then incubated with the secondary antibody at 37°C for 2h. For SOX17 staining, a rabbit anti-goat antibody (1:400 dilution) and for Tubulin III staining, a goat anti-mouse antibody (1:200), both FITC-conjugated, were used.

The cells were washed again and treated with DAPI (1:1000 dilution), as a nuclear dye, for 10min. Cells were analyzed and images were recorded using an Olympus CKX41 microscope and the Axiovision 4.8 software.

3 Results

3.1 Patient case

We are introducing a patient, who has been diagnosed with severe congenital neutropenia (CN) at one year of age. Throughout his childhood, he experienced frequent infections of the skin, abscesses of the mucosa (anal abscesses and gingivostomatitis) as well as pneumonitis, enteritis and tonsillitis (Welte *et al.*, 1990). The bone marrow shows a maturation arrest at the promyelocytic stage (slightly elevated cell count) and a lack of subsequent cells starting from the stage of myelocytes. Despite a regular white blood cell count, a substantial neutropenia, as well as a modest eosinophilia and lymphocytosis can be seen. Furthermore, an exceptionally high percentage of monocytes (5-18x the reference) was observed. Analyzes of bone marrow and peripheral blood are seen in Table 8.

Table 8. Patient bone marrow and differential blood count prior to rhG-CSF and rhGM-CSF treatment

Bone marrow:	Patient	Reference (Isermann, 2013)
Promyelocytes (%)	5	0-7.5
Myelocytes (%)	1 (↓↓)	5-25

Peripheral blood:	Patient	Reference (Isermann, 2013)
White blood cells ($10^9/L$)	8.0	4.0-9.0
Neutrophils (%)	0 (↓↓↓)	50-70
Eosinophils (%)	7 (↑↑)	2-4
Basophils (%)	0	0-1
Monocytes (%)	37 (↑↑↑)	2-8
Lymphocytes (%)	41 (↑)	25-40
Platelets ($10^9/L$)	231	150-300
Hemoglobin (g/dl)	14	14-17.5 (male)

Comparison between the index patients cell count and the reference cell count in healthy individuals (Welte *et al.*, 1990; Isermann, 2013).

The histological analysis of bone marrow samples emphasizes differences between healthy individuals, typical severe congenital neutropenia (CN) patients and this particular patient (index patient): while healthy donors show a variety of progenitor cells at different stages of differentiation and typical CN patients display the maturation arrest of granulopoiesis at the promyelocytic stage, our index patient has an increased number of monocytic progenitor (Figure 5).

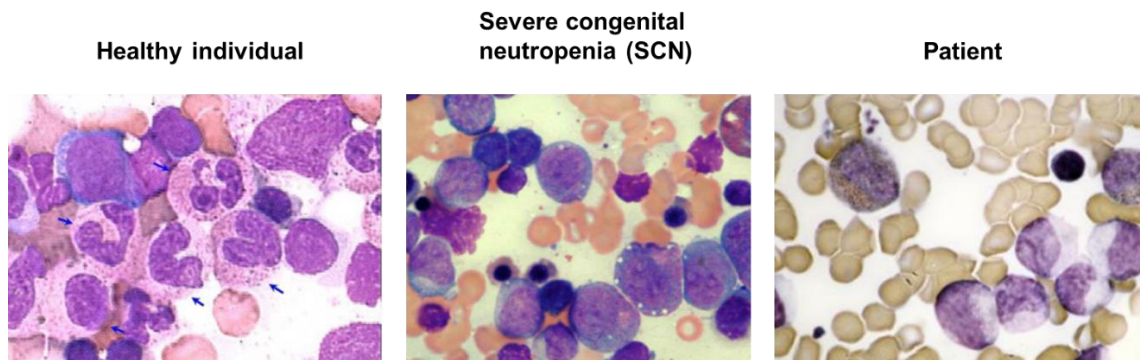


Figure 5. Histological comparison of bone marrow samples from healthy individuals, a typical CN patient and the index patient

Unusual is the extremely high number of monocytes, that were detected in the peripheral blood of this patient (AMC=3.438/ μ l), which increased even further after G-CSF treatment (AMC=24.800/ μ l) (reference AMC is 70-840/ μ l) (Welte *et*

al., 1990; Isermann, 2013). The neutrophil count in this patient increased only modestly to approx. 1000/ μ l at a G-CSF dosage of 5 μ g/kg/day (Welte *et al.*, 1990).

Interestingly, this patient has no known mutations in CN-related genes such as *ELANE*, *HAX1* or *G6PC3*. Next-generation whole genome sequencing of DNA samples of patient and his mother (father is not available) has revealed several heterozygous and homozygous mutations and single nucleotide polymorphisms (SNP), which have been analyzed for their importance in hematopoiesis and myelopoiesis. Furthermore, microarray analyses of G-CSF and GM-CSF treated CD34⁺CD33⁺ cells (patient and healthy donor) have been evaluated to find differences in gene expression. Ingenuity Pathway Analysis (IPA) has been used to find affected pathways with relevance to hematopoiesis.

We performed whole exome sequencing and identified two candidate SNPs that might be responsible for his disease: a heterozygous mutation in the Fms-like tyrosine kinase 3 (*FLT3*) gene (c.C662T, NM_004119.2, rs146030737), leading to a Valine to Methionine change (V194M), shared with his healthy mother, and a heterozygous *FLT1* mutation (P1201L, rs140861115), that was not presented in mother's DNA. We were not able to perform genetic analysis of patients' father.

Considering *FLT3*'s role in myelomonocytic differentiation (1.3), we decided to focus in this thesis on the *FLT3* V194M mutation. It is located in exon 5 which translates to the extracellular part of the receptor. This missense mutation has been identified as possibly damaging by PolyPhen-2 (<http://genetics.bwh.harvard.edu/pph2/>) (Adzhubei *et al.*, 2010). Using SIFT and PMUT web tools, Fröhling *et al.* have predicted no pathological consequence for this mutation on AML pathogenesis (Fröhling *et al.*, 2007). Nevertheless, in 2017 it was found that this particular mutation can be associated with a monocytic phenotype (Mousas *et al.*, 2017).

The heterozygote missense *FLT1* mutation is not being shared by the healthy mother of the index patient, making it an interesting candidate for studies researching the combined effect of *FLT3* and *FLT1* genetic variants on the

myelo-monocytic differentiation. It has been predicted by PolyPhen-2 as possibly damaging.

3.2 Analysis of V194M-*FLT3* mutation using an overexpression system

HEK293FT cells were transfected with a wildtype-*FLT3*-vector, a V194M-*FLT3*-mutated vector and a negative control (“empty vector”) containing the lentiviral backbone of the plasmid. The effect of the *FLT3* mutation on the expression levels of *FLT3* mRNA- and protein was evaluated using qRT-PCR, WB and FACS.

3.2.1 Production of a wildtype *FLT3* vector

For the backbone of the new *FLT3* wild type vector, a lentiviral vector containing an ampicillin resistance as well as a Blue Fluorescence Protein (BFP) sequence was chosen. The vector contained originally the RUNX1 cDNA with the restriction sites of Age1 and Afe1, which was extracted by enzymatic digestion and replaced by the *FLT3* template.

pDONR223-*FLT3* plasmid (Addgene) was used to acquire a wild type *FLT3* template. The extraction of the *FLT3* sequence was accomplished using the Age1-KZ*FLT3*-for and Afe1-*F*-rev, simultaneously adding the restriction sites of Age1 and Afe 1 as well as a Kozak region for additional yield. The primers had been previously designed by members of Skokowa Lab. Furthermore, a Kozak-Sequence was used to increase the translational yield of the plasmid. The *FLT3* template was extracted from pDONR223-*FLT3* plasmid and multiplied by PCR (2.2.1). The PCR product was separated on a 0,8% Agarose gel at 150V. The 3 kB band matched the size of *FLT3*, as reported by the manufacturer (Addgene). The band was extracted and the *FLT3* template was separated from the gel as described in 2.2.2. The cloning process was performed using protocols described in 2.2.3.

To ensure the success of the *FLT3* wild type vector production, the new WT-*FLT3* vector (717) as well as the original RUNX1 containing vector (641) were digested by Age1/Afe1 restriction enzymes and separated at 140V on 0,8% electrophoresis gel (Figure 6A). Additionally, the sequence of the new wild type

FLT3 vector was examined by Sanger Sequencing confirming that no new mutations had appeared in the *FLT3* cDNA (Figure 6B). Several primers were designed to cover the entire *FLT3* cDNA sequence (2.2.5) (Figure 6C).

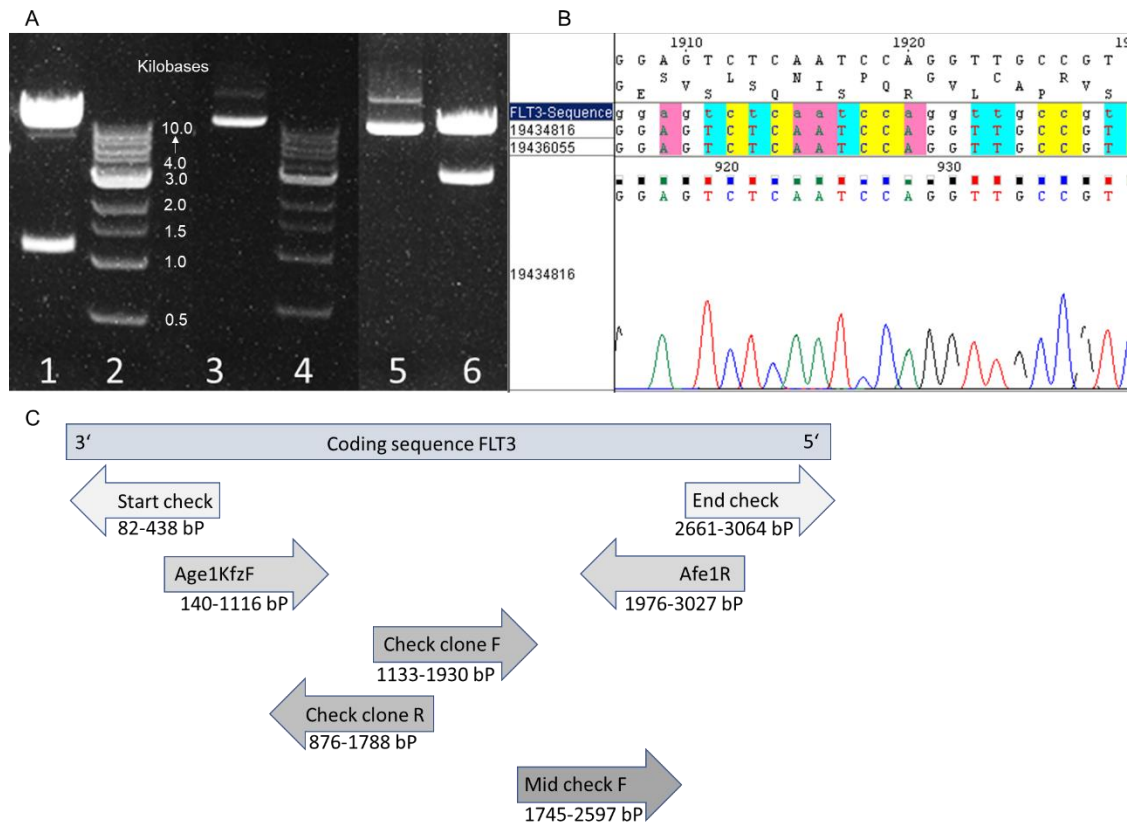


Figure 6. Electrophoresis of lentiviral vector backbone and *FLT3* insert, Sanger Sequencing of *FLT3*-WT vector and sequencing primer coverage of the *FLT3* gene

A) Electrophoresis of original RUNX1 containing vector (641) in digested (column 1) and undigested (column 3) form, as well as the WT-*FLT3* vector (717) in undigested (column 5) and digested form (column 6). Column 2 and 4 show the Quick-load 1kb DNA ladder.

B) Representative section of Sanger Sequencing of *FLT3*-WT vector compared to known *FLT3*-Sequence.

C) Coverage of the *FLT3* coding sequence by newly designed primers (2.1.8). Base pair (bP) number refers to the base pair coverage of the primer in the coding sequence of *FLT3*.

3.2.2 Production of V-194M-*FLT3* vector using site directed mutagenesis

To analyze the patient specific mutation in the *FLT3* gene and its impact on the *FLT3* receptor tyrosine kinase, the V194M-*FLT3* mutation was inserted into the wild type *FLT3* vector using site directed mutagenesis. Site directed mutagenesis primer design and reaction was performed by Dr. Houra Loghmani and M.Sc. Tessa Skroblyn (Skokowa Lab, University Tübingen).

Forward and reverse primer of the mutation site were prepared, stretching from the 178 to the 210th amino acid, thus including the chosen amino acid change of valine to methionine at position 194 (2.1.8).

Using thermal cycling, following the protocol of the QuickChange II Site directed Mutagenesis kit (Agilent Technologies, Santa Clara, USA), an expression vector with *FLT3* mutation was generated and multiplied via mini- and maxipreparation.

The sequence with the inserted mutation was confirmed by Sanger sequencing (Figure 7).

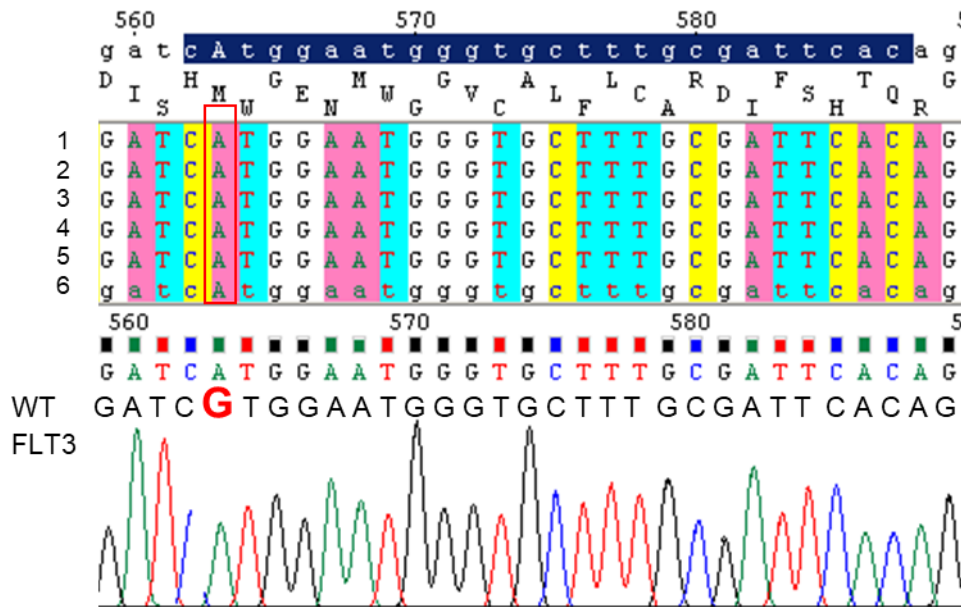


Figure 7. Sanger Sequencing of V194M-*FLT3* mutated vector

Sequencing of 5 clones produced using site directed mutagenesis (no. 1 - 5) compared to the mutated patient-derived V194M-*FLT3* sequence (no. 6). All clones present with the V194M-*FLT3* mutation site marked by the red square. Wild type *FLT3* sequence is shown below with the original "G" at the mutation site marked red.

3.2.3 Comparison of the expression levels of WT- and mutant *FLT3* in transfected 293FT cells

In a comparative experiment, HEK293FT cells were transfected with the "empty vector" (# 644), the wild type *FLT3* vector (# 717) and the mutant *FLT3* vector (# 736) as described in 2.2.6. 48-72h after transfection the cells were collected by trypsinization and divided for three different purposes:

- RNA was reverse-transcribed to cDNA by the reverse transcriptase

(2.2.7) and used for qRT-PCR (2.2.8) to study mRNA expression levels of transfected *FLT3*.

- Western blot was used to analyze *FLT3* protein expression.
- Surface expression of the *FLT3* receptor was evaluated by FACS.

Gene expression, as measured by qRT-PCR and normalized to the untransfected “no plasmid” sample of HEK293FT cells or cells transfected with an empty vector, showed markedly elevated *FLT3* levels for both WT-*FLT3* transfected cells and mutant V194M-*FLT3* transfected cells. Interestingly, gene expression of the WT-*FLT3* samples was almost two times higher than the mutant *FLT3* samples (Figure 8A).

While the *FLT3* mRNA was expressed in wild type and mutant samples, no V194M-*FLT3* protein band was detectable by Western blot. Equally, no *FLT3* protein was detected in the control samples (empty vector and no plasmid). Wildtype *FLT3* protein however was detectable and showed a strong double band at 130kDa and 160kDa indicating the non-glycosylated and glycosylated form of *FLT3* (Figure 8B).

Likewise, FACS analysis revealed low *FLT3* surface expression in the negative control group (empty plasmid) and the mutant *FLT3* transfected HEK293FT cells, as compared to the WT-*FLT3* transfected cells (Figure 8C). All cells were gated for PI (PerCP-Cy5-5) negativity, a characteristic of cell viability, and for BFP positivity to measure transfected cells.

In conclusion, a WT-*FLT3* expression in transfected HEK293FT cells is detectable on mRNA and protein levels. For the mutant-*FLT3* transfected cells, however, only mutant-*FLT3* mRNA was measurable. Mutant-protein expression was lacking.

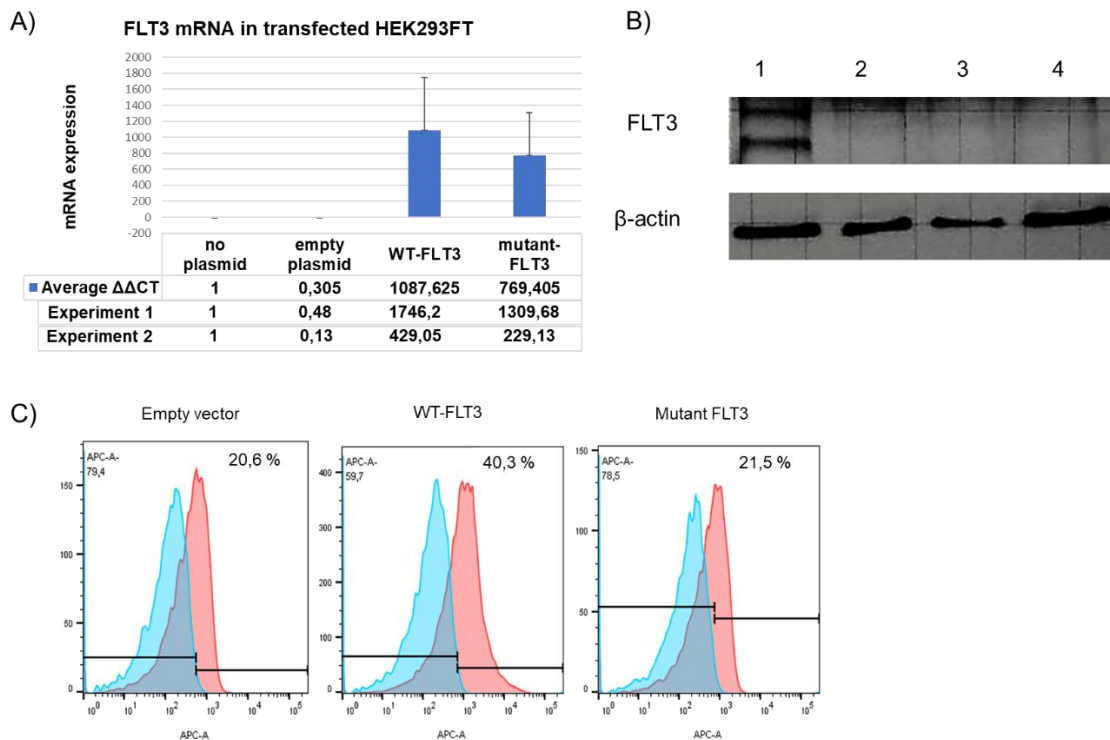


Figure 8. Results of the *FLT3* mRNA/protein expression analysis in transfected 293FT cells

A) qRT-PCR results. B) Western blot: 1= wild type sample; 2= mutant *FLT3*; 3= empty plasmid sample; 4= untransfected 293FT/ no plasmid
 C) FACS *FLT3* expression in “empty plasmid” negative control, Wildtype *FLT3* transfected cells and mutant *FLT3* transfected cells.

3.2.4 Production of the *FLT3* mutant- and *FLT3* WT – lentiviral particles

For the Wild-type *FLT3*-Vector (717), the mutant *FLT3*-Vector (736) and, as a negative control, the “empty-vector” (644), containing only the vector backbone, virus particles were produced and titrated following the protocol described in 2.2.10. Analysis of the potency of the virus was performed by flowcytometry.

One sample of untreated 293FT cells as well as of virus-transduced cells in four subsequently diluted concentrations (2.2.10) were collected. The cells were stained for PI (viability marker), BFP and *FLT3*.

As demonstrated in Figure 9, at a virus dilution of 1:100, 24,4% of alive cells were transduced by the empty-vector virus. In stronger dilutions, the percentage of transduced cells decreases, as expected. For the wild type *FLT3* virus at a dilution of 1:100, only 13,3% of the live HEK293FT cells were transduced, thus rendering the wild type *FLT3* virus less potent. To increase the success of the transduction process of the mutant *FLT3* virus, which in previous experiments

had shown signs of weakness, the dilution row was started at 1:20. At this concentration, 40,2% of the alive cells were transduced with mutant *FLT3* virus (Figure 9).

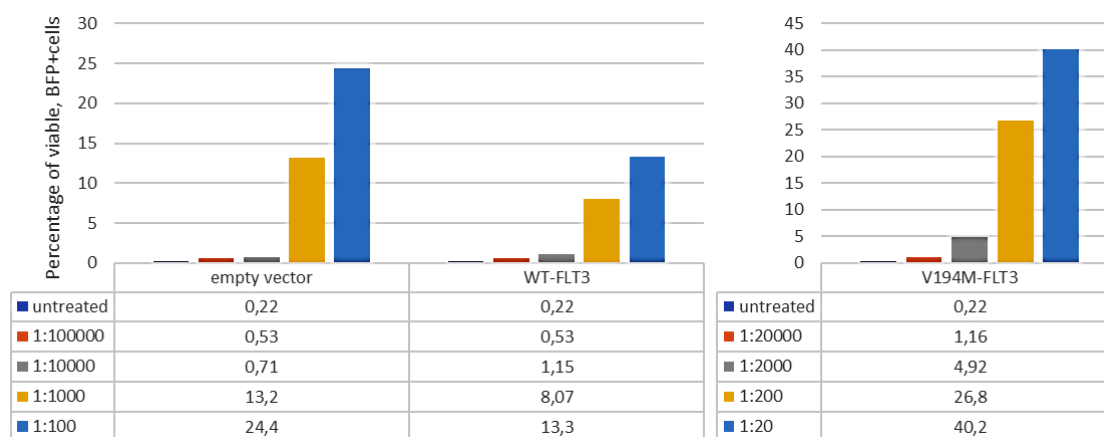


Figure 9. Virus titration of *FLT3* control/empty virus, WT-*FLT3* virus and mutant V194M-*FLT3* virus

Flow cytometry of PI negative (live) and BFP positive (transduced) 293FT cells. Transduction rates are shown as percentages of BFP positive cells following the experiments dilution row.

In a second step, the *FLT3* expression in the transduced and viable cells population was measured: Empty-vector/virus and mutant-*FLT3*-vector/virus showed a similarly low *FLT3* receptor expression (6,12% and 4,6%), while the WT-*FLT3*-vector/virus lead to a receptor expression of 80,9% (data not shown).

3.3 Evaluation of the effect of Bortezomib on the expression level of V194M *FLT3*

To examine a possible reason for the lack of mutant *FLT3* protein expression, the role of the 26S proteasome for the decay of mutant *FLT3* protein was investigated. Bortezomib was used as an inhibitor of the 26S proteasome, to investigate whether upon inhibition of the proteasome, the mutant-*FLT3* transfected cells will express *FLT3* on protein level.

293FT cells were transfected with the empty vector backbone (negative control), the WT-vector and the mutant-vector. After 24h, transfected cells were treated with increasing concentrations of Bortezomib (1µM, 10µM, 100µM) as well as the corresponding amounts of DMSO, which, as the solvent of

Bortezomib, was considered the solvent control. Furthermore, of each transfection group, one sample was kept untreated.

After an incubation time of 24h with Bortezomib or DMSO, the cells were collected and prepared for flow cytometry or Western blot analysis.

3.3.1 *FLT3* receptor surface expression in *FLT3* vector transfected and Bortezomib treated 293FT cells (flow cytometry)

Cells were collected and prepared for FACS following the standard protocol as described in 2.2.15. PI (PerCP-Cy5-5) negativity and BFP positivity was measured to select all viable transfected cells. Furthermore, *FLT3* receptor expression in the untreated group as well as in groups with increasing amounts of DMSO and Bortezomib treatment was measured. The mean fluorescence intensity (MFI) of the negative control (vector backbone) was subtracted from the WT and mutant *FLT3* MFI.

No increase of *FLT3* receptor in the Bortezomib treated groups compared to the untreated group was found (Figure 10). This seems to be the case for both WT-*FLT3* transfected cells and mutant-*FLT3* cells. Some experiments showed a small increase in *FLT3* expression upon Bortezomib treatment. However, similarly and sometimes even higher *FLT3* levels could be observed in the untreated group (Figure 10). Therefore, we concluded that Bortezomib does not influence *FLT3* receptor expression in WT-*FLT3* transfected and V194M-*FLT3* transfected HEK293FT cells.

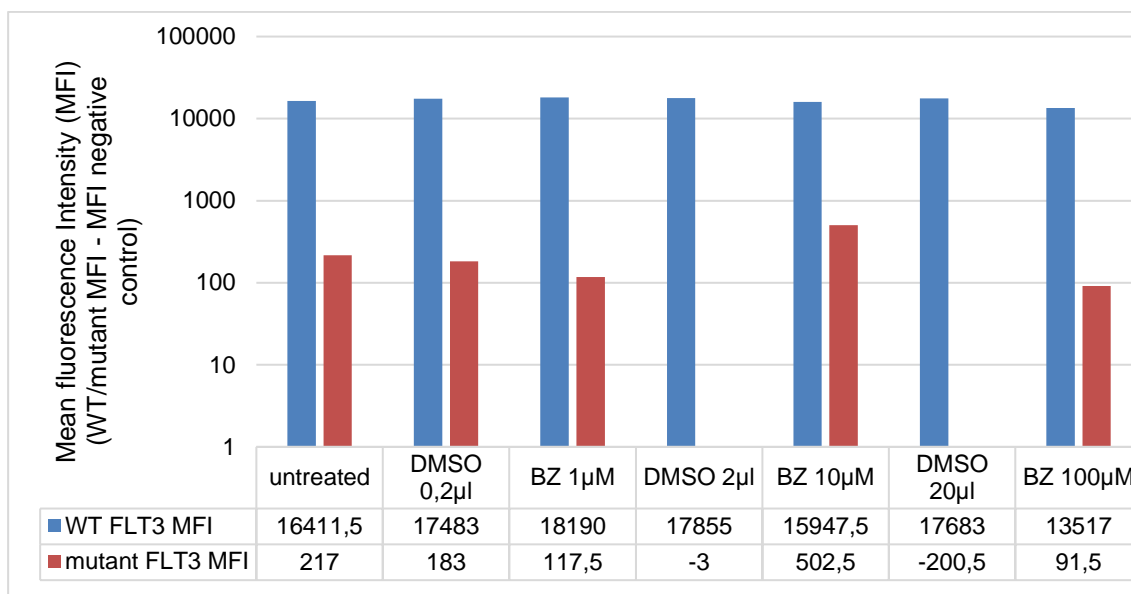


Figure 10. Mean fluorescence intensity (MFI) of *FLT3* in *FLT3*-vector transfected and Bortezomib (BZ)/DMSO treated HEK293FT cells

MFI of the empty control is subtracted from the MFI of WT- or V194M-*FLT3*-vector transfected HEK293FT cells. In paired comparison (DMSO 0,2µl-BZ 1µM, DMSO 2µl-BZ 10µM, DMSO 20µl-BZ 100µM), we have seen no increase in *FLT3* expression in the WT-*FLT3* transfected group upon BZ treatment. In the mutant *FLT3* V194M transfected group, higher *FLT3* levels were detected in the BZ 10µM and BZ 100µM groups compared to their solvent control. However, compared to the untreated group, this difference in *FLT3* expression is rather due to a decrease in the DMSO group than an increase in the BZ-treated group.

3.3.2 *FLT3* protein expression in *FLT3* vector transfected and Bortezomib treated 293FT cells (Western blot)

Western blot was performed according to protocol as described in 2.2.9. Empty vector-, WT-*FLT3* vector- and mutant V194M-*FLT3* vector transfected HEK293FT cells in untreated, DMSO treated or Bortezomib treated subgroups were analyzed for their *FLT3* protein expression levels.

Interestingly, while a strong *FLT3* band could be seen in all three WT-*FLT3* groups, the Bortezomib and DMSO treatment showed no effect on the *FLT3* protein expression in the empty vector and mutant *FLT3* group (Figure 11). The same result was seen when using 1µM and 10µM of Bortezomib (data not shown).

In conclusion, Bortezomib treatment in concentrations up to 100µM and with an incubation time of 24h showed no increase in mutant *FLT3* protein expression.

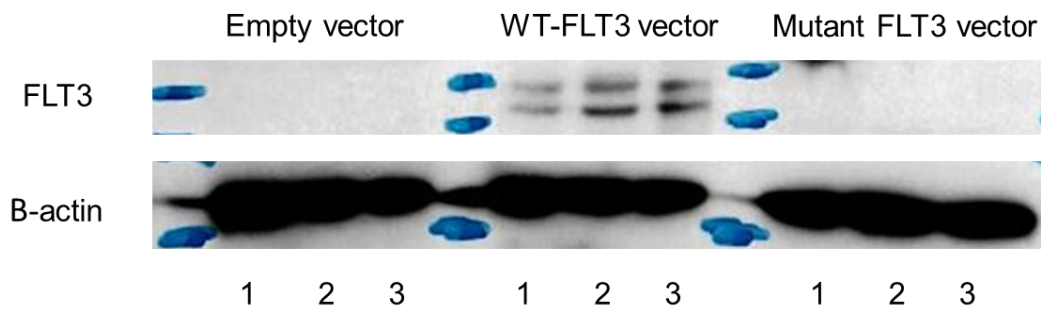


Figure 11. Western blot of *FLT3* protein in *FLT3* vector (control, WT and mutant) transfected and treated 293FT cells

Cells were transfected with empty vector, WT-*FLT3* vector and mutant *FLT3* vector. Subgroups: 1=untreated, 2=DMSO 1:100 and 3=Bortezomib 100µM. Representative WB images are shown.

3.4 Production and characterization of CN patient iPS cells

To produce patient iPS cells, mononuclear cells from the peripheral blood (PBMNC) of the index patient were used. These cells were expanded in a cytokine cocktail for a week to induce CD34⁺ cells expansion and were reprogrammed with the OSKM-Virus (2.2.11). Colonies which showed the characteristic phenotype of iPS cells were collected, maintained and passaged. To prove pluripotency and the ability to differentiate into all three germ layers, further characterization experiments were performed.

3.4.1 Alkaline Phosphatase staining of undifferentiated iPSC colonies

Alkaline phosphatase (AP) staining is a well-established method for stem cell characterization (O'Connor *et al.*, 2008). Undifferentiated iPSC colonies were stained according to the alkaline phosphatase assay protocol (2.2.17).

The dark purple color of the pluripotent stem cell colonies indicates AP-positivity. The SNL-feeder cells which surround the colonies served as a negative control (Figure 13).

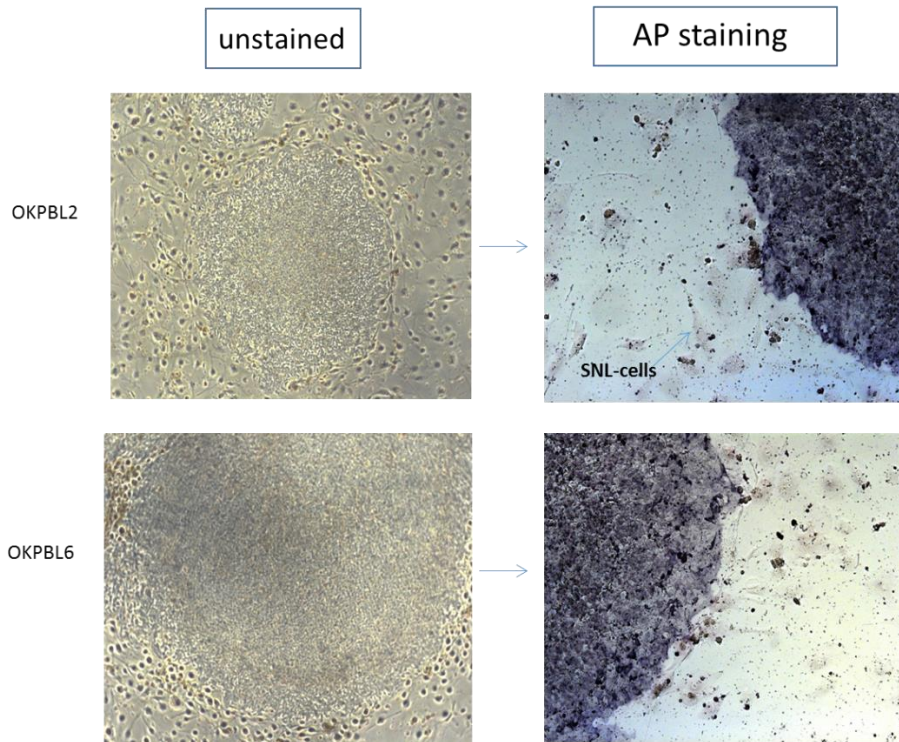


Figure 12. AP staining of patient derived IPS colonies

AP staining of two different patient IPS clones (OKPBL2 and OKPBL6). On the left side: unstained, bright field microscopy of colonies (5x). On the right side: AP-stained colonies + unstained SNL-cells (10x). Representative images are shown.

3.4.2 Flow cytometry of undifferentiated patient iPS cells for pluripotency markers

To further characterize the pluripotency of generated iPSC clones, their surface markers expression was assessed by flow cytometry. Phenotypically undifferentiated cells were collected and prepared as described in 2.2.15.1.

The samples were double stained with Tra1-85 (FITC), as a marker for human cells, and Tra1-60 or SSEA4 (PE) as pluripotency markers (Adewumi *et al.*, 2007). For each sample, an isotype control for the FITC- and PE-conjugated antibodies was prepared. As a positive control for this experiment, the healthy donor iPS cell line CD34IPSC16 was used, which previously had been characterized as a true and fully reprogrammed iPS cell line (Lachmann *et al.*, 2014).

The cells were gated for DAPI negativity (live cells). Tra1-85 as a marker for human cells was chosen to distinguish between human iPSC and the mouse MMC-SNL feeder cell. In the overlay of the isotype (blue population) control and

the sample (red population), a distinct shift towards double positivity was visible in all three iPSC cell lines: a strong positivity for SSEA4 and Tra1-60 was measurable in the previously confirmed healthy donor cell line (CD34IPSC16) and in both patient derived iPSC clones (OKPBL2 and OKPBL6) (Figure 13).

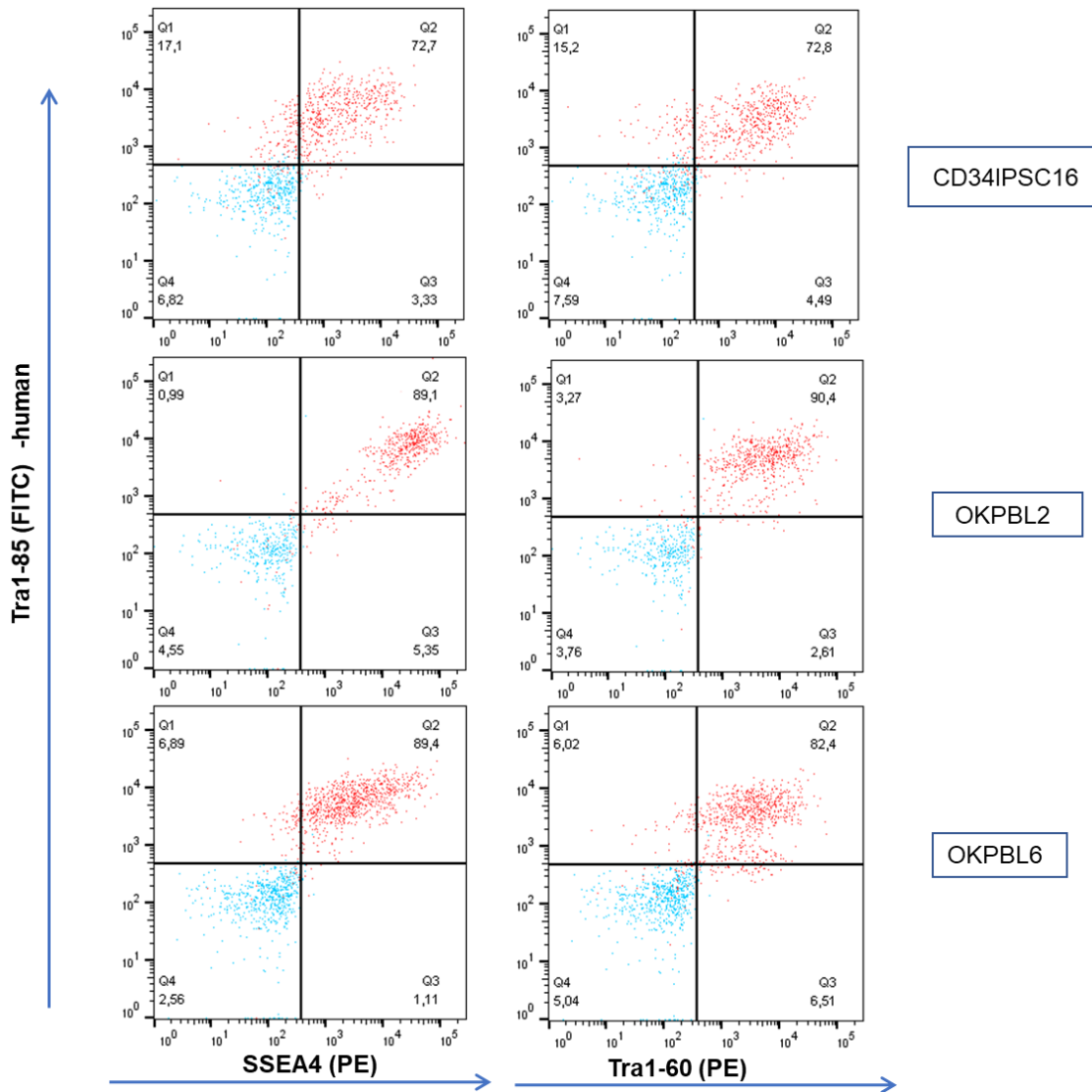


Figure 13. Flow cytometry evaluation of SSEA4 and Tra1-60 expression in undifferentiated iPSC cells of CN patient (OKPBL2 and OKPBL6) and healthy donor (CD34IPSC16)

The population was gated for live cells and Tra1-85, SSEA4 and Tra1-60 positivity. The Ab staining sample (red) was overlaid with the isotype control (blue). In all three iPSC lines, a high percentage (72-90%) of double positive cells for the pluripotency markers was measured. Representative FACS images are depicted.

3.4.3 Real-time PCR for the pluripotency- and 3-germ layer markers

An important step in the characterization of iPS cells is to prove their pluripotency and more precisely their ability to differentiate to all 3-germ layers: mesoderm, endoderm and ectoderm. Real-time PCR is an established method to do so. Furthermore, pluripotency can be documented by gene expression levels of Nanog, SOX2 and DNMT3B in undifferentiated iPS cells compared to primary CD34⁺ cells (Adewumi *et al.*, 2007).

iPS colonies were cultured with an elongated passage cycle of > 11 days with decreased medium changes (3 times per week). They underwent spontaneous differentiation which could be observed as their phenotype and colony integrity changed. As in 3.4.2, the CD34IPSC cell line was considered the positive control, since its pluripotency has been previously proven (Lachmann *et al.*, 2014). Primary bone marrow CD34⁺ cells on the other hand were used as a negative control. Cells were collected and lysed in RLT-Buffer. RNA was isolated and cDNA synthesized (2.2.7). Real-time PCR was performed (2.2.8). The gene expression levels of the iPS cell lines were analyzed by calculating the $\Delta\Delta CT$, thus comparing the mRNA expression of the samples with the negative control (CD34⁺ cells). Though the patient derived OKPBL2 and OKPBL6 iPSC lines showed lower levels of NANOG, SOX2 and DNMT3B mRNA levels, than the CD34IPSC16 cell line, they still express the pluripotency markers to a higher degree than the negative control CD34⁺ cells (Figure 15). Thus, the pluripotency of patient iPS cells (OKPBL2 and OKPBL6) is proven by qRT-PCR.

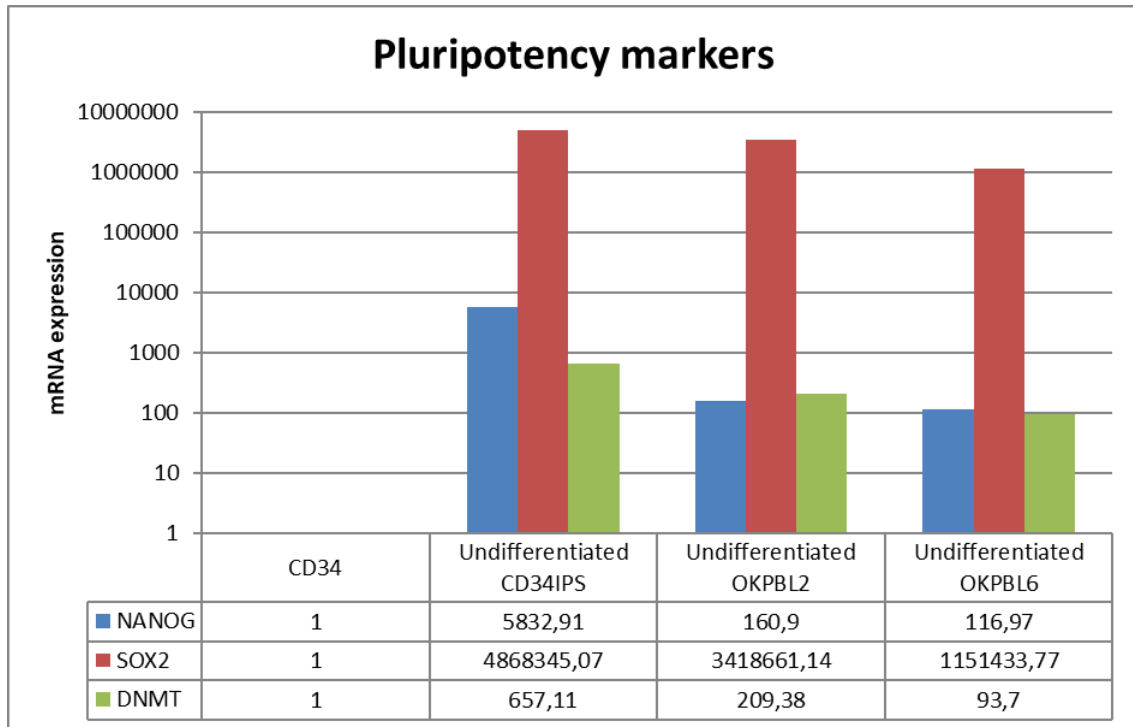


Figure 14. Real-time PCR analysis of pluripotency markers in undifferentiated CN patient (OKPBL2 and OKPBL6) and healthy donor (CD34iPS) iPS cells compared to mature CD34⁺ cells

Expression of Nanog, Sox2 and DNMT was compared to the normalized expression in CD34⁺ positive cells. Elevated levels of NANOG, SOX2 and DNMT were measured in both patient derived undifferentiated iPSC and healthy donor iPSC.

To prove the ability of iPS cells to differentiate to ectoderm and endoderm, the two specific markers, PAX6 and AFP, respectively, were chosen. Comparing their mRNA expression levels in spontaneously differentiated iPSC to the levels in undifferentiated IPS cells, an increase of PAX6 and AFP mRNA expression upon spontaneous differentiation was observed in both CN patient iPSC clones as well as in the CD34iPS cell line (Figure 16). OKPBL2 has a higher expression of the endodermal marker AFP ($\Delta\Delta\text{CT}=648,07$), while OKPBL6 has an approx. three times higher expression level of PAX6 ($\Delta\Delta\text{CT}=10,3$) than AFP. Based on these results, we concluded that CN patient iPSC have the ability to differentiate to endoderm and ectoderm. The potential for mesodermal differentiation, here at the example of hematopoietic cells, was shown by FACS (CD45⁺, CD11b⁺ cells) and morphological analyses below (3.4.2).

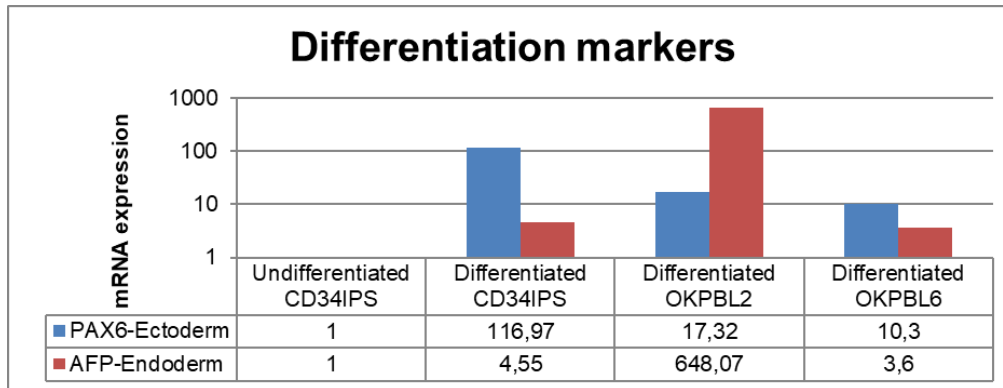


Figure 15. mRNA expression levels of markers of ectodermal and endodermal differentiation in spontaneously differentiated CN patient and healthy donor iPS cell- vs. undifferentiated iPS cells

mRNA expression of PAX6 (ectoderm) and AFP (endoderm) in differentiated iPS cells compared to the normalized result of undifferentiated healthy donor iPS cells (CD34IPSC16). $\Delta\Delta$ CT analysis was performed. Elevated levels of PAX6 and AFP were measured in the differentiated iPS-derived patient and healthy donor cells.

3.4.4 Immunocytochemistry of spontaneously differentiated CN patient iPS cells

To confirm the ability of the CN patient iPSC to differentiate in endoderm and ectoderm, immunocytochemistry with Tubb3 and PAX6 as ectodermal- and SOX17 as endodermal markers was performed on spontaneously differentiated iPS colonies. The immunocytochemistry was achieved as described in 2.2.19. Positivity of the ectodermal markers PAX6 and Tubb3 as well as the endodermal marker Sox17 was observed (Figure 16).

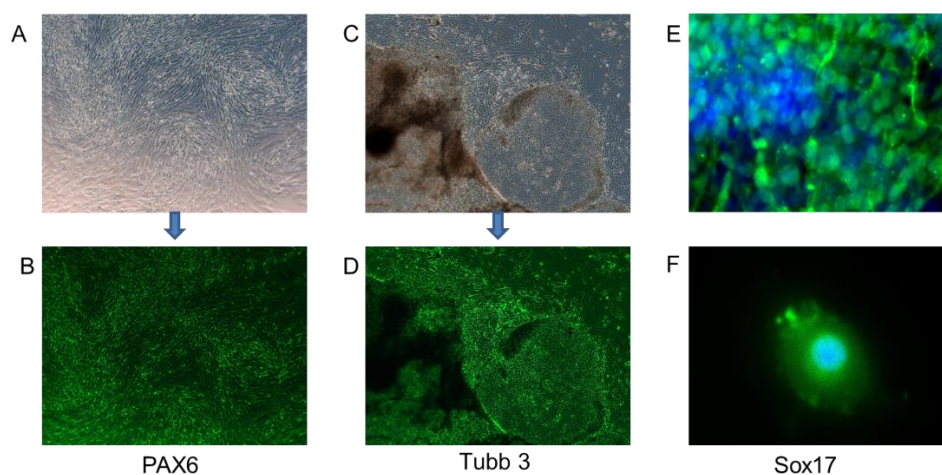


Figure 16. Immunocytochemistry of spontaneously differentiated patient iPS cells

A,C: Brightfield images of spontaneously differentiated CN patient iPS cells. B: Pax6-FITC ectoderm staining of cells from A. D: Tubb 3-FITC ectoderm staining of cells from C. E,F: Sox17-FITC endoderm staining. Overlay with DAPI-blue nuclear stain.

3.5 Comparison of CN patient vs. healthy donor iPS cell hematopoietic and myeloid differentiation

Having synchronized the passaging cycle of a healthy donor iPS cell line (CD34IPSC16) with two CN patient iPSC clones (OKPBL2 and OKPBL6), embryoid bodies (EBs) were formed and through specific cytokine stimulation, hematopoietic differentiation was induced (2.2.14).

3.5.1 Early differentiation: *FLT3* and *FLT1* expression analysis

EBs were collected on the first, second, fourth and eighth day and disintegrated by enzymatic reaction (accutase, trypsin) as well as through vigorous pipetting. The cell surface expression levels of receptors *FLT3* and *FLT1* were compared between healthy donor and CN patient iPSC lines.

Both, healthy donor and CN patient iPSC showed the same pattern of low *FLT3* expression on day one of EB culture with increasing expression on day 2. However, CN patient iPS expressed *FLT3* to a much lower degree (MFI=350; MFI=402,4) than the healthy donor control group (MFI=1025; MFI=1128; MFI=1165). On day four of culture (48h in APEL+bFGF+BMP4), most iPS cell lines showed decreased *FLT3* expression. *FLT3* in CN patient EBs decrease even further towards day eight.

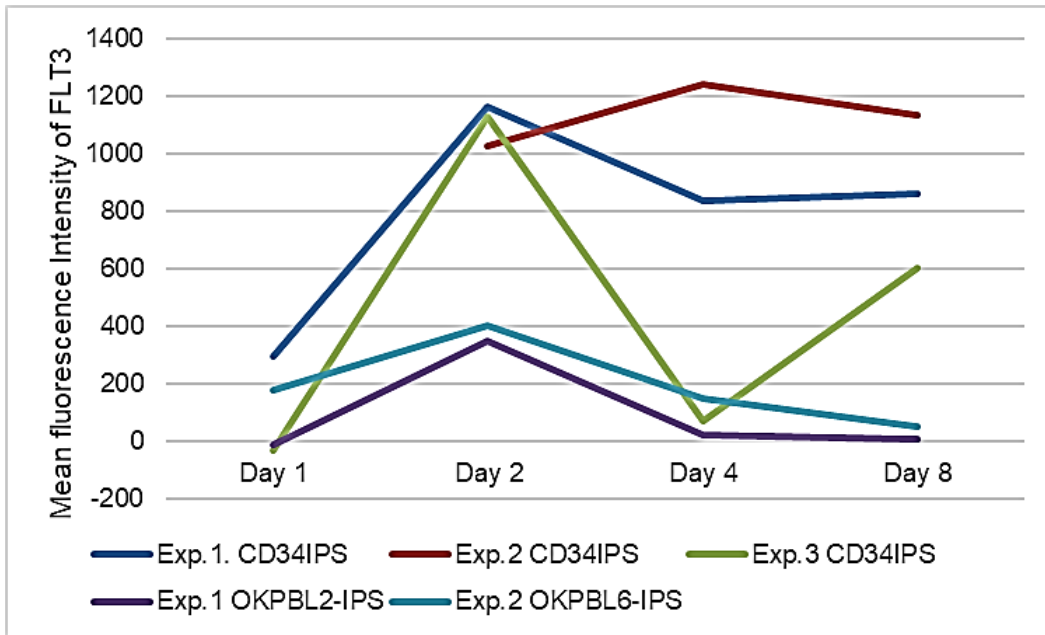


Figure 17. Mean fluorescent intensity (MFI) (Mean sample-mean isotype) of *FLT3* expression at early stages of hematopoietic differentiation of CN patient vs. healthy donor EBs

FLT3 expression in index patient EBs is depressed compared to the healthy donor cells during the early differentiation period (day 1-8).

Furthermore, the *FLT1* expression level was compared in CN patient vs. healthy donor iPSCs during the early development of embryoid bodies (EBs). *FLT1* is one of the index patients single nucleotide polymorphism (SNPs) (heterozygote mutation G/A at position 3887 leading to the amino acid change P1201L, rs140861115) with relevance to hematopoietic differentiation. Again, an increase in *FLT1* expression was observed on day 2 of EB-culture in healthy donor and index CN patient iPSCs. While different cell lines varied in expression, all of them followed the same expression pattern of having the maximum *FLT1* expression on day 2.

While there was no difference between CN patient and healthy donor iPSCs, a difference in *FLT1* expression was detectable between EBs, which attached and differentiated to hematopoietic cells and those, which spontaneously disintegrated and failed to develop further. Detached EBs (both healthy donor and index CN patient) expressed high levels of *FLT1* on the day 1 of treatment, which decreased on day 2 of culture (data not shown).

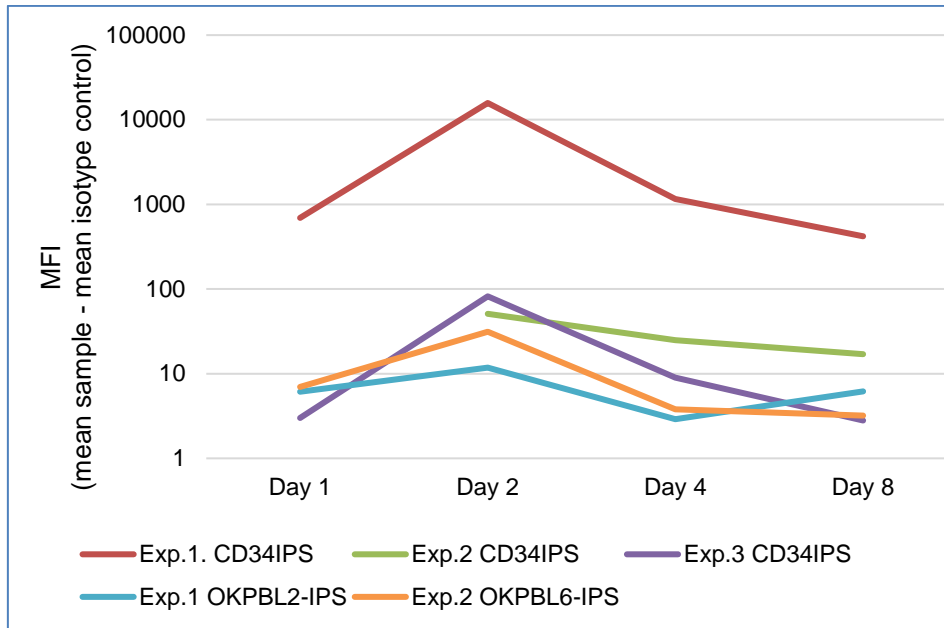


Figure 18. MFI of *FLT1* expression at early stages of hematopoietic differentiation of CN patient vs. healthy donor EBs.

Repeat experiments show elevated *FLT1* expression on day 2 of differentiation in patient and healthy donor derived EBs.

3.5.2 Intermediate and late differentiation: comparison of CN patient vs. healthy donor iPS cells

Starting on day 12, EBs produce suspension cells (floating cells), which can be collected for flow cytometry analysis as well as phenotypical analysis when fixated on cytospin slides and Wright-Giemsa stained. Floating cells were collected on day 12, 19, 26, 29 and 32. Per cell line (CD34IPSC16, OKPBL2, and OKPBL6), three different treatment groups were established starting from day 8 of culture:

- IL3= IL3 (100 µg/ml)
- IL3-GCSF= IL3 (100 µg/ml) + G-CSF (100 µg/ml)
- IL3-GCSF-*FLT3L*= IL3 (100 µg/ml) + G-CSF (100 µg/ml) + *FLT3L* (100 µg/ml)

3.5.2.1 Multicolor FACS analysis of suspension cells

Suspension cells were collected and prepared for flow cytometry according to protocol 2.2.15.2 and measured with the FACS Canto II Cytometer. The data was analyzed using the FlowJo-Software.

3.5.2.1.1 Myeloid differentiation of iPSCs

Cells were gated for viability (7AAD negativity) and for the leukocyte marker CD45. CD11b was chosen as a marker for myeloid cells, CD14 as a marker for monocytes and CD16 as a marker for mature neutrophils.

Development of these viable CD45⁺ cells was compared over time in healthy donor iPSC line (CD34iPSC16) and 2 patient iPSC lines (OKPBL2 and OKPBL6). All cell lines were cultured in the standard cytokine cocktail IL3-GCSF (3.5.2).

CD45⁺CD11b⁺ suspension cells appeared starting at day 12 in healthy donor (72%) and in CN patient (79%) (Figure 19A). The relative cell count of CD45⁺CD11b⁺ cells increased even further and reached its maximum on day 19 (79,1-87,3%) (Figure 20B), and on day 26 (69,6-70% in the CN iPSCs and 82% in the healthy donor iPSCs) (Figure 19C).

Monocytic differentiation was evaluated by analyzing CD14 positivity and more specifically CD11b-CD14 double positivity. Throughout differentiation, both healthy donor and patient derived iPSCs showed an affinity for monocytic differentiation. While the relative cell count for CD11b⁺CD14⁺ cells were similar on day 12 in all three cell lines (Figure 19A), both patient derived iPSCs surpassed the healthy donor cells on day 19 in monocyte production (Figure 19B). In the OKBL2 iPSC line, 60% of the viable CD45⁺ cells were CD11b⁺CD14⁺, while the healthy donor iPSCs developed only 42,4% monocytes. Monocytic differentiation decreased towards day 26 (Figure 19C). The maximum monocyte development was observed on day 19.

Neutrophil differentiation, defined as CD11b and CD16 double positivity, was most prominent on day 19, reaching 15,8-25,5% of viable CD45⁺ suspension cells (Figure 19B). Interestingly, one patient cell line (OKPBL2) surpassed neutrophil development of the healthy donor cell line (CD34IPSC16), while one patient iPSC line (OKPBL6) developed fewer double positive cells on day 19. On day 12 and 26, very few neutrophils were detectable in both healthy donor and patient cell lines (Figure 19A/C).

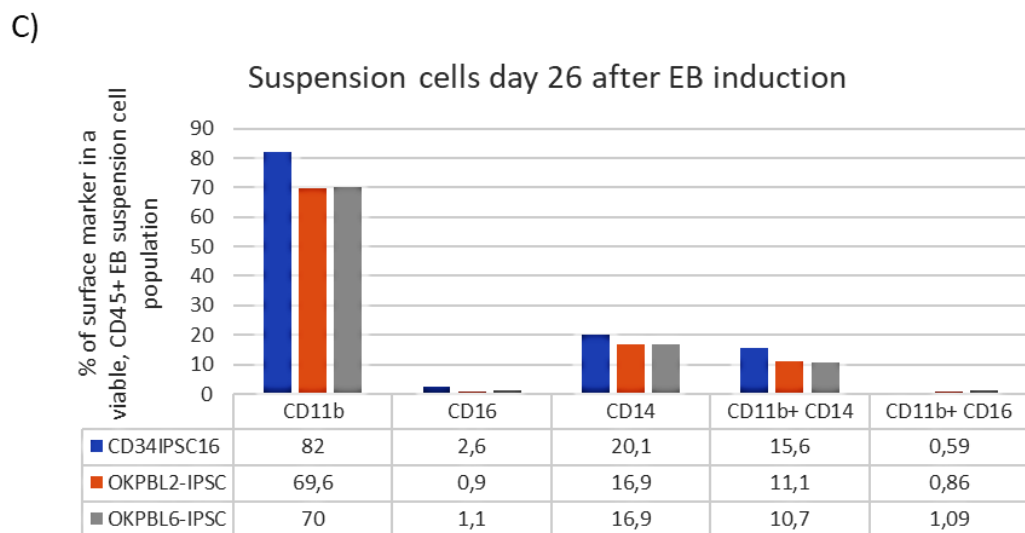
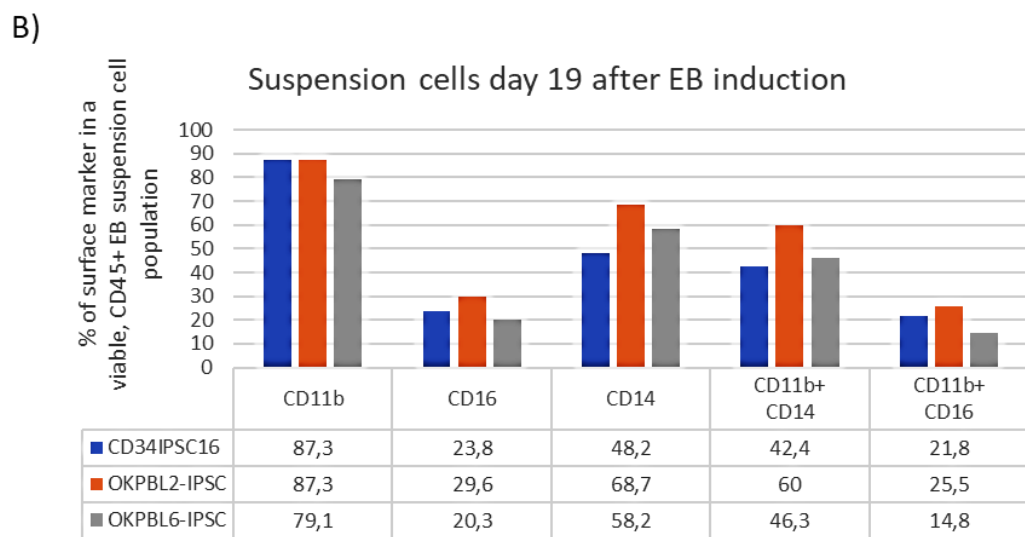
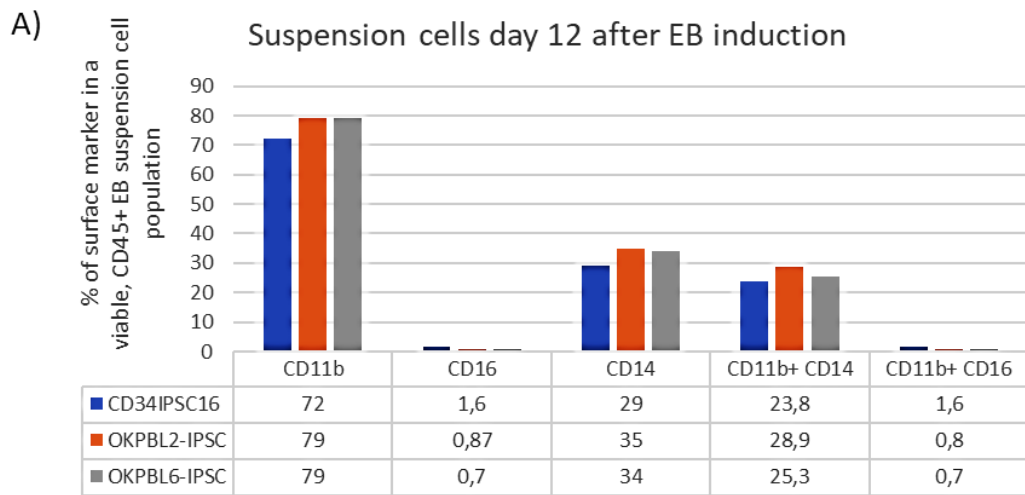


Figure 19. Analysis of myeloid differentiation of healthy donor and patient derived iPSC-Suspension cells day 12-26

Viable CD45 positive suspension cells were gated for CD11b, CD16, CD14 as well as double positivity of CD11b/CD14 (monocytes) and CD11b/CD16 (mature neutrophils).

3.5.2.1.2 Myeloid differentiation using various culture conditions

Cells were gated for viability (7AAD negativity), CD45 positivity (white blood cell marker), CD11b as a marker for myeloid cells, CD14 as a marker for monocytes and CD16 as a marker for mature neutrophils.

Cell differentiation was compared on day 19 in healthy donor and patient derived iPSC, each of which treated with three different cytokine cocktails starting at day 8 of differentiation: IL3, IL3-GCSF and IL3-GCSF-*FLT3L*.

G-CSF induces generation of CD45⁺ cells in all three iPSCs lines (Figure 20A/B), even further so in the healthy donor cell line upon *FLT3L* treatment, while the patient derived iPSCs showed no difference upon *FLT3L* stimulation compared to the IL3-GCSF treated sample (Figure 20B/C).

CD11b⁺ cell counts in healthy donor cells were highest in the IL3-GCSF treated group (Figure 20B). It decreased upon stimulation with *FLT3L* (Figure 20C). The CD11b expression in patient cells, however, was not affected by differences in G-CSF and *FLT3L* cytokine treatment.

Healthy donor derived iPSCs presented the highest monocyte cell count in the IL3 treated group. With the addition of G-CSF to the cytokine mix, CD11b⁺CD14⁺ cells decreased, even more so with the addition of *FLT3L* (Figure 20A/B/C). In contrast, the patient derived iPSCs (OKPBL2+6) demonstrated an increase in monocytes upon G-CSF treatment (Figure 20B). The cell count rose even further upon *FLT3L* treatment (Figure 20C).

Neutrophil differentiation, increased upon G-CSF treatment in healthy donor and patient derived iPSCs (Figure 20B) compared to the IL3 treated cell lines (Figure 20A). The addition of *FLT3L* had no great impact on the patient cell lines, while the healthy donor cells produced less CD11b⁺CD16⁺ cells than the IL3-GCSF treated sample (Figure 20B/C).

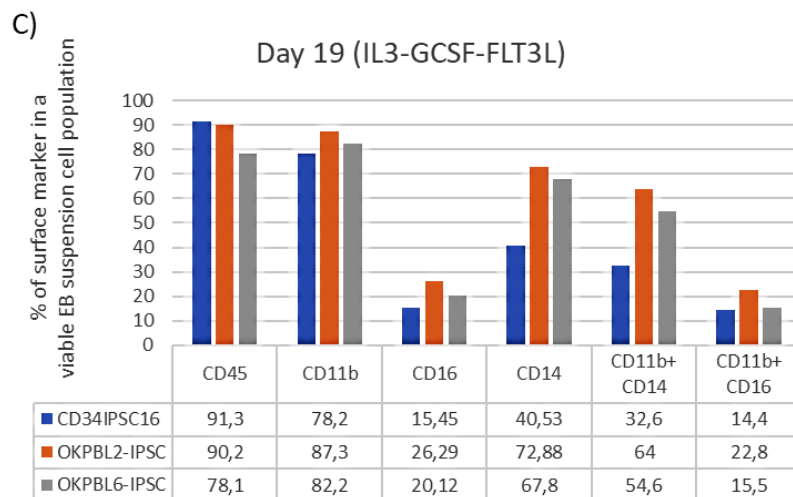
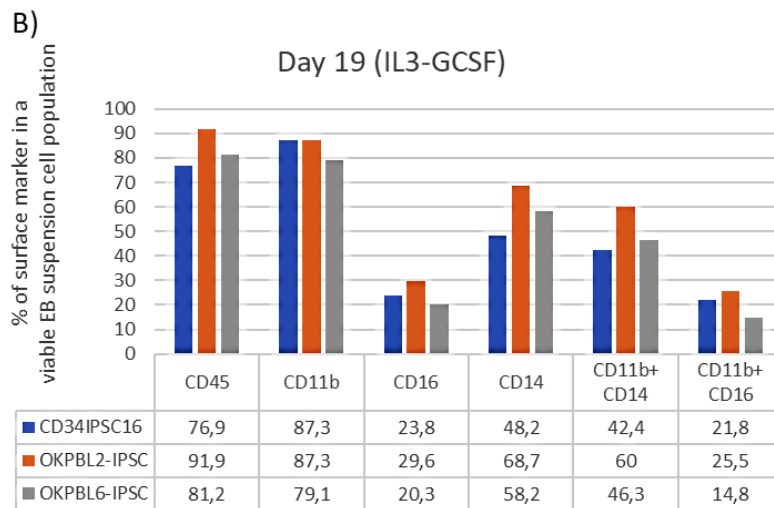
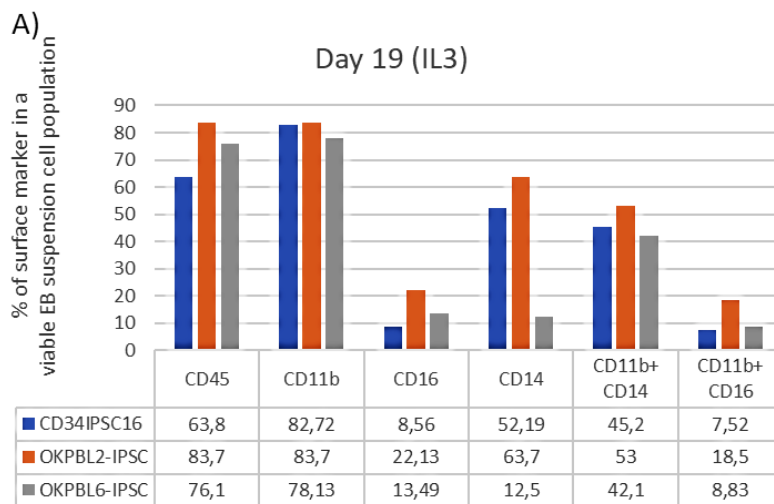


Figure 20. Assessment of myeloid differentiation of healthy donor and patient derived iPSCs stimulated with different cytokine mixes (IL3, IL3-GCSF, IL3-GCSF-FLT3L)

Viable suspension cells were gated for CD45, CD11b, CD16, CD14 as well as double positivity of CD11b/CD14 (monocytes) and CD11b/CD16 (mature neutrophils). Analysis was performed on day 19 of culture.

3.5.2.2 Morphology analysis of iPSC suspension cells

Parallel to FACS analysis, the morphology of floating cells derived from each iPSC cell line, organized into different cytokine treatment groups, was observed over time.

As mentioned previously, three different treatment groups were established starting from day 8 of culture:

- IL3= IL3 (100 µg/ml)
- IL3-GCSF= IL3 (100 µg/ml) + G-CSF (100 µg/ml)
- IL3-GCSF-*FLT3L*= IL3 (100 µg/ml) + G-CSF (100 µg/ml) + *FLT3L* (100 µg/ml)

Considering the cell morphology, the cells were characterized as immature-, intermediate- and mature granulocytes as well as macrophages.

On one hand, cell composition of differentiated CN patient iPSC cell clones (OKPBL2 and OKPBL6) were compared to the healthy donor cells (CD34iPS) of the same treatment. On the other hand, differences of hematopoietic differentiation between different groups were analyzed.

Phenotypical characterization was performed by Regine Bernhardt (MTA, Skokowa Lab).

Interestingly, considering the CN patient's peripheral blood phenotype with high numbers of macrophages and low numbers of neutrophils (3.1), in this *in vitro* model a stable and even adequate production of mature granulocytic cells (day 26-32: 59-85%) was achieved (Figure 21 A+B). Moreover, the development of equal percentages of mature neutrophils in the patient iPSC differentiation compared to the healthy donor cell line was observed (Figure 21C).

The healthy donor IL3-GCSF and IL3-G-CSF-*FLT3L* treated groups showed an earlier (day 19) increase of mature neutrophils (31-36%) then the G-CSF deprived cells/ IL3 treated (11,76%) of the same cell line (Figure 21C). Moreover, this pattern of development (late increase of mature granulocytes on day 26) was mirrored by all the patient cell lines regardless of their G-CSF stimulation (Figure 21A+B).

Though the two patient iPSC cell clones show a similar pattern of cell distribution at the late stages of differentiation (day 26, 29, 32), they differ quite strongly

during the first two measuring time points (day 12 and 19): while OKPBL2 IL3 and IL3-GCSF produces mainly immature cells (82,91-94,26%) on day 12, rapidly dropping the production towards day 19 (13,97-18,05%), the intermediate cells are increased from day 12 to day 19 at approximately 4,5-10 fold (Figure 21A). OKPBL6 iPSC line on the other hand shows in the IL3 and IL3-GCSF group the opposite changes of cell development: a high number of intermediate cells on day 12 which drops soon, and an increase of immature cell number on day 19 (Figure 21B). The healthy donor, CD34IPSC16 IL3 treated and IL3-GCSF, presents itself with a similar development of intermediately differentiated cells as OKPBL6, starting with a high cell count on day 12 which rapidly drops on day 19. The immature cell count, however, does not rise on day 19 as we see for the equivalent OKPBL6 groups, as cell production shifts to mature cells (Figure 21C, IL3 and IL3-GCSF).

At the early stages of treatment (Day 12 + 19) the G-CSF exposed patient iPSC clones (IL3 and IL3-GCSF-*FLT3*) demonstrate a noticeable increase of intermediately differentiated cells compared to the result in the G-CSF deprivation sample (IL3) of the same cell line (OKPBL2: 59,51%→72,02%; OKPBL6: 16,46%→41,94%) (Figure 21 A IL3 and IL3-GCSF; Figure 21B IL3 vs. IL3-GCSF). Treatment with *FLT3L* does not augment this effect (Figure 21 A+B IL3-GCSF-*FLT3L*). In the healthy donor cell line, however, there is no visible increase of intermediate cells upon G-CSF treatment (Figure 21C IL3 vs. IL3-GCSF).

In all three cell lines, it can be noticed, that while the “IL3” and the “IL3-GCSF” group show a similar pattern of cell development and distribution over time, the addition of *FLT3L* (IL3-GCSF-*FLT3L*) changes the ratio of immature and intermediate cells in early development while leaving the late development unaffected (Figure 21 day 12+19, IL3-GCSF-*FLT3L* vs. other cytokine treatment).

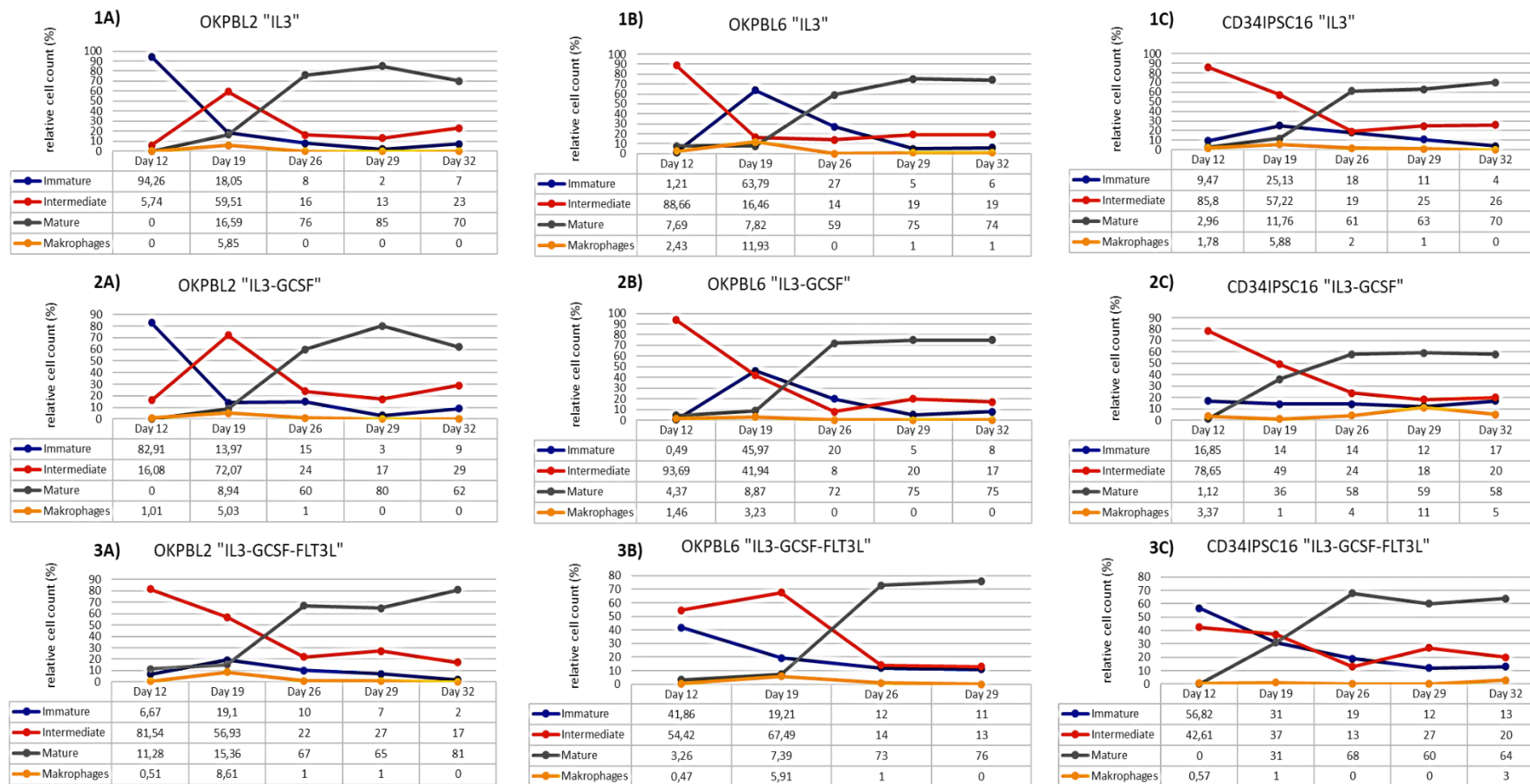


Figure 21. Morphology analysis of CN patient vs. healthy donor floating cell development in different treatment groups

Relative cell count of immature (blue)-, intermediate (red)-, and mature granulocytic cells (grey) as well as macrophages (yellow). A) OKPBL2; B) OKPBL6; C) CD34IPSC16; 1=IL3, 2=IL3-GCSF, 3=IL3-GCSF-FLT3L.

In contrast to the patient peripheral blood count, the relative cell count of mononuclear cells in the patient cell line was low (0-1% on day 26-32). Furthermore, in this cell line no increases/decreases of monocyte numbers were noticed upon different cytokine stimulations. The highest monocyte/macrophage count for all CN patient iPSC groups was observed on day 19 (Figure 22B/C).

This was also the case for the G-CSF deprived group of the healthy donor iPSC (Figure 22A, "IL3"). However, in the IL3-GCSF and - *FLT3L* treated healthy donor samples, the main development of mononuclear cells shifted to a later point (day 29 and 32) (Figure 22A, IL3-GCSF and IL3-GCSF-*FLT3L*). Interesting is the high percentage (Day 26-32: 4%→11%→5%) of monocytes, that have developed overall in the healthy donor control group with IL3-GCSF (Figure 22A, "IL3-GCSF"). With the deprivation of G-CSF as well as the addition of *FLT3L*, noticeable smaller percentages of mononuclear cells in healthy donor suspension cells can be seen (Figure 22A, IL3 and IL3-GCSF-*FLT3L*).

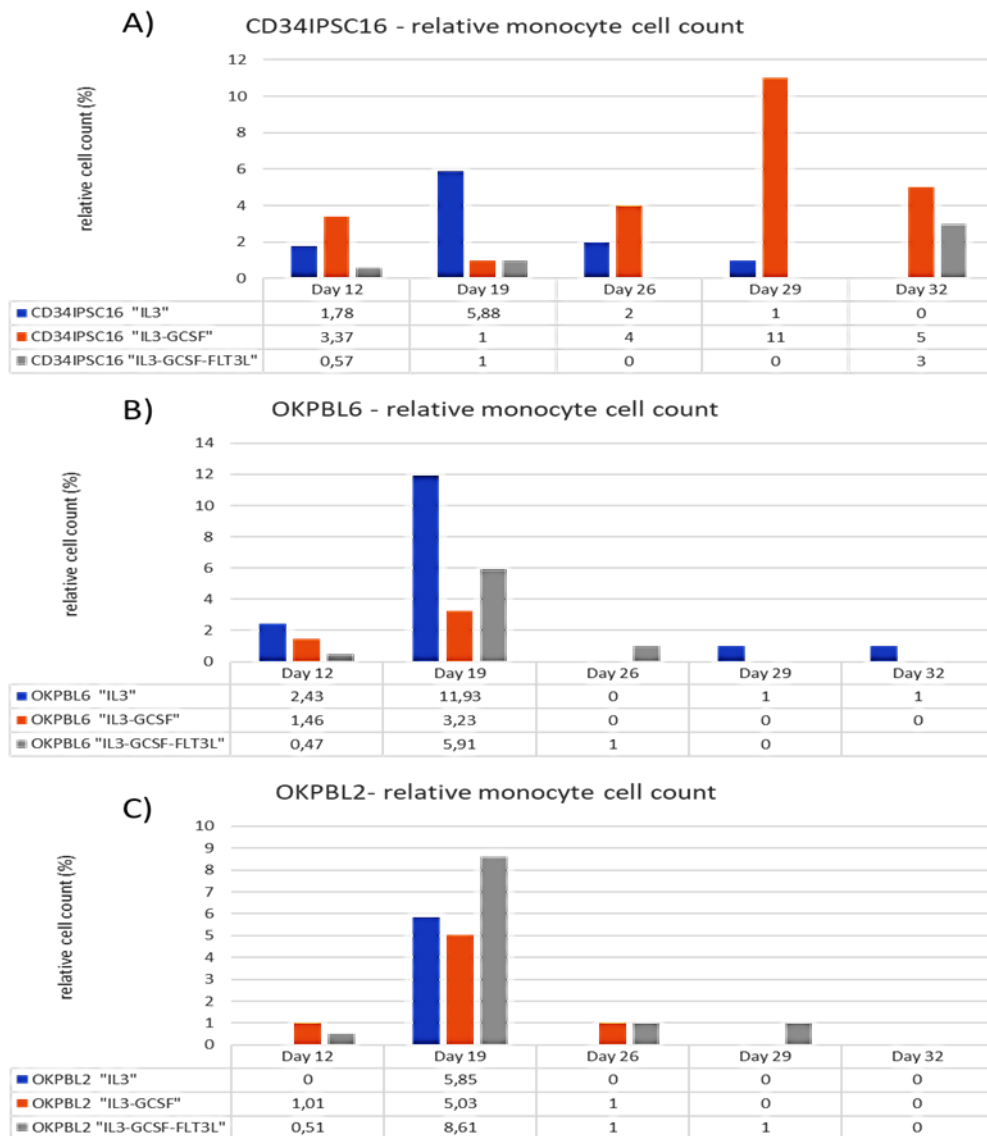


Figure 22. Morphology analysis of monocyte development of CN patient vs. healthy donor iPSC suspension cells development in different treatment groups (IL3, IL3-GCSF, IL3-GCSF-FLT3L)

A) healthy donor suspension cells, B) and C) patient derived iPSC. Monocyte development day 12-32 during different cytokine stimulations.

4 Discussion

A thorough understanding of the regulation of hematopoietic stem cells differentiation and identification of critical genes and mutations affecting this process is the basis for comprehension and treatment of hematological diseases. Despite extensive research in this field, many questions remain unanswered. Among these are uncertainties about transcriptional regulation of myeloid differentiation beyond the effects of the PU.1:C/EBP α expression ratio. For many years, the orphan disease Severe Congenital Neutropenia (CN) has been studied for a better understanding of myeloid differentiation. CN patients experience an arrest of bone marrow granulopoiesis at the promyelocytic stage leaving them without mature neutrophils and thus relatively unprotected from many life-threatening pathogens. However, while the granulopoiesis is severely impaired, patients develop monocytosis with an absolute monocyte count (AMC), elevated 2-4 times above average (Bonilla *et al.*, 1994). The reason for this phenomenon is unclear. In discussion is a stimulation of monocytic development to compensate abrogated granulocyte functions in the innate immune system defense. Another hypothesis is an inadvertent stimulation of monocytic development through an excess of myeloid progenitor stimulation as part of an active neutrophilic feedback system. Fact is that LEF1 and C/EBP α transcription factors are downregulated in CN-progenitors, but not in cyclic or idiopathic neutropenia (Skokowa *et al.*, 2006). Furthermore, PU.1 expression in bone marrow cells of CN patients is slightly upregulated compared to healthy donor cells (Skokowa *et al.*, 2006). While these results are in line with our current knowledge of myeloid decision making, a clear genotype-phenotype relationship has yet to be discovered. Even though most cases of CN can be explained through mutations in one of the typical CN related genes (e.g., *ELANE*, *HAX1*, *G6PC3*), there are also patients with CN phenotype and an atypical or even unknown mutation profile.

One of these patients has been at the center of this study. This index CN patient has not only the unique genotype, but also a strong monocytic shift with an AMC 4-18 times above average and an even stronger AMC when treated

with G-CSF (Welte *et al.*, 1990). This raises the questions, what this strong monocytosis provokes, whether an answer to monocytic development can be found in his genotype, and how his early hematopoiesis compares to healthy individuals. Further understanding of the genetic background of the neutropenia and excessive monoopoiesis will lead to the establishment of novel therapeutic opportunities for CN patients with these hematopoietic phenotypes.

Using next generation sequencing of the patients and healthy mother DNA, we found that the index patient harbors *FLT3* and *FLT1* single nucleotide polymorphisms.

In hematology, *FLT3* appears in more than one context. First, *FLT3* mutations are key mutations in 1/3 of acute myeloid leukemias (AML). Thus, *FLT3* internal tandem duplications (ITD) or mutations of the *FLT3* intracellular tyrosine kinase domain (TKD) lead to ligand independent receptor activation and subsequently unrestricted cell proliferation (Hayakawa *et al.*, 2000; Kiyoi *et al.*, 2002; Spiekermann *et al.*, 2002; Papaemmanuil *et al.*, 2016).

On the other hand, *FLT3* is being studied for its role in hematopoietic differentiation. It has been named as a marker for the loss of self-renewal in HSC, being expressed in ST-HSC and increasingly so in MPPs (Adolfsson *et al.*, 2001; Christensen and Weissman, 2002). Furthermore, isolated stimulation of hematopoietic progenitors and stem cells with *FLT3L* triggers predominantly monocytic differentiation (Gabbianelli *et al.*, 1995).

Our index patients' V194M-*FLT3* (rs146030737) variant and its effects on hematopoiesis are unknown. Multiple predictor programs SIFT and PMUT (Fröhling *et al.*, 2007) as well as PolyPhen-2 (<http://genetics.bwh.harvard.edu/pph2/>) (Adzhubei *et al.*, 2010) have come to different conclusions estimating it to have either no pathological significance or predicted it to be possibly damaging.

FLT1 on the other hand transcribes for the vascular endothelial growth factor receptor 1 (VEGFR1), a receptor tyrosine kinase with seven extracellular immunoglobulin like domains. It exists in a membrane bound as well as in a shortened, soluble form (Shibuya, 2001). *FLT1* is known to modulate embryonic angiogenesis and endothelial cell migration (Ji *et al.*, 2018). *FLT1* mRNA is

upregulated in activated monocytes and the binding of VEGF to *FLT1* promotes monocyte migration (Shibuya, 2001). Furthermore, *FLT1* expression was found to be stimulated by Wnt ligand in retinal myeloid cells, leading ultimately to a suppression of angiogenesis (Stefater *et al.*, 2011). The heterozygote missense mutation *FLT1* - P1201L (rs140861115) has been graded by PolyPhen-2 (<http://genetics.bwh.harvard.edu/pph2/>) (Adzhubei *et al.*, 2010) as possibly damaging.

FLT1 and *FLT3* share a similar structure as receptor tyrosine kinases (Shibuya, 2001) and are both located in close proximity on chromosome 13 at the positions 13q12.2 and 13q12.3, respectively.

Since the index patient's healthy mother shares the *FLT3*, but not *FLT1* SNP, we propose that the combination of the rare SNPs in *FLT1* and *FLT3* that were detected in the index CN patient, cause severe neutropenia and extensive monocytosis. Combined effects from *FLT1* and *FLT3* SNPs would be an explanation, why index CN patient and his healthy mother display different phenotypes despite sharing the genetic variant in *FLT3*. The healthy mother has WT *FLT1*.

One of the aims of this thesis was to evaluate the role of the identified *FLT3* mutation on the hematopoietic and myeloid differentiation. Evaluation of *FLT1* genetic defect was out of the scope of the study.

Considering the fact that the patients mother has the same heterozygous *FLT3* mutation without any pathological phenotype, it is safe to say that this mutation, located in the extracellular part of the receptor, does not have an activating and proliferative function. However, its role in hematopoietic differentiation remains to be studied. Interestingly, the V194M-*FLT3* mutation has been associated with a monocytic phenotype (Mousas *et al.*, 2017). It is not clear why the patient's mother does not display this phenotype and if compensatory epigenetic/genetic mechanisms are at work. The combined effects of multiple mutations in relevant hematological genes and pathways in our index patient have to be considered.

4.1 V194M-*FLT3* mutation and its implication on mRNA, protein and receptor expression levels

We have produced a wild type (WT)-*FLT3* vector with a blue fluorescence protein region for investigative purposes. Site directed mutagenesis allowed the introduction of the patient-specific V194M-*FLT3* mutation (performed by Dr. Houra Loghmani and Tessa Skroblyn, Skokowa Lab, Tübingen).

We transfected HEK-293FT cells with WT-*FLT3* vector, mutant *FLT3* vector as well as a negative control containing the vector backbone (empty vector). Interestingly, we found that we could detect high levels of *FLT3* mRNA in both WT and mutant samples (average $\Delta\Delta CT$ (n=2): no plasmid=1; empty plasmid=0.305; WT=1087.6; mutant=769.4). However, on protein level (Western blot, FACS) the mutant-*FLT3* was undetectable.

To explain these results, we considered an error in the antibody binding due to the extracellular character of the V194M mutation. However, this proves to be an unlikely explanation: Even though the supplier of the FACS-*FLT3*-antibody has not performed epitope mapping to establish the exact binding site (Email technical service BioLegend, J. Dickow, 21.05.2019) the western blot antibody binds to the Ser740 region of human *FLT3* (<https://www.cellsignal.com/products/primary-antibodies/FLT3-8f2-rabbit-mab/3462>) and thus interference with the mutation site is not to be expected.

We can assume therefore that the reduced *FLT3* protein expression does not display an error in antibody binding but rather a translational stop resulting in low protein levels or degradation of mutated protein.

Two systems regulate the degradation of proteins: the lysosomal system is mostly responsible for extracellular proteins, while 80-90% of intracellular proteins are disintegrated by the ubiquitin-proteasome system (UPS) (Ciechanover, 1994; Dou and Zonder, 2014). The 26S proteasome complex contains the cylindrical 20S proteasome and two regulatory 19S proteasomes (Borissenko and Groll, 2007). Bortezomib is an inhibitor of the 26S proteasome and binds to the chymotryptic-like active site (Borissenko and Groll, 2007). It is most widely used in the treatment of multiple myeloma and mantle cell lymphoma (Dou and Zonder, 2014). Our lab has found previously, that

Bortezomib inhibits LEF1 degradation thus improving granulopoiesis in CN patient cells (Gupta *et al.*, 2014). Whether the proteasome has any influence on V194M-*FLT3* expression is yet to be discovered.

4.2 Evaluation of the impact of Bortezomib on the expression level of V194M *FLT3*

To evaluate the importance of the 26S proteasome on the degradation of mutated V194M-*FLT3* protein, we treated *FLT3*- (WT, mutant and empty vector) transfected HEK293FT cells for 24h with increasing dose of Bortezomib (1µM, 10µM or 100µM) or the corresponding amount of DMSO as a vehicle control.

We found that the *FLT3* receptor expression in wildtype and V194M-*FLT3* transfected cells did not increase upon Bortezomib treatment. Moreover, we detected no V194M-*FLT3* protein in Bortezomib-, DMSO- or untreated groups.

Considering the broad spectrum of Bortezomib molarity (1-100µM) we used, compared to similar experiments (Gupta *et al.*, 2014; Shi *et al.*, 2017), and the lack of noticeable changes in protein expression, we conclude that the 26S proteasome is not responsible for the V194M-*FLT3* protein/receptor degradation. Though it is possible that the proteasomal system is only activated following an *FLT3* ligand -*FLT3* receptor interaction, there is a different ubiquitination system to be considered as well.

Interestingly, another tyrosine kinase receptors type III, the SCF receptor c-kit, has been identified in a ligand dependent ubiquitination and degradation process (Miyazawa *et al.*, 1994). The process of ubiquitination and degradation could be partially reversed by treatment with chloroquine in its capacity as lysosomal inhibitor (Miyazawa *et al.*, 1994). Membrane-bound receptors can be ubiquitinated intracellularly while the extracellular domains are open to endosomal and lysosomal recycling processes (Ciechanover, 1994). Under stress conditions, intracellular proteins can be degraded by the lysosomal system as well (Ciechanover, 1994). Considering our results which negate the importance of the 26S proteasome in *FLT3* degradation and the similarities of the tyrosine kinase receptor group III in structure and sequence, it is not far-fetched to hypothesize a lysosomal degradation system for the *FLT3* receptor.

Experiments to prove ubiquitination, lysosomal involvement and restitution through lysosomal blockage (chloroquine) would have to follow.

Newly discovered research techniques as e.g. generation of patient specific induced pluripotent stem cells offer the opportunity to explore early hematopoiesis in an *in vitro* model. Moreover, iPSC system, also partially artificial, provides us with almost unlimited amounts of hematopoietic cells at different stages of hematopoietic development for the downstream analysis of the functional significance of identified genetic defects during hematopoietic cell differentiation. It is particularly essential for the investigations of the inherited bone marrow syndromes, including severe congenital neutropenia, with very limited amounts of primary bone marrow hematopoietic cells available for the downstream analysis.

Therefore, the next aim of this thesis was to generate iPS cells of the index CN patient and to characterize hematopoietic and myeloid differentiation of these cells.

4.3 Production and characterization of patient derived iPSC

Patient specific iPSCs were generated using peripheral blood mononuclear cell (PBMNC) which were expanded in a cytokine containing stem cell expansion medium (2.2.12). For reprogramming, we used the classic transcription factor combination OSKM (Oct4, Sox2, Klf4, c-Myc) in a lentivirus. After 30 days of cytokine stimulation (bFGF, L-ascorbic acid, valproic acid), single colonies were collected and expanded (2.2.12, 2.2.13). We confirmed morphological characteristics of iPSCs in generated iPSC clones. To define pluripotency and stem cell characteristics, specific tests are essential:

- Positive alkaline phosphatase staining
- Pluripotency markers in undifferentiated iPSCs (RT-PCR and FACS)
- Differentiation potential into three germ layers (RT-PCR, FACS and immunocytochemistry)

Alkaline phosphatase (AP) staining has been used for years to identify undifferentiated human embryonic stem cells (hESC) (O'Connor *et al.*, 2008).

Since the discovery of iPSCs, it has also been applied to prove their embryonic stem cell characteristics (Takahashi *et al.*, 2007; Štefková, Procházková and Pacherník, 2015; Plotnikov *et al.*, 2017).

Markers for pluripotency (SSEA4, Tra1-60, SOX2, NANOG and DNMT3B) were chosen as recommended by the International Stem Cell Initiative which have defined a panel for human embryonic stem cell characterization (Adewumi *et al.*, 2007).

Instead of the classic xenografted teratoma assay, we proved the potential for tri-lineage differentiation (endoderm, mesoderm, ectoderm) by choosing endodermal (AFP, SOX17) and ectodermal (PAX6, TUBB3) markers and showed upregulated mRNA expression and positive protein expression in immunocytochemistry (Kanai-Azuma *et al.*, 2002; Adewumi *et al.*, 2007; Zhang *et al.*, 2010). Interestingly, some ectodermal markers as for example TUBB3 have recently been discredited in their specificity for differentiated iPSC colonies (Kuang *et al.*, 2019). However, the same lab found PAX6 to be a reliable ectodermal marker in iPSC-characterization (Kuang *et al.*, 2019), thus supporting the legitimacy of our characterization. We investigated mesodermal development through hematopoietic differentiation as measured by FACS (3.5). Tra1-60 and DNMT3B have been described to rule out partial reprogramming as iPSC-like cells can be very similar to fully reprogrammed cells in phenotype, AP staining and even gene expression (NANOG and SSEA4) (Chan *et al.*, 2009).

All of the above-mentioned tests indicate a successful and complete induction of the index CN patient derived pluripotent stem cells displaying all necessary characteristics (pluripotency and three germ layer differentiation potential) of iPSCs.

4.4 Comparison of the hematopoietic differentiation of the index CN patient vs. healthy donor iPSC

4.4.1 Early differentiation into mesodermal lineage: *FLT3* and *FLT1* expression analysis

The *FLT3* tyrosine kinase receptor is a crucial player in early hematopoietic development as evident in the high number of *FLT3* positive malignant but also normal hematopoietic progenitor cells. In human hematopoiesis, the *FLT3* expression starts to a low degree at the earliest LT-HSC level and increases towards the granulocyte/macrophage- and lymphoid progenitors (Kikushige *et al.*, 2008). Differences between human and murine receptor expression in early hematopoiesis have been discovered, not in the least in *FLT3* expression (Kikushige *et al.*, 2008; Doulatov *et al.*, 2012). Mice hematopoietic progenitors express *FLT3* later and much more selectively on multipotent progenitors (MPPs) and common lymphoid progenitors (Kikushige *et al.*, 2008).

To have an accurate impression of the early hematopoietic differentiation and *FLT3* expression of human cells carrying the *FLT3* V194M mutation, we compared embryoid body differentiation in index CN patient iPSCs and healthy donor cells.

We found an increase in *FLT3* expression within 24h of embryoid body formation (APEL-medium+bFGF+Rock inhibitor). Surprisingly, this increase occurred before the stimulation with BMP4 which is known to induce mesodermal differentiation (Brickman and Serup, 2017). *FLT3* expression remained high in most iPSC lines and started to decrease in (the healthy donor) suspension cells starting at day 13 (data not shown). We have noticed a reduced *FLT3* expression in V194M mutated cells compared to the WT-*FLT3* healthy donor cells at early stages of differentiation. As this is comparable to the reduced *FLT3* expression we have seen in the V194M-*FLT3* transfected HEK-293FT cell experiment, protein degradation is a likely explanation here as well. Experiments blocking the ubiquitination-degradation process as well as further repeat experiments are needed.

Interestingly, it has been discovered, that Wnt signaling regulates the internal structure and cell arrangement of EBs and is ultimately responsible for mesendodermal induction (ten Berge *et al.*, 2008). An increase in *FLT1* expression over the course of the first week of human EB differentiation, has been described before (Gerecht-Nir *et al.*, 2005).

We have found differences in *FLT1* expression in embryoid bodies which have shown the ability to attach and differentiate compared to those that have not. Overall, *FLT1* expression was higher in unattached EBs at day 1-8 of culture, especially on day 1. A premature loss of pluripotency in these iPSCs could be an explanation. Interestingly, *FLT1* has been suggested to negatively regulate VEGF levels and *FLT1*^{-/-} mice have shown an excess of hemangioblast formation (Shibuya, 2001). One could speculate that high levels of *FLT1* decrease VEGF levels which in turn hinders EB formation through downregulated Wnt signaling and furthermore leads to a lack of hemangioblast- and hematopoietic differentiation. While this remains highly speculative at this point, it would be interesting to evaluate the possible connection between Wnt mediated EB-axis formation, VEGF levels in medium and VEGFR1/*FLT1* expression in EBs in the future. Even though *FLT1* (rs 140861115, NM_002019.4) is one of the heterozygous SNPs of unknown significance that was detected in our index CN patient, we have seen no difference in *FLT1* cell surface expression at early stages of hematopoietic differentiation. It would be essential to study whether the mutated *FLT1* is functionally active.

4.4.2 Analysis of the late hematopoietic differentiation of iPSCs

Next, we compared myeloid differentiation of iPSCs derived for the index CN patient and healthy donor. The following are observations from one duplicate experiment. In this experiment, we gained a first impression on patient vs healthy donor myeloid differentiation as apparent in cell surface receptor expression profile and cell morphology.

Surface antigen profiles of myeloid progenitors and mature neutrophils, as well as monocyte progenitors and mature monocytes have been characterized previously by different labs (van Lochem *et al.*, 2004; Wood, 2004). Based on

these studies, we defined the CD45⁺CD11b⁺CD14⁺ population as monocytes and the CD45⁺CD11b⁺CD16⁺ population as mature neutrophils.

Most interestingly, in morphological analysis, we have found sufficient levels of neutrophils in the index CN patients' samples during the late stages of differentiation (day 26 – 29; 62 - 85% mature neutrophils) (Figure 21). Patient cells differentiated to neutrophils to the same degree as the healthy donor cells did. This is very interesting, considering the neutropenia and severe monocytosis in the index patient blood count. One possible explanation is that we used high doses of G-CSF in our cell culture. Similar to the elevated neutrophil production of the index patient upon high G-CSF doses, we might see a correction of neutrophil differentiation in the *in vitro* culture as well. To mirror the patients neutropenia, further experiments with decreased G-CSF doses in the *in vitro* culture are in order.

Cell morphology is not mirrored in the multicolor FACS analysis of the respective samples. Healthy donor and CN patient cell lines showed similar and rather high levels of CD45⁺CD11b⁺CD16⁺ neutrophils on day 19 of culture. Depending on the cytokine treatment between 7.5 - 21.8% neutrophils were detected in healthy donor and between 18.5 - 25.5% in the index CN patient (Figure 20). However, on day 26 – 29 of differentiation, the CD45⁺CD11b⁺CD16⁺ cell population decreased in all cell lines, leaving only a small population in healthy donor and none in patient cells. This discrepancy between cell morphology and cell surface marker is interesting. Further so, as cell viability and the percentage of CD45⁺ and CD11b⁺ cells were continuously high in late differentiation (day 26) (Figure 19C). While neutrophils display a surprising plasticity in their surface profile, depending on their activation status and in response to cell-cell interactions, three markers are known to be neutrophil specific: CD11b, CD16 and CD66b (Scapini and Cassatella, 2014; Lakschevitz *et al.*, 2016). Cell sorting using a combination of these three antigens yielded a high purity of neutrophils (Lakschevitz *et al.*, 2016). However, Weston et al. found that CN patients treated with G-CSF showed lower expression levels of CD16 and higher levels of CD11b on their neutrophils (Weston R. F.;Axtell, R.;Balazovich, K.;Stewart, J.;Locey, B.

J.; Mayo-Bond, L.; Loos, P.; Hutchinson, R.; Boxer, L. A., 1991). This was confirmed in the works of Elsner et al. who found constant CD11b expression, reduced CD16 expression and elevated CD14 expression in CN patient neutrophils (Elsner *et al.*, 1992). This is in line with our observations of a high percentage of CD11b positive cells, while having much less CD16 positive cells. (Figure 20). However, this was regardless of the cytokine stimulation with or without G-CSF. We are suspecting an autocrine/paracrine G-CSF stimulation as aberrant myeloid cells have been known for (Jiang *et al.*, 1999). Since we never changed the complete medium in our cell culture, always keeping half of the old and half new medium (2.2.14), an accumulation of cytokines might be an explanation for the decrease in CD14 and CD16 positivity in late differentiation (day 26) as well (Figure 19C). Analysis of the cytokine spectrum in the cell medium would have to follow.

Immunophenotyping of G-CSF treated healthy donor peripheral blood cells has shown an increase of the CD11b⁺ population in the CD45⁺ gate compared to untreated donor samples (34.9%→90.1%) (Luyckx *et al.*, 2012). We have found an increase of CD45⁺ cells and subsequently CD11b⁺ cells in healthy donor IL3-GCSF treated samples as well (Figure 20B). However, while the CD45⁺ cell count increased further upon *FLT3L* treatment, the number of CD11b⁺ healthy donor cells decreased (Figure 20C). The patient samples reacted with an increase in CD45⁺ cells upon G-CSF treatment as well, though the amounts of CD11b⁺ cells stayed similar in the IL3, IL3-GCSF and IL3-GCSF-*FLT3L* treatment groups (Figure 20). *FLT3L* treatment had no impact on myeloid differentiation of patient iPSCs (Figure 20B/C).

Contrary to Luyckx et al., high CD11b⁺ cell counts were measurable regardless of G-CSF deprivation (=IL3 treatment) or G-CSF treatment. Again, as mentioned above, an autocrine/paracrine G-CSF stimulation could be an explanation.

Overall we conclude that in the ongoing studies more neutrophil-specific surface markers are needed for reliable cell identification.

Analysis of monocytic differentiation revealed that monocytic development showed the maximum at day 19 of differentiation and was elevated in the index

CN patient iPSC lines. Thus, we have found 42.4% of CD11b⁺CD14⁺ cells in the CD45⁺ gate in healthy donor cells and in the patient derived cells 60% (OKPBL2) / 46,3% (OKPBL6) of the CD45⁺ cells were CD11b⁺CD14⁺ monocytes. This is in agreement with the exceptionally high absolute monocyte counts (AMC) in the peripheral blood of this patient.

Morphologically, in all the patient groups as well as the G-CSF deprived healthy donor group ("IL3" CD34IPSC16), we found a similar pattern of monocytic differentiation with a maximum around day 19 (Figure 22). The addition of G-CSF shifted monocytic development to a latter point in differentiation in healthy donor cells (days 29 - 32) (Figure 22).

We must question whether parameter of our experiments namely cell maintenance and cytokine stimulation are responsible for this discrepancy between morphology and immunophenotype. While some labs reculture their suspension cells in a M-CSF or G-CSF focused medium to improve monocyte or granulocyte yield (Lachmann *et al.*, 2015; Pittermann *et al.*, 2017), we refrained from doing so and analyzed cell morphology and immunophenotype directly after collection. Our lab has established a protocol for hematopoietic differentiation using initial embryoid body formation and mesodermal differentiation of EBs induced by bFGF + BMP4 + VEGF + SCF + IL3 followed by myeloid differentiation of hematopoietic cells that is triggered by IL3 and G-CSF (Dannenmann *et al.*, 2019). Suspension cells were collected and directly analyzed (morphology and surface antigen profile) displaying the typical CN phenotype with smaller percentages of granulocytic cells in the healthy donor samples (up to 20%) (Dannenmann *et al.*, 2019). It remains unclear, why we were not able to reproduce CN typical cell distribution in our CN patient samples. One possible explanation is the protocol modification to change only half of the medium every three days thus allowing existing cytokine stimulation to proceed. Therefore, measurement of the cytokine profile in the medium of these samples would be interesting to detect any possible autocrine stimulation and cytokine accumulation. Furthermore, functional neutrophil assays to establish neutrophil-like cells as active players of the innate immune system would be of interest.

4.5 Conclusion

In course of this thesis, we have pursued research to broaden the understanding of myeloid-specific decision making. We have studied the genotype of a CN patient with agranulocytosis and an exceptionally high monocyte count and have found a combination of rare *FLT3* SNP (V194M, rs 146030737) and *FLT1* SNP (P1201L, rs 140861115). To evaluate the role of *FLT3* SNP on *FLT3* mRNA and protein expression, we have produced WT-*FLT3* and V194M-*FLT3* mutated vectors. We found that the V194M-*FLT3* SNP affects its protein expression as transfected cells express *FLT3* mRNA, but no *FLT3* protein was detectable. Furthermore, we precluded the possibility, that proteasome inhibition with Bortezomib might repair protein and receptor expression.

We have successfully established two new CN patient derived pluripotent stem cell lines. We have studied *FLT1* and *FLT3* expression in early embryoid bodies. There we found that we were able to distinguish successful and disintegrating embryoid bodies early on when comparing *FLT1* expression. We found that *FLT3* was not as prominently expressed in patient EBs than in healthy donor EBs.

We have modified an established myeloid differentiation protocol of iPSCs to compare patient and healthy donor hematopoietic differentiation. Morphologically, patient cells differentiated similarly to healthy donor cells. The neutrophil to monocyte ratio was in agreement with the reference peripheral blood count (Isermann, 2013). Interestingly, we found differences in cell morphology and the expected cell surface marker expression. Measuring the surface antigen expression, we found high numbers of CD45 and CD11b positive cells. The cell marker CD14, CD15 and CD16 on the other hand were only temporarily expressed on these cells on day 19 of embryoid body differentiation. Considering the surface marker expression on day 19, the *in vitro* patient cell lines mirrored the monocytosis the patient is known for, while the morphological analysis suggested a sufficient neutrophil cell count.

In continuation of our work, several paths are open to be pursued:

The impact of lysosomal inhibitors on the destruction process of V194M-*FLT3* protein as well as evidence of ubiquitination. Furthermore, WT- and mutant *FLT3* virus has been produced to allow transduction of CD34⁺ cells and comparison of differentiation carrying this particular mutation. Moreover, further experiments with the patient derived iPSC are of interest with special consideration to the morphology and surface antigen profile. CRISPR/Cas9-based correction of the V194M-*FLT3* mutation and the evaluation of the impact on differentiation of this cell line could follow. Introduction of the *FLT3* and *FLT1* SPNs in healthy donor iPSCs would be an alternative. An evaluation of the frequency of *FLT3* and *FLT1* mutations in CN patients with unknown genetic defects as well as further analysis of the combined effect of *FLT3* and *FLT1* SNPs are of importance.

5 Abstract/Zusammenfassung

5.1 Abstract

Severe congenital neutropenia (CN) is a heterogenous group of disorders of the myeloid differentiation, defined by a maturation arrest of granulopoiesis at the promyelocyte/myelocyte stage and an absolute neutrophil count (ANC) of $< 0,5 \times 10^9/L$. Furthermore, characteristic for CN patients are elevated monocyte counts. The reason for this shift in myelomonocytic differentiation is being studied in attempts for better understanding of myeloid decision making beyond the effects of the PU.1 to C/EBP α transcription factors expression ratio.

We analyzed an index CN patient with an unusually strong shift from granulocytic to monocytic development and no mutations in the known CN-associated genes (e.g. *HAX1*, *ELANE*, *G6PC3*, *JAGN1*, *SRP54*). Next generation sequencing has revealed rare single nucleotide polymorphisms in the *FLT3* and *FLT1* genes. To evaluate the role of the V194M-*FLT3* variant on the myelomonocytic development, we produced expression constructs with wild type and V194M mutated *FLT3*. We found the mutated *FLT3* to be inadequately expressed on protein level. Furthermore, we found that inhibition of the 26S proteasome through Bortezomib treatment does not increase V194M-*FLT3*

protein expression. We concluded that the degradation process of mutated *FLT3* seems to be independent of the functionality of the proteasomes.

Furthermore, we successfully established two new induced pluripotent stem cell lines (iPSC) from the index CN patient to study early hematopoietic development. Multiple characterization experiments have shown this cell line to bear all characteristics of iPSCs. We have found *FLT3* to be expressed less in the early embryoid body (EB) cells derived from patient iPSCs compared to healthy donor EBs. Late hematopoietic differentiation of index patient and healthy donor iPSCs have shown disparities in morphology vs. antigen expression profile: Both healthy donor and index patient iPSCs differentiation results in sufficient neutrophil production. However, after day 19 of EB formation, cells, while being viable, CD45 and CD11b positive, express limited CD15 and CD16. Reasons might be found in the specific cytokine stimulation and cell maintenance protocols. The monocytosis, the index patient is known for, is reflected in the surface marker analysis of the *in vitro* cell lines.

5.2 Zusammenfassung

Schwere Kongenitale Neutropenie (CN) ist eine heterogene Krankheitsentität aus dem Bereich der myeloiden Differenzierung, welche über einen Entwicklungsstopp auf Stufe der Promyelozyten/Myelozyten, eine absolute Neutrophilenzahl (ANZ) von $< 0,5 \times 10^9/L$, sowie erhöhte Monozytenzahlen definiert ist. Durch ihre Erforschung werden neue Einblicke in das Verständnis der myeloiden Differenzierung über die Effekte der Transkriptionsfaktoren PU.1/c/EBP α hinaus gewonnen.

Wir stellen hier einen CN-Indexpatienten mit ungewöhnlich ausgeprägter Monozytose vor, der des Weiteren keine Mutationen in den CN-typischen Genen (z.B. *HAX1*, *ELANE*, *G6PC3*, *JAGN1*, *SRP54*) vorweist. Über Next generation sequencing konnten eine Reihe von seltenen Genvariationen aufgedeckt werden, unter anderem single nucleotide polymorphisms in dem *FLT3* und *FLT1* Gen. Um den Einfluss der V194M-*FLT3* Variation auf die myelomonozytäre Entwicklung zu ermitteln, entwickelten wir einen Wildtyp und V194M mutierten Vektor. Wir stellten fest, dass V194M-*FLT3* Rezeptor und

Protein deutlich geringer exprimiert wird als Wild-Typ *FLT3*. Eine Inhibition des 26S Proteasoms durch Bortezomib korrigiert die V194M-*FLT3* Protein Expression nicht. Wir schlussfolgerten, dass der Degradierungsprozess des mutierten *FLT3* unabhängig von der Funktionalität des Proteasoms ist.

Zusätzlich etablierten wir zwei neue induzierte pluripotente Stammzelllinien (iPSC) von somatischen Indexpatientenzellen und verglichen die frühe hämatopoetische Entwicklung mit gesunden Spenderzellen. Multiple Charakterisierungsexperimente bestätigten, dass die neuen iPSC Linien alle Merkmale von iPS Zellen tragen.

Wir sahen, dass *FLT3* in Embryoid Body (EB) Zellen des Indexpatientens in der frühen Differenzierung geringer exprimiert war als in gesunden Spender EBs.

In der späten hämatopoetischen Differenzierung unterschied sich die Zellmorphologie mit der Oberflächenmarkerexpression der Suspensionszellen: Morphologisch differenzierten sowohl gesunde Spender- als auch Indexpatienten iPS Zellen zu einem ausreichenden Anteil zu neutrophilen Granulozyten. Jedoch nach Tag 19 der EB Formation exprimierten die meisten lebensfähige CD45⁺CD11b⁺ Zellen nur zu einem geringem Anteil CD15 oder CD16. Gründe dafür können gegebenenfalls in der Zytokin Stimulation und den Differenzierungsprotokollen gefunden werden.

6 References

Adewumi, O. *et al.* (2007) 'Characterization of human embryonic stem cell lines by the International Stem Cell Initiative', *Nature Biotechnology*. doi: 10.1038/nbt1318.

Adolfsson, J. *et al.* (2001) 'Upregulation of Flt3 expression within the bone marrow Lin-Sca1+c-kit+ stem cell compartment is accompanied by loss of self-renewal capacity', *Immunity*. doi: 10.1016/S1074-7613(01)00220-5.

Adolfsson, J. *et al.* (2005) 'Identification of Flt3 + lympho-myeloid stem cells lacking erythro-megakaryocytic potential: A revised road map for adult blood lineage commitment', *Cell*. doi: 10.1016/j.cell.2005.02.013.

Adzhubei, I. A. *et al.* (2010) 'A method and server for predicting damaging missense mutations', *Nature Methods*. doi: 10.1038/nmeth0410-248.

Agnès, F. *et al.* (1994) 'Genomic structure of the downstream part of the human FLT3 gene: exon/intron structure conservation among genes encoding receptor tyrosine kinases (RTK) of subclass III', *Gene*. doi: 10.1016/0378-1119(94)90021-3.

Akashi, K. *et al.* (2000) 'A clonogenic common myeloid progenitor that gives rise to all myeloid lineages', *Nature*, 404(6774), pp. 193–197. doi: 10.1038/35004599.

Attar, A. (2014) 'Changes in the Cell Surface Markers During Normal Hematopoiesis: A Guide to Cell Isolation', *Global Journal of Hematology and Blood Transfusion*. doi: 10.15379/2408-9877.2014.01.01.4.

Avilion, A. A. *et al.* (2003) 'Multipotent cell lineages in early mouse development depend on SOX2 function', *Genes and Development*. doi: 10.1101/gad.224503.

Bacher, U. *et al.* (2008) 'Prognostic relevance of FLT3-TKD mutations in AML: The combination matters an analysis of 3082 patients', *Blood*. doi: 10.1182/blood-2007-05-091215.

Back, J. *et al.* (2005) 'Visualizing PU.1 activity during hematopoiesis', *Experimental Hematology*. doi: 10.1016/j.exphem.2004.12.010.

Barreda, D. R., Hanington, P. C. and Belosevic, M. (2004) 'Regulation of myeloid development and function by colony stimulating factors', *Developmental and Comparative Immunology*. doi: 10.1016/j.dci.2003.09.010.

ten Berge, D. *et al.* (2008) 'Wnt Signaling Mediates Self-Organization and Axis Formation in Embryoid Bodies', *Cell Stem Cell*, 3(5), pp. 508–518. doi: 10.1016/j.stem.2008.09.013.

Bernard, T. *et al.* (1998) 'Mutations of the granulocyte-colony stimulating factor receptor in patients with severe congenital neutropenia are not required for transformation to acute myeloid leukaemia and may be a bystander phenomenon', *British Journal of Haematology*. doi: 10.1046/j.1365-2141.1998.00652.x.

Bonilla, M. A. *et al.* (1989) 'Effects of recombinant human granulocyte colony-stimulating factor on neutropenia in patients with congenital agranulocytosis', *New England Journal of Medicine*.

Bonilla, M. A. *et al.* (1994) 'Long-term safety of treatment with recombinant human granulocyte colony-stimulating factor (r-metHuG-CSF) in patients with severe congenital neutropenias', *British Journal of Haematology*. doi: 10.1111/j.1365-2141.1994.tb05110.x.

Borissenko, L. and Groll, M. (2007) '20S Proteasome and Its Inhibitors: Crystallographic Knowledge for Drug Development', *Chemical Reviews*. doi: 10.1021/cr0502504.

- Borregaard, N. (2010) 'Neutrophils, from Marrow to Microbes', *Immunity*. doi: 10.1016/j.immuni.2010.11.011.
- Brickman, J. M. and Serup, P. (2017) 'Properties of embryoid bodies', *Wiley Interdisciplinary Reviews: Developmental Biology*. doi: 10.1002/wdev.259.
- Cartwright, P. (2005) 'LIF/STAT3 controls ES cell self-renewal and pluripotency by a Myc-dependent mechanism', *Development*. doi: 10.1242/dev.01670.
- Chan, E. M. *et al.* (2009) 'Live cell imaging distinguishes bona fide human iPS cells from partially reprogrammed cells.', *Nature biotechnology*, 27(11), pp. 1033–7. doi: 10.1038/nbt.1580.
- Christensen, J. L. and Weissman, I. L. (2002) 'Flk-2 is a marker in hematopoietic stem cell differentiation: A simple method to isolate long-term stem cells', *Proceedings of the National Academy of Sciences*. doi: 10.1073/pnas.261562798.
- Ciechanover, A. (1994) 'The ubiquitin-proteasome proteolytic pathway', *Cell*. doi: 10.1016/0092-8674(94)90396-4.
- Dahl, R. *et al.* (2003) 'Regulation of macrophage and neutrophil cell fates by the PU.1:C/EBPalpha ratio and granulocyte colony-stimulating factor', *Nat Immunol*, 4(10), pp. 1029–1036. doi: 10.1038/ni973.
- Dakic, A. *et al.* (2005) 'PU.1 regulates the commitment of adult hematopoietic progenitors and restricts granulopoiesis', *The Journal of Experimental Medicine*, 201(9), pp. 1487–1502. doi: 10.1084/jem.20050075.
- Dale, D. C. *et al.* (1993) 'A randomized controlled phase III trial of recombinant human granulocyte colony-stimulating factor (filgrastim) for treatment of severe chronic neutropenia.', *Blood*, 81(10), pp. 2496–2502.
- Dale, D. C. *et al.* (2000) 'Mutations in the gene encoding neutrophil elastase in congenital and cyclic neutropenia.[see comment]', *Blood*, 96(7), pp. 2317–2322.
- Dale, D. C. *et al.* (2003) 'Severe chronic neutropenia: Treatment and follow-up of patients in the Severe Chronic Neutropenia International Registry', *American Journal of Hematology*. doi: 10.1002/ajh.10255.
- Dancey, J. T. *et al.* (1976) 'Neutrophil kinetics in man.', *Journal of Clinical Investigation*, 58(3), pp. 705–715. doi: 10.1172/JCI108517.
- Dannenmann, B. *et al.* (2019) 'Human iPSC-based model of severe congenital neutropenia reveals elevated UPR and DNA damage in CD34 + cells preceding leukemic transformation', *Experimental Hematology*. doi: 10.1016/j.exphem.2018.12.006.
- DeKoter, R. P. and Singh, H. (2000) 'Regulation of B lymphocyte and macrophage development by graded expression of PU.1', *Science*. doi:

10.1126/science.288.5470.1439.

Diecke, S. *et al.* (2014) 'Recent technological updates and clinical applications of induced pluripotent stem cells', *Korean Journal of Internal Medicine*, pp. 547–557. doi: 10.3904/kjim.2014.29.5.547.

Donadieu, J. *et al.* (2013) 'Epidemiology of Congenital Neutropenia', *Hematology/Oncology Clinics of North America*, pp. 1–17. doi: 10.1016/j.hoc.2012.11.003.

Donadieu, J. *et al.* (2017) 'Congenital neutropenia in the era of genomics: classification, diagnosis, and natural history', *British Journal of Haematology*. doi: 10.1111/bjh.14887.

Dong, F. *et al.* (1995) 'Mutations in the Gene for the Granulocyte Colony-Stimulating–Factor Receptor in Patients With Acute Myeloid Leukemia Preceded By Severe Congenital Neutropenia', *New England Journal of Medicine*. doi: 10.1056/NEJM199508243330804.

Dong, F. *et al.* (1998) 'Stimulation of Stat5 by granulocyte colony-stimulating factor (G-CSF) is modulated by two distinct cytoplasmic regions of the G-CSF receptor.', *Journal of immunology (Baltimore, Md. : 1950)*.

Dou, Q. P. and Zonder, J. A. (2014) 'Overview of proteasome inhibitor-based anti-cancer therapies: perspective on bortezomib and second generation proteasome inhibitors versus future generation inhibitors of ubiquitin-proteasome system.', *Current cancer drug targets*.

Doulatov, S. *et al.* (2012) 'Hematopoiesis: A human perspective', *Cell Stem Cell*. doi: 10.1016/j.stem.2012.01.006.

Drissen, R. *et al.* (2016) 'Distinct myeloid progenitor-differentiation pathways identified through single-cell RNA sequencing', *Nature Immunology*. doi: 10.1038/ni.3412.

Elsner, J. *et al.* (1992) 'Altered function and surface marker expression of neutrophils induced by rhG-CSF treatment in severe congenital neutropenia', *European Journal of Haematology*. doi: 10.1111/j.1600-0609.1992.tb01787.x.

Fioredda, F. *et al.* (2015) 'Stem cell transplantation in severe congenital neutropenia: An analysis from the European Society for Blood and Marrow Transplantation', *Blood*, 126(16). doi: 10.1182/blood-2015-02-628859.

Forsberg, E. C. *et al.* (2006) 'New Evidence Supporting Megakaryocyte-Erythrocyte Potential of Flk2/Flt3+ Multipotent Hematopoietic Progenitors', *Cell*. doi: 10.1016/j.cell.2006.06.037.

Fröhling, S. *et al.* (2007) 'Identification of Driver and Passenger Mutations of FLT3 by High-Throughput DNA Sequence Analysis and Functional Assessment of Candidate Alleles', *Cancer Cell*, 12(6), pp. 501–513. doi:

10.1016/j.ccr.2007.11.005.

Gabbianelli, M. *et al.* (1995) 'Multi-level effects of flt3 ligand on human hematopoiesis: expansion of putative stem cells and proliferation of granulomonocytic progenitors/monocytic precursors', *Blood*, 86(5), pp. 1661 LP – 1670. Available at: <http://www.bloodjournal.org/content/86/5/1661.abstract>.

Gekas, C. *et al.* (2005) 'The placenta is a niche for hematopoietic stem cells', *Developmental Cell*. doi: 10.1016/j.devcel.2004.12.016.

Gerecht-Nir, S. *et al.* (2005) 'Vascular gene expression and phenotypic correlation during differentiation of human embryonic stem cells', *Developmental Dynamics*, 232(2), pp. 487–497. doi: 10.1002/dvdy.20247.

Germeshausen, M. *et al.* (2010) 'Digenic mutations in severe congenital neutropenia', *Haematologica*, 95(7), pp. 1207–1210. doi: 10.3324/haematol.2009.017665.

Gilman, P. ., Jackson, D. . and Guild, H. . (1970) 'Congenital agranulocytosis: prolonged survival and terminal acute leukemia.', *Blood*, 36(5), pp. 576–585. Available at: <http://www.embase.com/search/results?subaction=viewrecord&from=export&id=L90477974>.

Gupta, K. *et al.* (2014) 'Bortezomib inhibits STAT5-dependent degradation of LEF-1, inducing granulocytic differentiation in congenital neutropenia CD34+ cells', *Blood*, 123(16), pp. 2550–2561. doi: 10.1182/blood-2012-09-456889.

Hayakawa, F. *et al.* (2000) 'Tandem-duplicated Flt3 constitutively activates STAT5 and MAP kinase and introduces autonomous cell growth in IL-3-dependent cell lines', *Oncogene*. doi: 10.1038/sj.onc.1203354.

Hirai, H. *et al.* (2006) 'C/EBP β is required for "emergency" granulopoiesis', *Nature Immunology*, 7(7), pp. 732–739. doi: 10.1038/ni1354.

Hoang, T., Lambert, J. A. and Martin, R. (2016) 'SCL/TAL1 in Hematopoiesis and Cellular Reprogramming', in *Current Topics in Developmental Biology*. doi: 10.1016/bs.ctdb.2016.01.004.

Hoffmann, D. *et al.* (2017) 'Detailed comparison of retroviral vectors and promoter configurations for stable and high transgene expression in human induced pluripotent stem cells', *Gene Therapy*. doi: 10.1038/gt.2017.20.

Horwitz, M. S. *et al.* (2007) 'Neutrophil elastase in cyclic and severe congenital neutropenia', Available at: <http://bloodjournal.hematologylibrary.org/content/109/5/1817.short>.

Horwitz, M. S. *et al.* (2013) 'ELANE Mutations in Cyclic and Severe Congenital Neutropenia. Genetics and Pathophysiology.', *Hematology/Oncology Clinics of North America*, pp. 19–41. doi: 10.1016/j.hoc.2012.10.004.

Ichikawa, M. *et al.* (2004) 'AML-1 is required for megakaryocytic maturation and lymphocytic differentiation, but not for maintenance of hematopoietic stem cells in adult hematopoiesis', *Nature Medicine*. doi: 10.1038/nm997.

Imashuku, S. *et al.* (1995) 'Myelodysplasia and acute myeloid leukaemia in cases of aplastic anaemia and congenital neutropenia following G-CSF administration', *British Journal of Haematology*. doi: 10.1111/j.1365-2141.1995.tb08928.x.

Isermann, B. (2013) 'Lexikon der Medizinischen Laboratoriumsdiagnostik', *Laboratoriumsmedizin*, 37(3). doi: 10.1515/labmed-2013-0032.

Ji, S. *et al.* (2018) 'FMS-like tyrosine kinase 1 (FLT1) is a key regulator of fetoplacental endothelial cell migration and angiogenesis', *Placenta*. doi: 10.1016/j.placenta.2018.08.004.

Jiang, X. *et al.* (1999) 'Autocrine production and action of IL-3 and granulocyte colony-stimulating factor in chronic myeloid leukemia.', *Proceedings of the National Academy of Sciences of the United States of America*, 96(22), pp. 12804–9. doi: 10.1073/pnas.96.22.12804.

Kalra, R. *et al.* (1995) 'Monosomy 7 and activating RAS mutations accompany malignant transformation in patients with congenital neutropenia.', *Blood*.

Kanai-Azuma, M. *et al.* (2002) 'Depletion of definitive gut endoderm in Sox17-null mutant mice.', *Development (Cambridge, England)*.

Karlsson, J. *et al.* (2007) 'Low plasma levels of the protein pro-LL-37 as an early indication of severe disease in patients with chronic neutropenia', *British Journal of Haematology*. doi: 10.1111/j.1365-2141.2007.06530.x.

Kayser, S. *et al.* (2009) 'Insertion of FLT3 internal tandem duplication in the tyrosine kinase domain-1 is associated with resistance to chemotherapy and inferior outcome', *Blood*. doi: 10.1182/blood-2009-03-209999.

Kikushige, Y. *et al.* (2008) 'Human Flt3 is expressed at the hematopoietic stem cell and the granulocyte/macrophage progenitor stages to maintain cell survival.', *Journal of immunology (Baltimore, Md. : 1950)*.

Kim, S.-I. *et al.* (2015) 'KLF4 N-Terminal Variance Modulates Induced Reprogramming to Pluripotency', *Stem Cell Reports*, 4(4), pp. 727–743. doi: 10.1016/j.stemcr.2015.02.004.

Kiyoi, H. *et al.* (2002) 'Mechanism of constitutive activation of FLT3 with internal tandem duplication in the juxtamembrane domain', *Oncogene*. doi: 10.1038/sj.onc.1205332.

Klein, C. *et al.* (2007) 'HAX1 deficiency causes autosomal recessive severe congenital neutropenia (Kostmann disease).', *Nature genetics*, 39(1), pp. 86–92. doi: 10.1038/ng1940.

Kolaczowska, E. and Kubes, P. (2013) 'Neutrophil recruitment and function in health and inflammation', *Nature Reviews Immunology*. doi: 10.1038/nri3399.

Köllner, I. *et al.* (2006) 'Mutations in neutrophil elastase causing congenital neutropenia lead to cytoplasmic protein accumulation and induction of the unfolded protein response', *Blood*, 108(2), pp. 493–500. doi: 10.1182/blood-2005-11-4689.

Kostmann, R. (1956) 'Infantile Genetic Agranulocytosis (Agranulocytosis infantilis hereditaria) A New Recessive Lethal Disease in Man', *Acta Paediatrica*, 45(3), pp. 309–310. doi: 10.1111/j.1651-2227.1956.tb06875.x.

Kostmann, R. (1975) 'Infantile Genetic Agranulocytosis', *Acta Paediatrica*, pp. 362–368. doi: 10.1111/j.1651-2227.1975.tb03847.x.

Kuang, Y. L. *et al.* (2019) 'Evaluation of commonly used ectoderm markers in iPSC trilineage differentiation', *Stem Cell Research*. doi: 10.1016/j.scr.2019.101434.

Lachmann, N. *et al.* (2014) 'Gene correction of human induced pluripotent stem cells repairs the cellular phenotype in pulmonary alveolar proteinosis', *American Journal of Respiratory and Critical Care Medicine*. doi: 10.1164/rccm.201306-1012OC.

Lachmann, N. *et al.* (2015) 'Large-scale hematopoietic differentiation of human induced pluripotent stem cells provides granulocytes or macrophages for cell replacement therapies', *Stem Cell Reports*, 4(2), pp. 282–296. doi: 10.1016/j.stemcr.2015.01.005.

Lakschevitz, F. S. *et al.* (2016) 'Identification of neutrophil surface marker changes in health and inflammation using high-throughput screening flow cytometry', *Experimental Cell Research*. doi: 10.1016/j.yexcr.2016.03.007.

Laslo, P. *et al.* (2006) 'Multilineage Transcriptional Priming and Determination of Alternate Hematopoietic Cell Fates', *Cell*. doi: 10.1016/j.cell.2006.06.052.

Li, H. L. *et al.* (2016) 'Efficient genomic correction methods in human iPSC cells using CRISPR–Cas9 system', *Methods*, 101, pp. 27–35. doi: 10.1016/j.ymeth.2015.10.015.

Li, Y. *et al.* (2005) 'Murine embryonic stem cell differentiation is promoted by SOCS-3 and inhibited by the zinc finger transcription factor Klf4', *Blood*. doi: 10.1182/blood-2004-07-2681.

van Lochem, E. G. *et al.* (2004) 'Immunophenotypic differentiation patterns of normal hematopoiesis in human bone marrow: Reference patterns for age-related changes and disease-induced shifts', *Cytometry*. doi: 10.1002/cyto.b.20008.

Luyckx, A. *et al.* (2012) 'G-CSF stem cell mobilization in human donors induces

polymorphonuclear and mononuclear myeloid-derived suppressor cells', *Clinical Immunology*. doi: 10.1016/j.clim.2012.01.011.

MACHEREY-NAGEL (2020) 'User manual Bioanalysis', (February). Available at: <https://www.mn-net.com/media/pdf/18/eb/8f/Instruction-NucleoBond-Xtra-EF.pdf>.

Mackarehtschian, K. *et al.* (1995) 'Targeted disruption of the flk2/flt3 gene leads to deficiencies in primitive hematopoietic progenitors', *Immunity*. doi: 10.1016/1074-7613(95)90167-1.

Makaryan, V. *et al.* (2017) 'Elastase inhibitors as potential therapies for ELANE-associated neutropenia', *Journal of Leukocyte Biology*. doi: 10.1189/jlb.5A1016-445R.

Manz, M. G. and Boettcher, S. (2014) 'Emergency granulopoiesis', *Nature Reviews Immunology*, 14(5), pp. 302–314. doi: 10.1038/nri3660.

Mikkola, H. K. A. *et al.* (2003) 'Haematopoietic stem cells retain long-term repopulating activity and multipotency in the absence of stem-cell leukaemia SCL/tal-1 gene', *Nature*. doi: 10.1038/nature01345.

Miller, R. W. (1969) 'Childhood cancer and congenital defects a study of U.S. Death certificates during the period 1960–1966', *Pediatric Research*. doi: 10.1203/00006450-196909000-00001.

Miyazawa, K. *et al.* (1994) 'Ligand-dependent polyubiquitination of c-kit gene product: a possible mechanism of receptor down modulation in M07e cells', *Blood*.

Morrison, S. J. and Weissman, I. L. (1994) 'The long-term repopulating subset of hematopoietic stem cells is deterministic and isolatable by phenotype', *Immunity*. doi: 10.1016/1074-7613(94)90037-X.

Mousas, A. *et al.* (2017) 'Rare coding variants pinpoint genes that control human hematological traits', *PLoS Genetics*. doi: 10.1371/journal.pgen.1006925.

Müller, A. M. *et al.* (1994) 'Development of hematopoietic stem cell activity in the mouse embryo', *Immunity*. doi: 10.1016/1074-7613(94)90081-7.

Nayak, R. C. *et al.* (2015) 'Pathogenesis of ELANE-mutant severe neutropenia revealed by induced pluripotent stem cells', *Journal of Clinical Investigation*, 125(8), pp. 3103–3116. doi: 10.1172/JCI80924.

Nutt, S. L. *et al.* (2005) 'Dynamic regulation of PU.1 expression in multipotent hematopoietic progenitors', *The Journal of Experimental Medicine*. doi: 10.1084/jem.20041535.

O'Connor, M. D. *et al.* (2008) 'Alkaline Phosphatase-Positive Colony Formation

Is a Sensitive, Specific, and Quantitative Indicator of Undifferentiated Human Embryonic Stem Cells', *Stem Cells*. doi: 10.1634/stemcells.2007-0801.

Okuda, T. *et al.* (1996) 'AML1, the target of multiple chromosomal translocations in human leukemia, is essential for normal fetal liver hematopoiesis', *Cell*. doi: 10.1016/S0092-8674(00)80986-1.

Orkin, S. H. and Zon, L. I. (2008) 'Hematopoiesis: An Evolving Paradigm for Stem Cell Biology', *Cell*. doi: 10.1016/j.cell.2008.01.025.

Papaemmanuil, E. *et al.* (2016) 'Genomic Classification and Prognosis in Acute Myeloid Leukemia.', *The New England journal of medicine*. doi: 10.1056/NEJMoa1516192.

Patnaik, M. M. (2018) 'The importance of FLT3 mutational analysis in acute myeloid leukemia', *Leukemia and Lymphoma*. doi: 10.1080/10428194.2017.1399312.

Pc, N. and Bac, N. (2011) 'Plasmid DNA Purification User Manual Plasmid DNA Purification', (January). Available at: <https://www.mn-net.com/media/pdf/0c/20/aa/Instruction-NucleoSpin-Plasmid-Easypure.pdf>.

Pittermann, E. *et al.* (2017) 'Gene correction of HAX1 reversed Kostmann disease phenotype in patient-specific induced pluripotent stem cells', *Blood Advances*, 1(14), pp. 903–914. doi: 10.1182/bloodadvances.2016003798.

Plotnikov, A. *et al.* (2017) 'A multiplexed screening method for pluripotency', *Stem Cell Research*. doi: 10.1016/j.scr.2017.07.014.

Pütsep, K. *et al.* (2002) 'Deficiency of antibacterial peptides in patients with morbus Kostmann: An observation study', *Lancet*, 360(9340), pp. 1144–1149. doi: 10.1016/S0140-6736(02)11201-3.

Radomska, H. S. *et al.* (1998) 'CCAAT/Enhancer Binding Protein α Is a Regulatory Switch Sufficient for Induction of Granulocytic Development from Bipotential Myeloid Progenitors', *Molecular and Cellular Biology*, 18(7), pp. 4301–4314. doi: 10.1128/MCB.18.7.4301.

Ray, R. J. *et al.* (1996) 'Flt3 ligand supports the differentiation of early B cell progenitors in the presence of interleukin-11 and interleukin-7', *European Journal of Immunology*. doi: 10.1002/eji.1830260715.

Reddy, V. A. *et al.* (2002) 'Granulocyte inducer C/EBP α inactivates the myeloid master regulator PU.1: Possible role in lineage commitment decisions', *Blood*. doi: 10.1182/blood.V100.2.483.

Rosenbauer, F. *et al.* (2006) 'Lymphoid cell growth and transformation are suppressed by a key regulatory element of the gene encoding PU.1', *Nature Genetics*. doi: 10.1038/ng1679.

Rosenbauer, F. and Tenen, D. G. (2007) 'Transcription factors in myeloid development: Balancing differentiation with transformation', *Nature Reviews Immunology*. doi: 10.1038/nri2024.

Rosenberg, P. S. *et al.* (2006) 'The incidence of leukemia and mortality from sepsis in patients with severe congenital neutropenia receiving long-term G-CSF therapy', *Blood*, 107(12), pp. 4628–4635. doi: 10.1182/blood-2005-11-4370.

Rosenberg, P. S. *et al.* (2010) 'Stable long-term risk of leukaemia in patients with severe congenital neutropenia maintained on G-CSF therapy.', *British journal of haematology*, 150(2), pp. 196–9. doi: 10.1111/j.1365-2141.2010.08216.x.

Rosnet, O. *et al.* (1993) 'Close physical linkage of the FLT1 and FLT3 genes on chromosome 13 in man and chromosome 5 in mouse', *Oncogene*.

Ross, S. E. *et al.* (2004) 'Phosphorylation of C/EBPalpha inhibits granulopoiesis.', *Molecular and cellular biology*, 24(2), pp. 675–686. doi: 10.1128/MCB.24.2.675.

Rothová, M. *et al.* (2016) 'Differentiation of Mouse Embryonic Stem Cells into Ventral Foregut Precursors', in *Current Protocols in Stem Cell Biology*. Hoboken, NJ, USA: John Wiley & Sons, Inc., pp. 1G.3.1-1G.3.12. doi: 10.1002/9780470151808.sc01g03s36.

Rusten, L. S. *et al.* (1996) 'The FLT3 ligand is a direct and potent stimulator of the growth of primitive and committed human CD34+ bone marrow progenitor cells in vitro.', *Blood*.

Scapini, P. and Cassatella, M. A. (2014) 'Social networking of human neutrophils within the immune system.', *Blood*. doi: 10.1182/blood-2014-03-453217.

Scheller, M. *et al.* (1999) 'Altered development and cytokine responses of myeloid progenitors in the absence of transcription factor, interferon consensus sequence binding protein.', *Blood*.

Schwarzenberger, P. *et al.* (2000) 'Requirement of endogenous stem cell factor and granulocyte-colony-stimulating factor for IL-17-mediated granulopoiesis.', *Journal of immunology (Baltimore, Md. : 1950)*.

Semerad, C. L. *et al.* (2002) 'G-CSF is an essential regulator of neutrophil trafficking from the bone marrow to the blood', *Immunity*. doi: 10.1016/S1074-7613(02)00424-7.

Shi, C.-X. *et al.* (2017) 'CRISPR Genome-Wide Screening Identifies Dependence on the Proteasome Subunit PSMC6 for Bortezomib Sensitivity in Multiple Myeloma', *Molecular Cancer Therapeutics*. doi: 10.1158/1535-7163.MCT-17-0130.

Shibuya, M. (2001) 'Structure and dual function of vascular endothelial growth factor receptor-1 (Flt-1)', *International Journal of Biochemistry and Cell Biology*. doi: 10.1016/S1357-2725(01)00026-7.

Shivdasani, R. A., Mayer, E. L. and Orkin, S. H. (1995) 'Absence of blood formation in mice lacking the T-cell leukaemia oncogene tal-1/SCL', *Nature*. doi: 10.1038/373432a0.

Shu, J. *et al.* (2013) 'Induction of Pluripotency in Mouse Somatic Cells with Lineage Specifiers', *Cell*, 153(5), pp. 963–975. doi: 10.1016/j.cell.2013.05.001.

Skokowa, J. *et al.* (2006) 'LEF-1 is crucial for neutrophil granulopoiesis and its expression is severely reduced in congenital neutropenia.', *Nature medicine*, 12(10), pp. 1191–7. doi: 10.1038/nm1474.

Skokowa, J. *et al.* (2009) 'NAMPT is essential for the G-CSF–induced myeloid differentiation via a NAD+–sirtuin-1–dependent pathway', *Nature Medicine*, 15(2), pp. 151–158. doi: 10.1038/nm.1913.

Skokowa, J. *et al.* (2012) 'Interactions among HCLS1, HAX1 and LEF-1 proteins are essential for G-CSF-triggered granulopoiesis', *Nature Medicine*. doi: 10.1038/nm.2958.

Skokowa, J. *et al.* (2014) 'Cooperativity of RUNX1 and CSF3R mutations in severe congenital neutropenia: a unique pathway in myeloid leukemogenesis', *Blood*, 123(14), pp. 2229–2237. doi: 10.1182/blood-2013-11-538025.

Skokowa, J. *et al.* (2018) 'Severe congenital neutropenias'. doi: 10.1038/nrdp.2017.32.Severe.

Skokowa, J. and Welte, K. (2009) 'Dysregulation of myeloid-specific transcription factors in congenital neutropenia', *Ann N Y Acad Sci*. doi: NYAS4963 [pii]10.1111/j.1749-6632.2009.04963.x.

Skokowa, J., Zeidler, C. and Welte, K. (2018) 'Chronic neutropenia in childhood', *Monatsschrift für Kinderheilkunde*, 166(11), pp. 977–986. doi: 10.1007/s00112-018-0545-8.

Smith, L. T. *et al.* (1996) 'PU.1 (Spi-1) and C/EBP alpha regulate the granulocyte colony-stimulating factor receptor promoter in myeloid cells.', *Blood*.

Sontag, S. *et al.* (2017) 'Modelling IRF8 Deficient Human Hematopoiesis and Dendritic Cell Development with Engineered iPS Cells', *Stem Cells*. doi: 10.1002/stem.2565.

Soufi, A., Donahue, G. and Zaret, K. S. (2012) 'Facilitators and impediments of the pluripotency reprogramming factors' initial engagement with the genome', *Cell*. doi: 10.1016/j.cell.2012.09.045.

Spangrude, G. J., Heimfeld, S. and Weissman, I. L. (1988) 'Purification and

characterization of mouse hematopoietic stem cells', *Science*. doi: 10.1126/science.2898810.

Spiekermann, K. *et al.* (2002) 'A new and recurrent activating length mutation in exon 20 of the FLT3 gene in acute myeloid leukemia', *Blood*. doi: 10.1182/blood-2002-03-0953.

Spoor, J., Farajifard, H. and Rezaei, N. (2019) 'Congenital neutropenia and primary immunodeficiency diseases', *Critical Reviews in Oncology/Hematology*. Elsevier, 133(October 2018), pp. 149–162. doi: 10.1016/j.critrevonc.2018.10.003.

Stefater, J. A. *et al.* (2011) 'Regulation of angiogenesis by a non-canonical Wnt - Flt1 pathway in myeloid cells', *Nature*. doi: 10.1038/nature10085.

Štefková, K., Procházková, J. and Pacherník, J. (2015) 'Alkaline Phosphatase in Stem Cells', *Stem Cells International*. doi: 10.1155/2015/628368.

Stirewalt, D. L. and Radich, J. P. (2003) 'The role of FLT3 in haematopoietic malignancies.', *Nature reviews. Cancer*, 3(9), pp. 650–665. doi: 10.1038/nrc1169.

Suzuki, Y. *et al.* (1997) 'HAX-1, a novel intracellular protein, localized on mitochondria, directly associates with HS1, a substrate of Src family tyrosine kinases', *Journal of immunology (Baltimore, Md : 1950)*.

Tak, T. *et al.* (2013) 'What's your age again? Determination of human neutrophil half-lives revisited', *Journal of Leukocyte Biology*. doi: 10.1189/jlb.1112571.

Takahashi, K. *et al.* (2007) 'Induction of Pluripotent Stem Cells from Adult Human Fibroblasts by Defined Factors', *Cell*, 131(5), pp. 861–872. doi: 10.1016/j.cell.2007.11.019.

Takahashi, K. and Yamanaka, S. (2006) 'Induction of Pluripotent Stem Cells from Mouse Embryonic and Adult Fibroblast Cultures by Defined Factors', *Cell*, 126(4), pp. 663–676. doi: 10.1016/j.cell.2006.07.024.

Tamura, T. *et al.* (2000) 'ICSBP Directs Bipotential Myeloid Progenitor Cells to Differentiate into Mature Macrophages', *Immunity*, 13(2), pp. 155–165. doi: 10.1016/S1074-7613(00)00016-9.

Uchida, N. and Weissman, I. L. (1992) 'Searching for Hematopoietic Stem Cells: Evidence That Thy-1.1^{lo} Lin⁻ Sca-1⁺ Cells Are the Only Stem Cells in C57BL/Ka-Thy-1.1 Bone Marrow.', *The Journal of experimental medicine*. doi: 10.1084/jem.175.1.175.

Untergasser, A. *et al.* (2012) 'Primer3-new capabilities and interfaces', *Nucleic Acids Research*. doi: 10.1093/nar/gks596.

- Weinblatt, M. E. *et al.* (1995) 'Transformation of congenital neutropenia into monosomy 7 and acute nonlymphoblastic leukemia in a child treated with granulocyte colony-stimulating factor', *The Journal of Pediatrics*. doi: 10.1016/S0022-3476(95)70557-0.
- Weissman, I. L., Anderson, D. J. and Gage, F. (2002) 'Stem and Progenitor Cells: Origins, Phenotypes, Lineage Commitments, and Transdifferentiations', *Annual Review of Cell and Developmental Biology*. doi: 10.1146/annurev.cellbio.17.1.387.
- Welte, K. *et al.* (1985) 'Purification and biochemical characterization of human pluripotent hematopoietic colony-stimulating factor.', *Proceedings of the National Academy of Sciences*. doi: 10.1073/pnas.82.5.1526.
- Welte, K. *et al.* (1990) 'Differential effects of granulocyte-macrophage colony-stimulating factor and granulocyte colony-stimulating factor in children with severe congenital neutropenia.', *Blood*.
- Weston R. F.;Axtell, R.;Balazovich, K.;Stewart, J.;Locey, B. J.;Mayo-Bond, L.;Loos, P.;Hutchinson, R.;Boxer, L. A., B. ;Tod. I. (1991) 'Severe congenital neutropenia: Clinical effects and neutrophil function during treatment with granulocyte colony-stimulating factor', *The Journal of Laboratory and Clinical Medicine*.
- Wood, B. (2004) 'Multicolor Immunophenotyping: Human Immune System Hematopoiesis', *Methods in Cell Biology*, 75, pp. 559–576. doi: 10.1016/S0091-679X(04)75023-2.
- Xia, J. and Link, D. C. (2008) 'Severe congenital neutropenia and the unfolded protein response.', *Current opinion in hematology*, 15, pp. 1–7. doi: 10.1097/MOH.0b013e3282f13cd2.
- Yamanaka, S. (2012) 'Induced Pluripotent Stem Cells: Past, Present, and Future', *Cell Stem Cell*, 10(6), pp. 678–684. doi: 10.1016/j.stem.2012.05.005.
- Ye, J. *et al.* (2012) 'Primer-BLAST: a tool to design target-specific primers for polymerase chain reaction.', *BMC bioinformatics*. doi: 10.1186/1471-2105-13-134.
- Zhang, D.-E. *et al.* (1997) 'Absence of granulocyte colony-stimulating factor signaling and neutrophil development in CCAAT enhancer binding protein - deficient mice', *Proceedings of the National Academy of Sciences*, 94(2), pp. 569–574. doi: 10.1073/pnas.94.2.569.
- Zhang, P. *et al.* (2004) 'Enhancement of Hematopoietic Stem Cell Repopulating Capacity and Self-Renewal in the Absence of the Transcription Factor C/EBP α ', *Immunity*, 21(6), pp. 853–863. doi: 10.1016/j.immuni.2004.11.006.
- Zhang, X. *et al.* (2010) 'Pax6 is a human neuroectoderm cell fate determinant', *Cell Stem Cell*. doi: 10.1016/j.stem.2010.04.017.

7 Declaration of authorship

This thesis was developed in the laboratory of Prof. Dr. Dr. Skokowa, department for translational oncology, *Medizinische Klinik II* of the University hospital Tübingen.

The concept of this thesis was designed by Prof. Dr. Dr. Skokowa in cooperation with Dr. H. Loghmani. All experiments and data analysis, except those explicitly marked otherwise or mentioned below, were performed by me under the supervision of Dr. H. Loghmani and Prof. Dr. Dr. Skokowa. The writing and correction process was supervised by Prof. Dr. Dr. Skokowa.

I was introduced to the experimental methods by the technicians of lab Skokowa (Regine Bernard, Karin Hähnel, Inge Steiert, and Ursula Hermanutz-Klein).

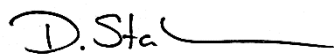
The analysis of the next generation sequencing results acquired from the index patients genome was performed by members of lab Skokowa before the start of this thesis. The site directed mutagenesis experiments were done by Dr. Loghmani and Tessa Skroblyn, M.Sc., of lab Skokowa.

The morphological cell count of the iPS suspension cells was performed by Regine Bernard, Lab Skokowa.

Karin Hähnel performed FACS for one V194M-FLT3 transfection and Bortezomib repeat experiment.

I hereby declare that this thesis is my original work. All sources of information, including those for figures, are referenced directly or mentioned above.

Tübingen, 23.07.2022



Dorothea Stalman

8 Acknowledgement

This thesis would not have been possible without the generous support, guidance, and patience of my advisor Prof. Dr. Dr. J. Skokowa.

I am forever grateful to her for giving me the opportunity to work and learn in her lab and for entrusting me with this particular thesis. She has given me the opportunity to gather insights to a broad spectrum of laboratory methods, to immerse myself in this fascinating field of medicine and to experience and partake in the labs research efforts. Her insightful suggestions have been an inspiration and a challenge for excellence. My special thanks extends as well to Prof. Dr. Karl Welte for his kind encouragement and helpful feedback during our lab meetings.

I would like to take the opportunity to thank my supervisor, Houra Loghmani, Ph.D., who introduced me to lab work and guided me along the ups and downs of the experimental part of this thesis with an infinite amount of positivity and ideas for improvement.

And lastly, I would like to express my deepest gratitude to the entire research group Skokowa. It has been a joy to work in this team. Their cooperative, friendly and welcoming way to integrate new members and work together is inspirational and exceptional. My thanks go out to the wonderful technicians (Regine Bernard, Karin Hähnel, Inge Steiert and Ursula Hermanutz-Klein) whose support, advice and help is at the foundation of this work and truly appreciated.